

Effects of polycations on structure and catalytic activity of cobalt phthalocyanine : mechanistic study of the ionene-promoted thiol autoxidation

Citation for published version (APA):

Welzen, van, J. (1989). *Effects of polycations on structure and catalytic activity of cobalt phthalocyanine : mechanistic study of the ionene-promoted thiol autoxidation*. [Phd Thesis 1 (Research TU/e / Graduation TU/e), Chemical Engineering and Chemistry]. Technische Universiteit Eindhoven. <https://doi.org/10.6100/IR316192>

DOI:

[10.6100/IR316192](https://doi.org/10.6100/IR316192)

Document status and date:

Published: 01/01/1989

Document Version:

Publisher's PDF, also known as Version of Record (includes final page, issue and volume numbers)

Please check the document version of this publication:

- A submitted manuscript is the version of the article upon submission and before peer-review. There can be important differences between the submitted version and the official published version of record. People interested in the research are advised to contact the author for the final version of the publication, or visit the DOI to the publisher's website.
- The final author version and the galley proof are versions of the publication after peer review.
- The final published version features the final layout of the paper including the volume, issue and page numbers.

[Link to publication](#)

General rights

Copyright and moral rights for the publications made accessible in the public portal are retained by the authors and/or other copyright owners and it is a condition of accessing publications that users recognise and abide by the legal requirements associated with these rights.

- Users may download and print one copy of any publication from the public portal for the purpose of private study or research.
- You may not further distribute the material or use it for any profit-making activity or commercial gain
- You may freely distribute the URL identifying the publication in the public portal.

If the publication is distributed under the terms of Article 25fa of the Dutch Copyright Act, indicated by the "Taverne" license above, please follow below link for the End User Agreement:

www.tue.nl/taverne

Take down policy

If you believe that this document breaches copyright please contact us at:

openaccess@tue.nl

providing details and we will investigate your claim.

**EFFECTS OF POLYCATIONS ON STRUCTURE AND
CATALYTIC ACTIVITY OF COBALT PHTHALOCYANINE**

Mechanistic study of the ionene-promoted thiol autoxidation



JOKE VAN WELZEN

**EFFECTS OF POLYCATIONS ON STRUCTURE AND
CATALYTIC ACTIVITY OF COBALT PHTHALOCYANINE**
Mechanistic study of the ionene-promoted thiol autoxidation

PROEFSCHRIFT

ter verkrijging van de graad van doctor aan de
Technische Universiteit Eindhoven, op gezag van
de Rector Magnificus, prof. ir. M. Tels, voor
een commissie aangewezen door het College van
Dekanen in het openbaar te verdedigen op
dinsdag 3 oktober 1989 te 16.00 uur

door

Johanna (Joke) van Welzen
geboren te Rotterdam

Dit proefschrift is goedgekeurd door
de promotoren: prof. dr. ir. A. L. German
 prof. dr. J. Reedijk
en de copromotor: dr. A. M. van Herk

*Wie bracht dit al tot stand ?
God schiep het door Zijn woord.*

(Gez. 30:5, Liedboek)

Aan mijn ouders

CONTENTS

1. INTRODUCTION

1.1 Catalysis	1
1.2 Polymers in catalysis	2
1.3 Scope of thesis; choice of model system	3
1.4 Outline of thesis	4

2. LITERATURE SURVEY ON THE COBALT PHTHALOCYANINE-CATALYZED AUTOXIDATION OF THIOLS

2.1 Mechanism of the polymer-free process	6
2.2 Effects of polymers	9

3. EXPERIMENTAL PART

3.1 Materials	13
3.2 Apparatus and techniques	17
3.3 Calculation methods	22

4. EFFECTS OF IONENES ON THE SOLUTION STRUCTURE OF $\text{CoPc}(\text{NaSO}_3)_4$

4.1 Polyelectrolyte-type ionenes	25
4.2 Comparison with model compounds	31
4.3 Polysoap-type ionenes	39
4.4 Conclusions	44

5. INTERACTION OF SUBSTRATES WITH THE $\text{CoPc}(\text{NaSO}_3)_4$ /IONENE COMPLEX

5.1 Interaction of O_2 with the catalyst	46
---	----

5.2 Interaction of thiol with the catalyst	48
5.3 Relation between structure and catalytic activity: the catalytic site	54
5.4 Conclusions and final remarks	59
6. KINETIC MODELLING OF THE IONENE-PROMOTED THIOL OXIDATION	
6.1 Introduction	62
6.2 The 2-substrate Michealis-Menten model	62
6.3 Side-reactions: accumulation of H ₂ O ₂	70
6.4 Conclusions	77
7. EFFECTS OF VARYING REACTION CONDITIONS ON THE KINETIC PARAMETERS; MECHANISTIC CONSIDERATIONS	
7.1 General features	79
7.2 Effects on individual kinetic parameters; reaction mechanism	84
7.3 Conclusions	94
8. POLYELECTROLYTE-PROMOTED CATALYTIC OXIDATION OF A HYDROPHOBIC THIOL	
8.1 Introduction	96
8.2 Results and discussion	97
8.3 Conclusions	106
9. GENERAL DISCUSSION	
9.1 Polymeric effects in catalysis	108
9.2 Prerequisites for application of polymer catalysts in thiol oxidation	109
LITERATURE REFERENCES	111

SUMMARY	117
SAMENVATTING	119
SAMENVATTING VOOR LEKEN	121
CURRICULUM VITAE	123

1.1 Catalysis

A catalyst is a compound that accelerates a chemical reaction without being part of the stoichiometric reaction equation or, in other words, without affecting the position of the equilibrium of the reaction. Rate enhancement is achieved by providing an alternative reaction pathway with a lower activation energy and/or a higher preexponential factor.

Apart from an increase in reaction rate, application of a catalyst may also lead to a change in selectivity, i.e. certain products will be formed in larger relative amounts than via the uncatalyzed process.

Due to both these kinetic and selectivity effects, it is not surprising that catalysts are widely applied in modern industrial chemistry. Nowadays, it is estimated that about 80 - 90% of all chemicals are produced by one or more catalytic steps.

Conventionally, catalysts are divided in two categories: homogeneous and heterogeneous systems. In homogeneous catalysis, catalyst and reactants are in the same (usually liquid) phase. The catalyst is then readily accessible to the substrates and, in general, high activities can be obtained. A disadvantage of these systems is, that separation of the catalyst from the reaction mixture is rather laborious and application in a continuous process difficult, for which reason homogeneous catalysis has only played a minor role in industry up to around 1970¹⁾. However, today the importance of these well-defined, highly active and selective systems is recognized, especially in the synthesis of fine-chemicals²⁾.

Heterogeneous catalysts are usually solids that catalyze reactions occurring in either the gaseous or the liquid phase. These catalysts are often heterogenized homogeneous catalysts, i.e. homogeneous catalysts attached to

(inert) supports. Unfortunately, upon heterogenization, generally part of the catalytic activity is lost, due to rate limitation because of slow transport of reactants to the catalyst particle surface. Therefore, extensive research is being carried out attempting to overcome this problem.

1.2 Polymers in catalysis

A possible solution to the above-mentioned mass transport problem in heterogeneous catalysis is offered by polymers: the catalytic compound may be bound to a polymer soluble in the reaction medium, which is then coupled to an insoluble support by way of single-link anchoring. In this way, the polymer chain acts as a spacer between the support particle surface and the catalytic site, so that transport of reactants from liquid to solid phase is no longer necessary. Interesting research in this field has been carried out by e.g. Van de Berg et al.³⁾, Ford et al.⁴⁾ and Van Streun et al.⁵⁾.

However, the interest in polymers in catalysis is much wider. It appears that polymers usually do not just behave as inert carriers but can exert certain positive effects on catalytic activity and selectivity as well.

These polymer catalytic effects comprise concentrational (1), structural (2) and geometric effects (3) as a result of interactions with both the catalyst and the substrate(s). Effects on activity are primarily due to enhancement of substrate concentration within the (catalyst containing) polymer coil domains by e.g. electrostatic or hydrophobic interactions⁶⁾ (1). Furthermore, the form in which the catalyst is stabilized by the polymer (catalyst structure (2)) may be of influence on activity: in the case of "site isolation", deactivating interaction between catalytic sites like e.g. dimerization^{7,8)} is prevented, while on the other hand it is also possible that the polymer enhances certain (desired) site-site interactions, as was found by Koning et al. for the polymer-catalyzed oxidative coupling of 2,6-dimethylphenol⁹⁾.

In determining the selectivity, the catalyst structure (2) is also an

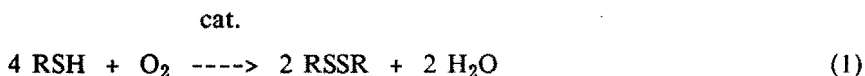
important factor¹⁰). In addition, geometry (3) may play a dominant role. For instance, it can be easily understood that selectivity may be affected by e.g. steric hindrance due to bulky side-groups on the polymer chains or by a stereospecific arrangement of polymer ligand groups¹¹).

In general, it can be stated that polymers thus offer a wide range of possibilities to create optimum conditions for catalytic reactions. They are especially interesting because various functional groups may be combined within the polymer chains, leading to "tailor-made" catalyst systems and even allowing the mimicking of the structure and reactivity of enzymes¹²).

Therefore, extensive research in the field of polymer catalysis is desired, in particular fundamental work, aimed at identifying and describing all types of polymer effects on catalytic processes. Elucidation of the mechanisms of polymer-promoted reactions, by means of kinetic and structural investigations, will be of help in systematically designing better catalyst systems.

1.3 Scope of this thesis: choice of model system

The work described in this thesis aims to contribute to the world-wide attempts to study and further understand the catalytic effects exerted by polymers. The (fundamental) research work comprises spectroscopic and kinetic measurements, in order to obtain a detailed mechanistic description of a polymer-promoted model reaction. As a model reaction, the catalytic autoxidation of thiols (eq. 1) was chosen. For several reasons, this is a very interesting and suitable process.



In the first place, thiol autoxidation is a process of industrial importance, since it is a necessary step in oil sweetening^{13,14}). Thiols are

present in hydrocarbon distillates and natural gases and can thus lead to poisoning of metal catalysts, corrosion of apparatus and, after combustion, environmental contamination. Therefore, thiols are oxidized into the corresponding, less harmful disulfides (that can be easily extracted), via the so-called Merox process (mercaptan oxidation), using sulphonato-phthalocyaninato-Co(II) complexes supported on activated carbon as catalysts^{15,16}).

Besides in industry, the oxidative coupling of thiols is also important in biological systems^{17,18}). The sulfhydryl group is one of the chemically most active groups in living cells, especially toward oxidation reactions. On the other hand, the relatively stable disulfide linkages are important structure elements in proteins. This explains the wide interest in e.g. the oxidation of cysteine, glutathione and other thiols catalyzed by vitamin B₁₂ derivatives^{19,20}).

Autoxidation of thiols can be catalyzed by a large variety of compounds^{15,16,21-25}), including simple inorganic salts like CuCl₂²⁴) and complex molecules like bis[dimercaptomaleonitrilato(2-)]cobaltate(2-)²⁵). The catalytically most active compounds appear to be four-coordinated cobalt species, viz. vitamin B₁₂ derivatives and phthalocyanines²²⁻²⁴).

Since tetrasulphonato-phthalocyaninato-Co(II) (abbrev.: CoPc(NaSO₃)₄) is used industrially, this system has been investigated most elaborately. The large amount of mechanistic information available on this conventional (i.e. polymer-free) system formed the basis of the polymer catalytic research described in this thesis.

1.4 Outline of thesis

After the above-given general introduction into the field of polymer catalysis and the argued choice of the model reaction, the next chapters will be concerned with the catalytic autoxidation of thiols and, especially, with the effects that polymers can exert on this process.

In chapter 2, an overview of the most important mechanistic information

about the polymer-free reaction is given, as well as a summary of the previously obtained results on polymer-promoted systems.

Chapter 3 contains all information on experimental methods used in the investigations described here.

In chapters 4 and 5 spectroscopic investigations are described, revealing the interactions between catalyst and polymer promotor (ch. 4) and the effects of substrates on the structure of the polymer catalyst system (ch. 5).

Chapters 6 and 7 deal with the kinetics of the catalytic thiol oxidation reaction in the presence of polymer promotors. In chapter 6 a general kinetic model is discussed, whereas chapter 7 contains more detailed information about the effects of reaction conditions on kinetic parameters. These are combined into a proposed reaction mechanism.

A study of the polymer-promoted oxidation of hydrophobic thiols is presented in chapter 8.

Finally, all obtained results are placed in context in the general discussion of chapter 9.

Parts of this thesis have already been published or will be published soon:

- parts of chapters 4 and 5 have been published in refs.²⁶⁻²⁸⁾
- chapter 6 contains major parts of the article of ref.²⁹⁾ (section 6.2) and the submitted paper of ref.³⁰⁾ (section 6.3) and a minor part of ref.³¹⁾ (section 6.2.3, stopped-flow)
- chapters 7 and 8 have been submitted for publication^{32,33)}.

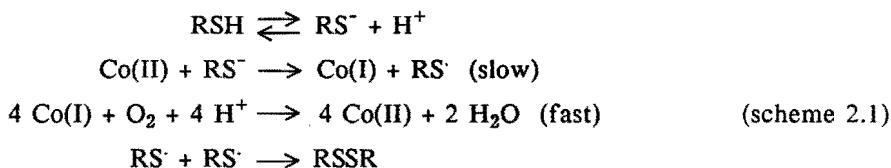
The co-authors A.H.J. Tullemans, H. Kramer and T.G.L. Thijssen have had a major part in the performance of the kinetic experiments of chapters 6 and 7.

2 LITERATURE SURVEY ON THE COBALT PHTHALOCYANINE-CATALYZED AUTOXIDATION OF THIOLS

2.1 Mechanism of the polymer-free process

The oxidation of thiols as catalyzed by $\text{CoPc}(\text{NaSO}_3)_4$ has been studied by several research groups, both via spectroscopic and kinetic measurements.

Kundo and Keier³⁴⁾ were the first to postulate a reaction mechanism of the process. Since they spectrophotometrically established, that the addition of cysteine to the catalyst (in the absence of dioxygen) leads to the same spectral change as the addition of one equivalent of the reductor TiCl_3 , they proposed that thiol oxidation proceeds by alternating electron transfer from thiol to the Co(II) species, generating thiyl radicals and Co(I) , and subsequent reoxidation of the catalyst by dioxygen (scheme 2.1).



The superior catalytic activity of $\text{CoPc}(\text{NaSO}_3)_4$ as compared with other transition metal phthalocyanines and other substituted cobalt phthalocyanines³⁵⁾ was explained from the relative ease of reduction of the $\text{CoPc}(\text{NaSO}_3)_4$ complex. Furthermore, it was shown that stabilization of the Co(III) state (e.g. by KCN ³⁵⁾ or ammonia³⁴⁾) increased reduction time and simultaneously lowered the catalytic activity.

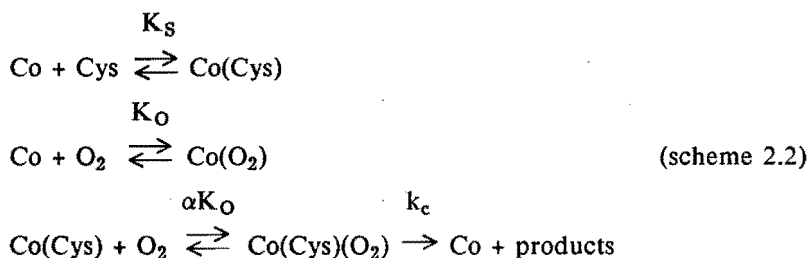
The model of Kundo and Keier was confirmed by Cookson et al.³⁶⁾, who studied cysteine oxidation by means of EPR spectroscopy. During reaction, they observed the disappearance of the Co(II) signal, which was ascribed to

reduction of the cobalt complex. It must be noted, that these experiments were carried out in frozen solutions (- 140 °C), presumably leading to dioxygen depletion. Therefore, the conclusion of $[\text{Co(I)Pc}(\text{NaSO}_3)_4]^-$ being present under reaction conditions is rather ambiguous.

Dolansky et al.³⁷⁾, who investigated the kinetics of the oxidation of cysteine, rejected the above-mentioned reaction mechanism. An important objection of these authors against scheme 2.1 concerned the proposed liberation of thiyl radicals in the absence of dioxygen. Since the production of cystine under anaerobic conditions could not be demonstrated, the occurrence of free thiyl radicals was thought to be improbable. Nevertheless, the occurrence of (unidentified) radicals has been proven by measuring the effects of addition of radical scavengers to the reaction mixture^{38,39)}.

Furthermore, Dolansky et al. argued that the assumption of Co(II) reduction by cysteine being the rate-determining step, is not compatible with the linear dependence of initial rate on $[\text{O}_2]$ they observed. Since in an earlier study, Wagnerova et al.⁴⁰⁾ had shown that $\text{CoPc}(\text{NaSO}_3)_4$ has the ability to form a stable adduct with dioxygen, and since it had been concluded⁴¹⁾ that catalytic activity in oxidation reactions is only exhibited by metal complexes possessing such ability, an alternative mechanism was postulated, involving the formation of a ternary complex of the form: $\text{RS}^- - \text{Co} - \text{O}_2$. The electron transfer leading to substrate oxidation was assumed to occur within this complex without the valency of the cobalt centre being altered.

A similar ternary complex (however, with variable Co valency⁴²⁾) was



proposed by Kozlyak et al., based on spectrophotometric⁴²⁾ and, especially, kinetic⁴³⁾ studies. A mechanism of the form of scheme 2.2 was proposed, in agreement with observed two-substrate Michaelis-Menten kinetics, described by eq. 2.1.

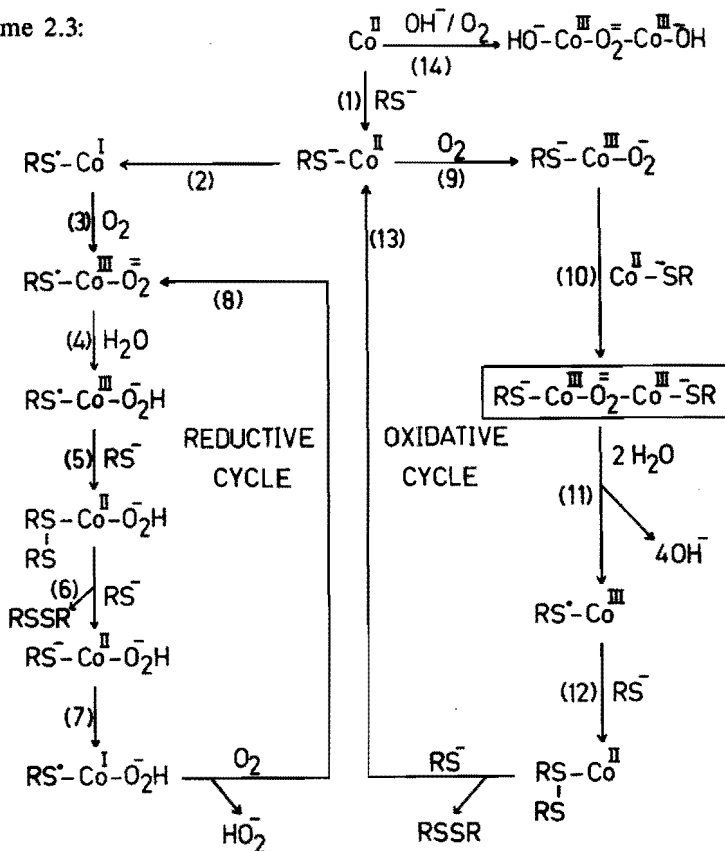
$$v_0 = \alpha k_c K_S K_O [Co]_0 [Cys][O_2] / (1 + K_S [Cys] + K_O [O_2] + \alpha K_O K_S [Cys][O_2]) \quad (2.1)$$

Reaction kinetics according to scheme 2.1 do not satisfy this rate law.

Two-substrate Michaelis-Menten kinetics was also reported by Hoffmann et al.⁴⁴⁾ for the catalytic oxidation of H₂S. This research group paid much attention to pH-effects on thiol oxidation rate^{38,44)}, which were described in terms of thiol and pyrrole nitrogen dissociation constants. They confirmed the findings of others that the thiolate anion is the reactive species.

Finally, an elaborate study of the CoPc(NaSO₃)₄ catalyzed oxidation of 2-mercaptoethanol and cysteine was performed by Zwart⁴⁵⁾. He combined kinetic and spectroscopic measurements, including steady-state spectral measurements. After carefully elucidating the origin of the obtained spectra by comparison with spectra of electrochemically generated catalyst species, it was concluded that the reaction mechanism of the thiol oxidation process consists of two parallel reaction paths (scheme 2.3), both involving ternary intermediate adducts. The reductive cycle, in which the cobalt(II) centre is first reduced to Co(I) before dioxygen addition takes place, proceeds at a high rate, as was clearly demonstrated from the rate increase upon prereduction of the catalyst. On the other hand, the oxidative cycle, where dioxygen is directly bound to the unreduced RS⁻ - Co complex, slows down the reaction, because via this cycle the relatively stable μ -peroxo complex (RS⁻ - Co(III) - O₂²⁻ - Co(III) - RS⁻) is formed, inactivating part of the catalyst. Occurrence of this complex formation was even shown to cause a negative kinetic order in dioxygen. Such kinetic behaviour was not found by other authors since they studied only limited dioxygen concentration ranges.

scheme 2.3:



2.2 Effects of polymers

Polymeric effects on the catalytic oxidation of thiols have been studied by several authors, both homogeneously⁴⁵⁻⁴⁷ (using polymers that are soluble in the reaction medium) and heterogeneously^{4,5,45-49}. Although, in general, the heterogeneous systems were, interestingly, found to exhibit higher activities than the polymer-free catalyst (by a factor of approx. 5 - 10), homogeneous systems have been investigated more elaborately. The latter systems not only have still higher activities, but also offer the possibility

of studying the intrinsic polymeric effects, without the measurements being complicated by inhomogeneities or mass transport problems.

Zwart^{45,50}) and Schutten^{46,51,52}), who did important work in this field, predominantly investigated the catalytic role of polyvinylamine, PVAm, which was chosen because of its bifunctionality: it contains basic groups to give the necessary thiol dissociation (since RS^- is the reactive species) as well as binding sites for the cobalt phthalocyanine complex. The complex could be bound to the polymer either covalently, by peptide linkage of a tetracarboxy phthalocyanine derivative to the amine groups, or coordinatively, by complexation of amine groups to the axial position of the cobalt. Both types of catalysts led to similarly high activities, up to 50 times the value observed for polymer-free $CoPc(NaSO_3)_4$.

The large rate enhancements achieved, were ascribed to two effects: (1) increase of the local thiolate anion concentration, i.e. $[RS^-]$ within the polymer coil domains in the vicinity of the catalyst, due to the presence of basic groups and (2) suppression of formation of the inactive μ -peroxo catalyst complex, which could be demonstrated spectrophotometrically⁵²). Prevention of μ -peroxo complexation was thought to be the result of isolation of monomeric $CoPc(NaSO_3)_4$ by the polymer chains ("site isolation").

Further research-work, carried out by Brouwer^{39,47,53,54,55}), revealed the importance of a high cationic charge density of the polymer. A series of copolymers of vinylamine and vinylalcohol was found to show a linear dependence of reaction rate on the linear charge density⁵³), as depicted in Fig. 2.1. Analogous results were obtained when using poly(quaternary ammonium)salts⁵⁴) (the so-called ionenes). From these results, it was concluded that electrostatic interaction plays an important role in increasing the catalyst activity by increasing the local thiolate anion concentration. The experiments with ionenes made clear that electrostatic interaction is sufficient to "bind" the catalyst complex (no binding sites are available) and that the presence of basic groups, like $-NH_2$, is not a prerequisite for

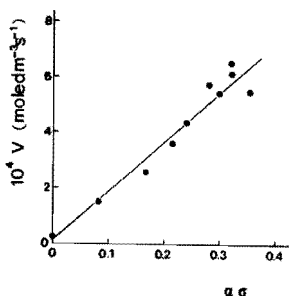


Fig. 2.1 Reaction rate versus the mole fraction of positively charged monomeric units in copolymers of vinylamine and vinylalcohol (taken from ref. 53).

efficient thiol oxidation.

The charge density effect also provided an explanation for the observed variations of reaction rate with ionic strength (Fig. 2.2) and pH (Fig. 2.3)⁵⁴). Upon increasing the ionic strength of the catalyst solution, reaction rate decreased drastically. This can be easily understood as the result of competition between thiolate and other anions for interaction with the polycation. The same phenomenon may cause (part of) the rate decrease at high pH found for ionenes, since, in studying the pH-dependence, the ionic strength was not kept constant. In the case of PVAm⁵⁵), however, the decrease of activity above pH 8 - 9 was too high to be explained on the basis of ionic strength only. Here, the reaction rate is further lowered due to deprotonation of the amine groups of the polymer, leading to very low (ultimately zero) charge density. Thus, although at high pH the thiolate anion concentration in the bulk of the solution is high, it is relatively low within the polymer domains.

Because of the pH-dependent behaviour of PVAm, ionenes are preferred in studying polymeric effects in catalysis, since these polymers carry a permanent, pH-independent cationic charge. Furthermore, ionenes have the advantage of simple synthesis, where the linear charge density can be fully

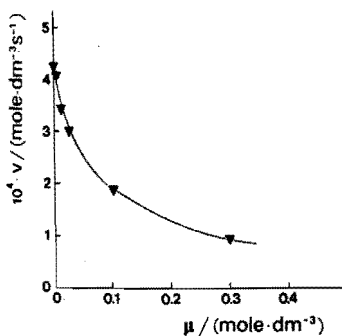


Fig. 2.2 Reaction rate as a function of ionic strength (NaCl) in the $\text{CoPc}(\text{NaSO}_3)_4/\text{PVAm}$ system (from ref.³⁹).

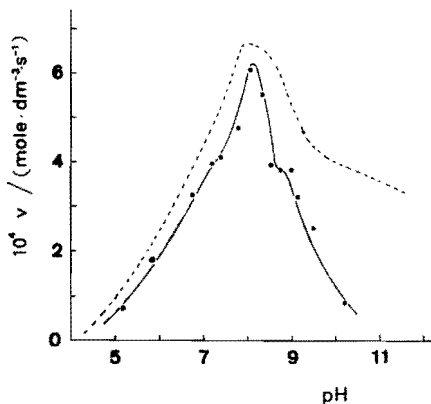


Fig. 2.3 Dependence of catalytic activity on pH for PVAm (●) and 2,4-ionene (---) (taken from ref.⁵⁴).

controlled (see section 3.1), and of being chemically inert with respect to various reagents. Therefore, the stability of ionene systems in successive catalytic runs was much better than of PVAm⁵⁴) that is probably decomposed by the catalytically produced disulfide.

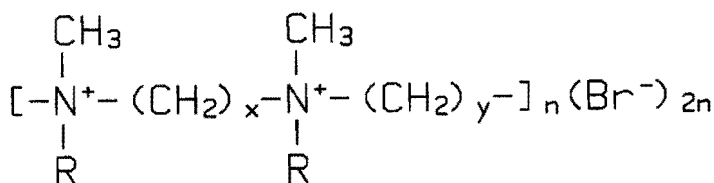
The investigations presented in this thesis have been performed with ionene systems. Effects of e.g. pH and polymer charge density were now studied keeping the ionic strength constant. In order to allow the investigations of pH-effects up to pH = 13, an ionic strength of 0.1 mol dm^{-3} was chosen, although the activity at this value is much lower than at zero ionic strength (Fig. 2.2).

3.1 Materials

3.1.1 α,γ -Ionen

2,4-Ionene (**1a**) was synthesized according to Rembaum et al.⁵⁶⁾, in mixtures of equivolumes of dimethylformamide and methanol, containing stoichiometric amounts of N,N,N',N'-tetramethylethylenediamine (TMEDA) and 1,4-dibromo-butane (1.5 mol dm⁻³). The solution was kept at room temperature for at least one week without stirring. The polymer was precipitated in acetone, filtered and purified by washing with acetone. The product was dried under vacuum (15 mm Hg) at 50 °C for ca. 12 hours.

To be able to determine molecular mass, the ionene chains were terminated with amine groups by reaction with an excess of amine (0.25 g TMEDA per gram of product) in water for another 8 hours. The N-terminated ionene was washed



	name	R	x	y
1a	2,4-ionene	CH ₃	2	4
1b	2,6-ionene	CH ₃	2	6
1c	2,8-ionene	CH ₃	2	8
1d	2,10-ionene	CH ₃	2	10
1e	2,12-ionene	CH ₃	2	12
1f	6,4-ionene	CH ₃	6	4
1g	6,6-ionene	CH ₃	6	6
1h	2,xyl-ionene	CH ₃	2	CH ₂ -Ø-CH ₂ instead of (CH ₂) _y
1i	6,2NH-ionene	CH ₃	6	CH ₂ -CH(CONHØ) instead of (CH ₂) _y
1j	3,3C ₁₂ -ionene	C ₁₂ H ₂₅	3	3

with acetone and dried at 50 °C under vacuum. M_n was then determined by titration of the amine endgroups with hydrochloric acid.

The 2,y-ionenes 1b, c, d and e were synthesized analogously, using the starting materials TMEDA and 1,y-dibromo-y-alkane. The ionenes 1f and g were prepared in a similar way, using the starting materials N,N,N',N'-tetramethyl-1,6-hexanediamine (TMHDA) and 1,4-dibromobutane for 1f and TMHDA and 1,6-dibromohexane for 1g.

C,H,N-analyses revealed the products were > 95% pure. Since the ionenes are very hygroscopic, they will have contained small amounts of water.

The M_n -values obtained were: 9200 for 1b, 10^4 for 1c, 5600 for 1d, 6200 for 1f and $1.3 \cdot 10^4$ for 1g. Since the 2,12-ionene (1e) could not be isolated after the N-termination procedure, M_n could not be determined in this case. The effect of this ionene was therefore studied only qualitatively.

The molecular mass of the 2,4-ionene (1a) was varied either by limiting the polymerization time (down to 6 hours) or by non-stoichiometric combination of the reagents. Products were obtained having M_n -values of 1800, 2200, 3400, 6100, 6300, 7300, 8600, 13000, 16000 and 22000.

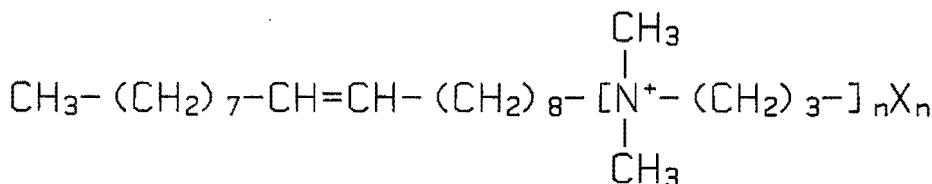
3.1.2 Other ionenes

2,xyl-Ionene (1h) was prepared analogously to the x,y-ionenes, using TMEDA and α,α' -dichloro-p-xylene as starting materials. M_n was determined to be 5300 by titration with hydrochloric acid (vide supra).

6,2Nø-Ionene (1i) was also prepared analogously, using TMHDA and 2,3-dibromo-N-phenyl-propionamide (see section 3.1.3) as starting materials. Since the overall yield (including monomer synthesis) was very low (18 %), the product was only studied qualitatively and M_n was not determined.

3,3C₁₂-Ionene (1j) was synthesized according to the method described in ref.⁵⁷. M_n was determined to be 10^4 by viscometric measurements.

Oleyl-ionene (2) was kindly provided by K.H. van Streun (Eindhoven University of Technology) and was synthesized as follows: 3.65 g dimethyl-



2 oleyl-ionene (X = Br⁻ or I⁻)

aminopropyl-chloride (isolated from its hydrochloric salt, according to the method of Yen et al.⁵⁸) and 0.69 g oleyliodide (see section 3.1.4) were refluxed for 48 hours in 5 ml water under nitrogen atmosphere. The iodide dissolved rapidly after the polymerization had started and a viscous reaction mixture resulted. After freeze-drying and washing the product with acetone, the yield was found to be quantitative.

3.1.3 2,3-Dibromo-N-phenyl-propionamide

The monomer 2,3-dibromo-N-phenyl-propionamide was prepared from 2,3-dibromopropionic acid via a two-step process.

10.00 g Of 2,3-dibromopropionic acid (Br-CH₂-CH(COOH)-Br) was reacted with 10 g of PCl₅ in 30 ml benzene at 0 °C under continuous stirring for 4 hours. Benzene was evaporated from the mixture under vacuum at 40 °C. The product, 2,3-dibromopropionic acidchloride (Br-CH₂-CH(COOCl)-Br), was purified by vacuum distillation (48 °C, 3 Torr), resulting in a transparent liquid (yield 67 %).

To a solution of 7.2 g of the product in ether, 2.9 g freshly distilled aniline was added dropwise, keeping the temperature at 0 °C. Excess of triethylamine (3.1 g) was added in order to bind the HCl formed. The resulting precipitate was washed with water and dried under vacuum (40 °C).

The rough product (Br-CH₂-CH(CONHØ)-Br) was then further purified, by dissolving in dichloromethane and extraction with base and acid solutions. After washing with water, the solution was dried over MgSO₄ and the product

was crystallized by slowly evaporating the solvent. A crystalline, white material was obtained (yield 53 %), with melting point 142-144 °C.

3.1.4 Oleyliodide

The monomer oleyliodide was prepared from oleylalcohol via a two-step process.

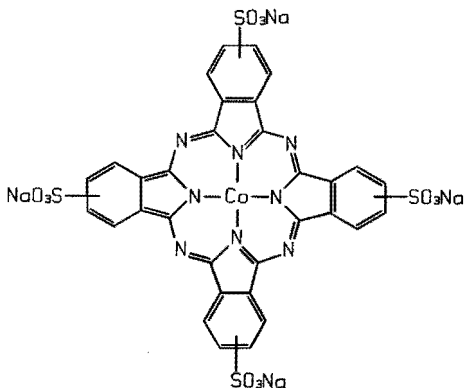
First, 5.0 g distilled oleylalcohol ($\text{CH}_3-(\text{CH}_2)_7-\text{CH}=\text{CH}-(\text{CH}_2)_7-\text{CH}_2\text{OH}$) and 3.91 g tosylchloride were dissolved in 50 ml pyridine and stored overnight at 4 °C. A precipitate was formed during reaction. The reaction mixture was poured into ice and extracted several times with dichloromethane. The combined organic fractions were washed with 5% HCl, followed by washing with water. After drying over MgSO_4 , the solvent was removed under reduced pressure. The yield of oleyltosylate ($\text{CH}_3-(\text{CH}_2)_7-\text{CH}=\text{CH}-(\text{CH}_2)_7-\text{CH}_2\text{OSO}_2-\text{C}_6\text{H}_4-\text{CH}_3$) was nearly quantitative. $^1\text{H-NMR}$ showed the absence of the starting material oleylalcohol.

In the second step, 5.5 g of the unpurified oleyltosylate was dissolved in 75 ml acetone together with 2.1 g NaI and refluxed under nitrogen atmosphere for three hours, during which a precipitate was formed. After filtration and evaporation of acetone a yellow oil remained (yield approx. 95%). $^1\text{H-NMR}$ showed the absence of the tosylate group. The quality of the oleyliodide ($\text{CH}_3-(\text{CH}_2)_7-\text{CH}=\text{CH}-(\text{CH}_2)_7-\text{CH}_2\text{I}$) was found to be satisfactory for synthesis of the oleyl-ionene.

3.1.5 Other materials

$\text{MtPc}(\text{NaSO}_3)_4$ (3), with Mt = Co, Cu, Fe, Mn and VO, were kindly provided by Dr. T.P.M. Beelen and were synthesized according to an adaptation by Zwart et al.⁴⁵⁾ of the method described by Weber and Busch⁵⁹⁾.

The thiols 2-mercaptoethanol, mercaptoacetic acid, aminoethanethiol and 1-dodecanethiol (all purchased from Fluka) were (vacuum) distilled prior to use, stored in the dark and were kept under nitrogen atmosphere in sealed ampoules.



3 tetrasulphonato-phthalocyaninato-cobalt(II) (CoPc(NaSO₃)₄)

All other materials used were of analytical purity and were used without further purification. During all experiments doubly distilled water was used.

3.2 Apparatus and techniques

3.2.1 Visible light spectroscopy

Spectroscopic measurements were performed with a Hewlett Packard 8451A Diode Array Spectrophotometer, equipped with a high intensity deuterium lamp; 1.000 cm quartz cuvettes were used, thermostatted at 25.0 ± 0.5 °C unless otherwise stated.

Whenever it was necessary, the measured phthalocyanine absorbances were corrected for absorption by ionenes.

From the absorbance values, apparent absorptivities ($\epsilon_{\lambda}^{\text{app}}$) were calculated according to

$$\epsilon_{\lambda}^{\text{app}} = \text{absorbance at } \lambda \text{ nm}/[\text{Co}] \quad (3.1)$$

with [Co] in mol dm⁻³.

3.2.2 Turbidimetry

The turbidity τ was obtained from visible light absorption measurements at 25.0 ± 0.5 °C, using the relationship:

$$\tau = (\log I_0/I)/b \quad (3.2)$$

where I_0 , I = intensity of incident and transmitted light, respectively, and
 b = optical path length in cm.

Measurements were carried out at a wavelength of 800 nm. In the case of the CoPc(NaSO₃)₄/ionene and the congo red/ionene systems, the values were corrected for minor dye absorbance at 800 nm.

3.2.3 Viscometry

Measurements were carried out at 25.00 ± 0.05 °C in a Ubbelohde viscometer. The solutions were filtered before use. All values reported were obtained by averaging the results of at least four repetitive measurements.

Apparent reduced viscosities (η_{red}) are presented, as defined by equation (3.3):

$$\eta_{red} = (\eta - \eta_i)/\eta_i c_i \quad (3.3)$$

with η = viscosity of solution, η_i = viscosity of 10^{-2} mol N⁺ dm⁻³ ionene solution and c_i = ionene concentration of the solution (= 10^{-2} mol N⁺ dm⁻³).

3.2.4 EPR

EPR measurements were performed at liquid nitrogen temperature on a Varian E-15 EPR-spectrometer with E-101 microwave bridge (X-band).

Samples were freed from dioxygen by degassing on a vacuum line (freeze-pump-thaw method). Concentrations of CoPc(NaSO₃)₄ were in the range of 2

10^{-4} to $5 \cdot 10^{-3}$ mol dm⁻³, of ionene around $0.1 \text{ mol N}^+ \text{ dm}^{-3}$.

3.2.5 Surface tension

In order to study the soap-like character of 2,10-ionene, surface tension was measured as a function of ionene concentration, using a Krüss Tensiometer K10T. The apparatus was thermostatted at 20.0 ± 0.1 °C, and equilibration times of at least 24 hours were allowed.

3.2.6 Catalytic activity measurements

Thiol oxidations were carried out in an all-glass double-walled Warburg apparatus, equipped with a powerful mechanical glass stirrer and thermostatted at 25.0 ± 0.5 °C. The total pressure was maintained at 0.1 MPa. The reaction volume was always 0.1 dm³. The stirring speed was 2600 rpm (at which no diffusion limitation occurs for the catalytic system under study, see chapter 8) unless stated otherwise. Reaction rate was measured by monitoring the dioxygen uptake rate with a digital mass flow controller (Inacom, Veenendaal), keeping the pressure (and thus the dioxygen concentration in the solution) constant. Mass flow controllers with capacities of 10 (only for slow reactions, especially with 2,10-ionene, section 5.3), 25 and 50 ml O₂/min were used. During reaction, the pH was measured with a pHM 62 pH meter equipped with a GK 2401B pH electrode (Radiometer, Copenhagen).

The polymer catalyst was prepared by mixing solutions of the appropriate amounts of ionene and CoPc(NaSO₃)₄. The cobalt concentration was varied between $1 \cdot 10^{-7}$ and $5 \cdot 10^{-6}$ mol dm⁻³ in such a way that the dioxygen uptake rate was kept within measuring range. To obtain the desired pH, either a few drops of concentrated NaOH solution were added (section 5.3, chapter 8) or a buffer was applied (chapters 6 and 7).

The following buffer compounds were used: TRIS (tris(hydroxymethyl)-aminomethane, pH 7.9 - 8.85), sodiumtetraborate (pH 9.5), carbonate (pH 10.5), phosphate (pH 11.5 and 12.3) and hydroxide (pH 13). The ionic strength of all

buffers was 0.1 mol dm^{-3} , achieved by dissolving the appropriate amounts of buffer components. No other salts were added, in order to obtain maximum buffer capacities. For the buffers of pH 10.5 and 11.5, buffer capacities were still found to be insufficient. Therefore, the results presented for these pH-values are somewhat less reliable.

The $\text{CoPc}(\text{NaSO}_3)_4$ /ionene mixture was degassed twice. The vessel was filled with nitrogen gas between evacuations. When the desired dioxygen partial pressure was lower than atmospheric, a dioxygen-nitrogen gas mixture was supplied to a total pressure of 0.1 MPa. The solution was saturated with the gas mixture for 5 minutes while stirring vigorously. Unless stated otherwise, dioxygen pressure was kept at 0.1 MPa.

In the case of 2-mercaptoethanol oxidations, reactions were started by the addition of the thiol (by means of a syringe) to the dioxygen-saturated catalyst mixture (containing ionene, cobalt complex and NaOH or buffer). When using 1-dodecanethiol as a substrate, it appeared to be more suitable to start reactions by injection of a concentrated $\text{CoPc}(\text{NaSO}_3)_4$ solution into the reactor containing an dioxygen-saturated mixture of ionene, thiol and NaOH (see chapter 8).

The addition of either thiol or catalyst solution to the closed reaction vessel, leads to an increase in gas pressure. Therefore, detection of dioxygen consumption can only start after a volume of dioxygen is consumed that equals the injected volume of liquid. Thus, only apparent initial reaction rates could be obtained, from the maximum observed uptake rates. Corrections were made for the (minor) amounts of thiol converted at $t = t_{\text{max}}$ (see Fig. 3.1). Since at these low conversions the amounts of accumulated H_2O_2 were still negligible, no corrections were made for the formation of this by-product and the stoichiometry of the reaction was taken to be 4:1 ($\text{RSH} : \text{O}_2$). Rates were expressed in mol converted thiol per second per mol Co, because previously³⁹, first order kinetics in Co had been demonstrated.

Prior to a subsequent experiment, the reactor was washed with water

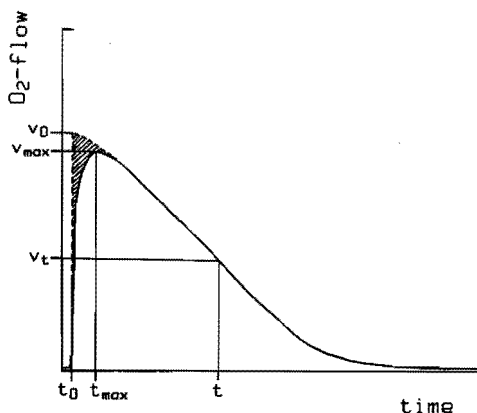


Fig. 3.1 Schematic representation of dioxygen uptake rate curves; experimental (—) and theoretical (---) curves (see text).

containing a soap solution (Hellma, Baden) while stirring for 5–10 minutes. In this way, catalyst components adsorbed to the glass wall of the vessel were dissolved and could be washed out.

3.2.7 Kinetic measurements of the reaction of $H_2O_2 + RSH$

The kinetics of the conversion of thiol by hydrogen peroxide was determined by investigating the absorbance increase at 280 nm with time (due to disulfide formation) in dependence of thiol and hydrogen peroxide concentrations.

Reactions were carried out under nitrogen atmosphere at pH 8, 8.3, 8.85 and 9, using TRIS-buffers with an ionic strength of 0.1 mol dm^{-3} .

3.2.8 H_2O_2 -accumulation measurements

During several catalytic oxidation experiments, H_2O_2 accumulation was determined as a function of time. Samples of 0.5 ml were taken from the reaction vessel by means of a syringe that contained 0.5 ml HCl (3 mol dm^{-3}) in order to quench further reactions (see section 6.2). The H_2O_2 content of the samples was measured spectrophotometrically using $TiCl_3-H_2O_2$ as

reagent⁶⁰).

H₂O₂ contents of reaction mixtures after complete thiol conversion were determined either by the spectrophotometric method or by iodometric titration (both methods were in good agreement).

3.2.9 Stopped-flow measurements

The stopped-flow measurements were carried out according to the method reported by Balt and Meuldijk⁶¹). The author is indebted to Prof. dr. S. Balt for providing the opportunity to use the stopped-flow apparatus.

3.3 Calculation methods

3.3.1 Calculation of dioxygen and thiolate anion concentrations

Concentrations of dissolved dioxygen were calculated according to Henry's law from the partial pressure of dioxygen, in combination with the solubility of dioxygen in 0.125 mol dm⁻³ NaCl⁶²) (0.0011 mol dm⁻³ at 1 atm. O₂).

Thiolate anion concentrations were calculated from thiol concentrations, applied pH and thiol-pK_a values at 0.1 mol dm⁻³ ionic strength. These pK_a values were obtained from the pK_a at zero ionic strength⁶³) and the Debye-Hückel equation⁶⁴) and were found to be: 8.2 for aminoethanethiol, 9.3 for 2-mercaptoethanol, 10.2 for mercaptoacetic acid (SH-group) and 8.2 for cysteine (SH-group).

3.3.2 Kinetics of the reaction of H₂O₂ + RSH

The obtained absorbance versus time curves were analyzed by means of the computer program FORK (First Order Reaction Kinetics), a modified version of the non-linear least squares program LSG of Detar⁶⁵).

When an (at least 10-fold) excess of thiol was used, the order in hydrogen peroxide could be determined. Its value appeared to be equal to 1, the data fitting very well the equation

$$- d[\text{H}_2\text{O}_2]/dt = k' [\text{H}_2\text{O}_2] \quad (3.4)$$

Using various excess concentrations of RS^- , a set of k' -values was obtained, yielding the actual rate constant k according to

$$k' = k [\text{RS}^-] \quad (3.5)$$

Analogously, k was determined by using various excess concentrations of H_2O_2 .

3.3.3 Simulation procedure

H_2O_2 -accumulation curves and oxygen uptake rate profiles were calculated numerically on the basis of equations (3.6) to (3.8), derived from scheme 6.2:

$$d[\text{H}_2\text{O}_2]/dt = v_f - v_d \quad (3.6)$$

$$d[\text{RSH}]/dt = -2(v_f + v_d) \quad (3.7)$$

$$d[\text{O}_2]/dt = -v_f \quad (3.8)$$

where v_f and v_d are calculated according to equations (6.2) and (6.6) (see sections 6.2 and 6.3). Numeric integration was carried out over time steps of typically 2 s (≤ 2.5 % of total reaction time).

3.3.4 Fit procedure (determination of 2-substrate Michaelis-Menten parameters)

Initial rates in dependence of $[\text{RS}^-]_0$ and $[\text{O}_2]$ were fitted to eq. 3.9, using a non-linear least squares procedure, where $\Sigma((v_{\text{calc}} - v_{\text{meas}})/v_{\text{meas}})^2$ was minimized (for explanation of variables: see section 6.2). For each set of data, matrices of v_{calc} as a function of kinetic parameters were calculated,

$$v_f = d[\text{P}]/dt = \frac{C_1[\text{Co}]_{\text{tot}}}{1 + C_2/[\text{S}_2] + C_3/[\text{S}_1] + C_2C_4/[\text{S}_1][\text{S}_2]} \quad (3.9)$$

the values of C_1 to C_4 being varied over a wide range.

With the knowledge on H_2O_2 accumulation, discussed in section 6.2, it was possible to analyze complete dioxygen uptake rate curves kinetically, deriving pairs of $[RS^-]_t$ and uptake rate at time t (see Fig. 3.1), where $[RS^-]_t$ was corrected for the amount of accumulated H_2O_2 . In order to test the reliability of this method, the effect of small variations in $[H_2O_2]_t$ (and thus $[RS^-]_t$) was studied. It appeared that, as a result of this, only k_1 was largely affected (see chapter 7).

In general, relative errors in the calculated kinetic parameters were: $k_1 \pm 40\%$; k_{-1} , k_2^{\min} and $K_2^{\min} \pm 30\%$; $k_3 \pm 10\%$.

4.1 Polyelectrolyte-type ionenes

4.1.1 Salt/polysalt effects

It is well known that CoPc(NaSO₃)₄ in neutral aqueous solution exhibits two absorption maxima in the visible region, due to partial dimerisation⁶⁶⁻⁶⁸ according to



with dimerisation constant $K_D = [D]/[M]^2$.

The dimeric complex D, presumably formed by overlap of the extended π -electron systems, shows a maximum at 628 nm, whereas the monomer M has its maximum at 662 nm. Formation of dioxygen-bridged dimers⁶⁸ ($\lambda_{\max} = 674$ nm) does not occur under these conditions, unless the pH of the solution is raised.

Upon addition of simple salts, like KCl, the absorptivity at 628 nm increases⁶⁸. This means K_D is increased, probably as a result of partial neutralisation (shielding effect) of the repulsive electrostatic forces caused by the anionic sulfonate substituents on the phthalocyanine rings. Larger amounts of salt cause loss of the isosbestic points and a shift of the dimer absorption maximum to lower wavelengths (620-622 nm). This shift is thought to be the result of the formation of polynuclear CoPc(NaSO₃)₄-aggregates, as was demonstrated for the copper analogue by Kratky and Oelschlaeger⁶⁹.

Similar effects should be expected in the case of ionene addition, since ionenes are in fact polysalts. Moreover, charged polymers in general are known to enhance association of oppositely charged dye molecules⁷⁰. Indeed, this behaviour was observed for the CoPc(NaSO₃)₄/ionene system (see Fig. 4.1). Even

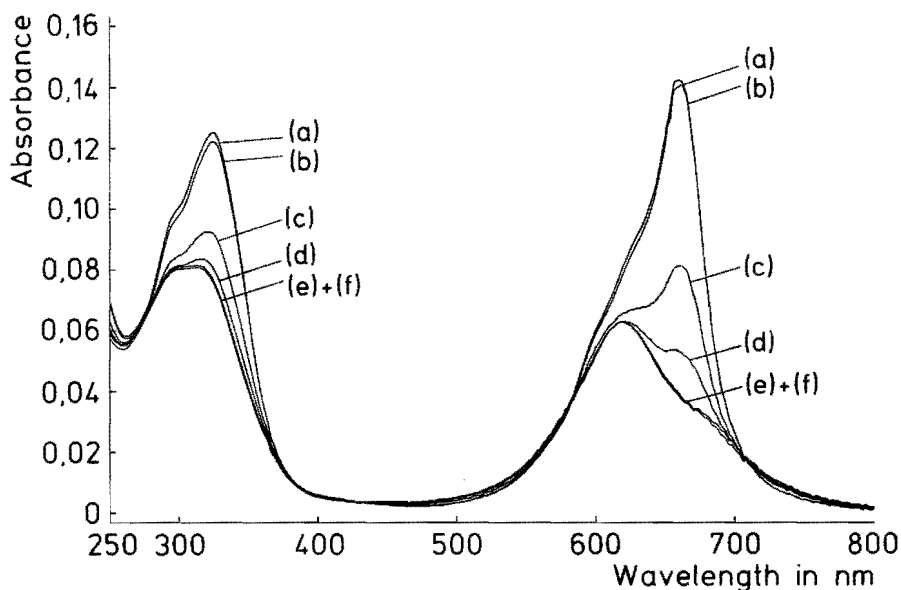


Fig. 4.1 Spectra of neutral aqueous solutions of $\text{CoPc}(\text{NaSO}_3)_4$ ($2 \cdot 10^{-6} \text{ mol dm}^{-3}$) in the presence of various amounts of 2,4-ionene ($M_n = 22000$).
 (a) $N^+/\text{Co} = 0$, (b) $N^+/\text{Co} = 0.1$, (c) $N^+/\text{Co} = 3$, (d) $N^+/\text{Co} = 4$, (e) $N^+/\text{Co} = 5$, (f) $N^+/\text{Co} = 100$.

a very dilute ionene solution (10^{-5} M in N^+ , 10^{-6} M in Co) showed the spectrum typical of phthalocyanine aggregates. The fact that no EPR-signal could be obtained, confirmed the absence of monomeric species. On these grounds it was concluded that ionenes strongly enhance the $\text{CoPc}(\text{NaSO}_3)_4$ aggregation process.

4.1.2 Effects of varying the N^+/Co -ratio; 2,4-ionene system

In order to obtain more detailed information about the effects of ionenes on the cobalt complex structure, visible light spectroscopic measurements were carried out over a wide range of N^+/Co -ratios. The results for 2,4-ionene ($M_n = 22000$) are given in Figures 4.1 and 4.2. Analogous measurements, performed with NaBr instead of ionene, led to the results shown in Fig. 4.3. The essential features of the figures are discussed below.

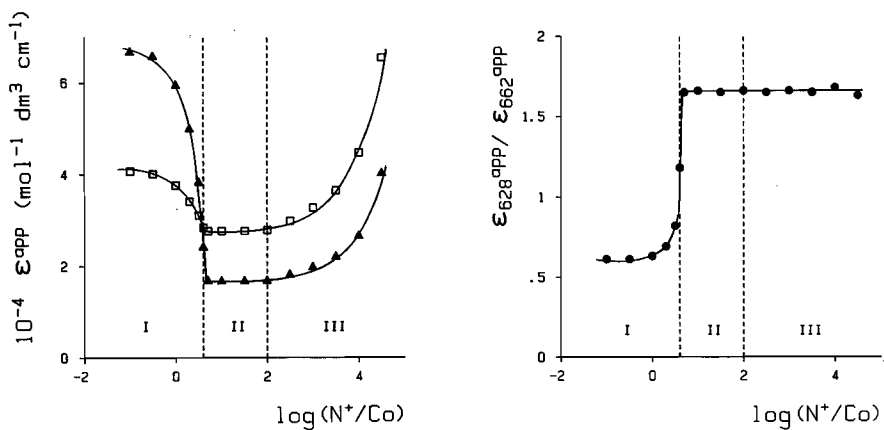


Fig. 4.2 a. Dependence of the apparent absorptivities at 628 nm (\square) and 662 nm (\blacktriangle) on the N^+/Co -ratio.

b. $\epsilon_{628}^{app} / \epsilon_{662}^{app}$ as a function of the N^+/Co -ratio.

[Co] was kept constant at $2 \cdot 10^{-6}$ mol dm⁻³, the ionene used was 2,4-ionene ($M_n = 22000$).

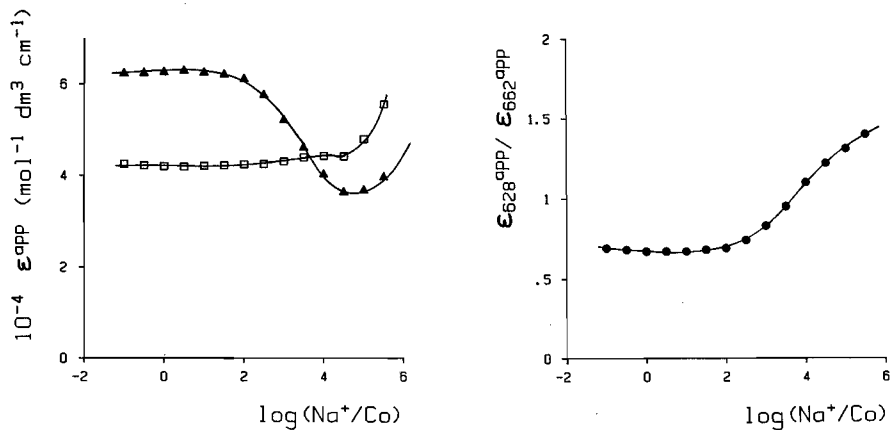


Fig. 4.3 Effect of varying the Na^+/Co -ratio for (a) the apparent absorp-

tivities at 628 nm (\square) and 662 nm (\blacktriangle) and (b) $\epsilon_{628}^{app} / \epsilon_{662}^{app}$.

[Co] was kept constant at $2 \cdot 10^{-6}$ mol dm⁻³.

Looking at Fig. 4.2, three regions can be distinguished: one where $N^+/Co < 4$ (I), one where $N^+/Co > 100$ (III) and the intermediate region (II). In region I, as N^+/Co increases from 0 to 4, it appears that $\epsilon_{628}^{app}/\epsilon_{662}^{app}$, which is a measure of the relative amount of aggregated cobalt species, gradually increases. This is obviously due to dimerisation (oligomerisation), as described in the previous section. Simultaneously, both ϵ_{628}^{app} and ϵ_{662}^{app} are gradually decreasing, probably as a result of strong interaction of $CoPc(SO_3)_4^{4-}$ with the highly positively charged ionene, thus lowering the molar absorptivities of both M and D.

At $N^+/Co = 4$ a discontinuity appears in the ϵ_{628}^{app} -, the ϵ_{662}^{app} - and the $\epsilon_{628}^{app}/\epsilon_{662}^{app}$ -plots. Beyond this point, up to $N^+/Co = \text{approx. } 100$ (region II), all three quantities remain constant. This strongly suggests the formation of an ionene/ $CoPc(NaSO_3)_4$ complex with fixed stoichiometry (4:1). Adding more ionene only appears to result in an increase of the concentration of cobalt-free ionene without the existing complex being affected.

When NaBr was used instead of ionene (Fig. 4.3), the plots of the apparent absorptivities versus the Na^+/Co -ratio did not show any discontinuity associated with the formation of strongly interacting complexes. The only effects observed were increasing aggregation of the cobalt complex due to increasing salt concentration and, at very high concentration, coordination of bromide ions (see below).

The fixed stoichiometry of 4:1 was found to hold for 2,4-ionenes with $M_n > 6100$. Samples with lower molecular mass that were also investigated, gave rise to lower values, down to 2:1 for $M_n = 1800$, presumably as a result of loss of coil structure for the small oligomer chains. Thus, it is clear that there is a strong tendency toward 4:1 N^+/Co complexation, provided the ionenes contain a sufficient number of ammonium groups.

It should be noted that at a ratio of 4:1 8 positive charges on the ionene are just matching the opposite charge on the dimeric cobalt complex. This suggests that the high electrostatic potential of the polymer plays a

dominant role in the interaction between the polymer and $\text{CoPc}(\text{NaSO}_3)_4$. Assuming this is true, it can be expected that other negatively charged molecules also show a tendency to form strong complexes with ionenes at the ratio where the charges are matching. Therefore, combinations of ionenes with several model compounds were studied, which will be discussed in section 4.2.

Regarding region III, it appears that a large excess of ionene ($\text{N}^+/\text{Co} > 100$) causes the absorptivities to increase again. A possible explanation of this absorptivity enhancement is, that the bromide ions, present as counterions of the ionene, coordinate to the axial positions of the cobalt complex⁷¹). In order to obtain supportive evidence to this hypothesis, the spectral change of a $\text{CoPc}(\text{NaSO}_3)_4$ /ionene solution with $\text{N}^+/\text{Co} = 10$ was measured upon the addition of KBr. Indeed, an absorptivity increase was found, which strongly supports the concept of coordinative interaction (see also Fig. 4.3).

In spite of the bromide coordination however, the cobalt complex remained in the aggregated form, as can be seen from the constancy of $\epsilon_{628}^{\text{app}}/\epsilon_{662}^{\text{app}}$ in region III. This is very surprising, since Co-site isolation was expected to occur due to redistribution of the cobalt complex over the ionene chains in such a way that each chain contains only one complex anion⁵²). However, no evidence of an increased occurrence of the monomeric species was found.

It must be noted, that bromide coordination apparently is possible within the aggregate structure. A possible explanation for this phenomenon is, that the aggregates do not consist of closely spaced, stacked oligomers, but in fact are groups of dimers, as was suggested by Elzing et al.⁷²). The accessibility to ligands of two of the four axial positions of the two cobalt atoms in each dimer, may be important with respect to substrate interaction in the thiol oxidation process (see chapter 5).

4.1.3 Effects of other ionenes

Apart from 2,4-ionene, a wide variety of ionenes was studied in combination with the cobalt catalyst complex. The results obtained were

similar to those presented above, except in the case of polysoap-type ionenes that will be discussed in section 4.3.

Variation of the number of methylene groups between adjacent ammonium groups in the polymer backbone (2,6-, 2,8- or 6,6-ionene), only affected the molar absorptivities of the polymer catalyst complexes, but qualitatively these systems behaved identically: aggregation of the phthalocyanine into poly-nuclear species ($\lambda_{\max} = 620\text{-}622\text{ nm}$) occurred, maximum degree of aggregation was reached at $N^+/Co = 4$ and no monomerization could be observed up to $N^+/Co = 10^5$ ($\epsilon_{628}^{\text{app}}/\epsilon_{662}^{\text{app}}$ constant), just as was found for the 2,4-ionene. The molar absorptivities of both M and D increased with increasing N^+ - N^+ linear distance (decreasing charge density, see Table 4.1). This suggests that the $CoPc(NaSO_3)_4$ /ionene interaction decreases in intensity in this order, as the electronic structure of the cobalt complex is apparently less affected. The $\epsilon_{628}^{\text{app}}/\epsilon_{662}^{\text{app}}$ -ratio (N^+/Co constant) also depended on charge density (Table 4.1). It is interesting to note that for the catalytic activity the same trend was found⁵⁴) (see also chapter 7).

Building aromatic groups into the polymer backbone (2,xyl-ionene) or attaching bulky side groups as in 6,2NØ-ionene, again led to interaction patterns with the catalyst complex analogous to the other investigated

Table 4.1 Effect of varying the type of ionene on spectroscopic parameters^a.

ionene	σ^b	$10^{-4} \epsilon_{628}^{\text{app}}$	$10^{-4} \epsilon_{662}^{\text{app}}$	$\epsilon_{628}^{\text{app}}/\epsilon_{662}^{\text{app}}$
2,4	1.45	2.8	1.7	1.6
2,6	1.15	2.9	2.0	1.4
2,8	0.96	3.4	3.0	1.2
6,6	0.82	4.1	3.5	1.2
2,xyl	1.25	3.0	2.3	1.3
6,2NØ	1.15	3.5	2.7	1.3
NaBr	--	4.2	6.2	0.7

^a $[Co] = 2 \cdot 10^{-6} \text{ mol dm}^{-3}$, $N^+/Co = 4$; $\epsilon_{\lambda}^{\text{app}}$ in $\text{dm}^3 \text{ mol}^{-1} \text{ cm}^{-1}$

^b linear charge density parameter⁵⁴)

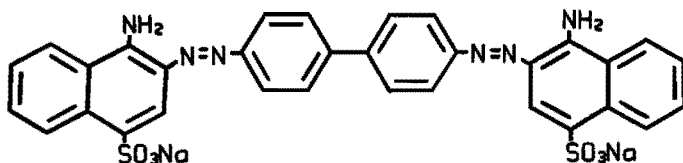
ionenes. Again, aggregation was induced, stoichiometric complexation occurred at $N^+/Co = 4$ and no site isolation was observed up to $N^+/Co = 10^4$. However, these ionenes showed spectra with $\lambda_{max} = 628$ nm, indicating only dimers are formed and no higher aggregates. In case of 6,2NØ-ionene, this is obviously the result of the bulky side groups, preventing interaction between individual dimers. Apparently, the same effect can be attained by the presence of xylyl-groups in the polymer backbone. Presumably, these chain-"stiffening" groups cause a too large separation between the dimers: the $N^+ - N^+$ distance along xylyl segments is about 8 Å, whereas the phthalocyanine ring-to-ring distance in aggregates is probably about 4 Å (3.4 Å in solid CoPc⁷³). The importance of this effect with respect to catalytic activities will be discussed in chapter 7.

4.2 Comparison with model compounds

4.2.1 Spectrophotometry

From the spectroscopic investigations described in section 4.1, it was concluded that ionenes strongly enhance the aggregation of CoPc(NaSO₃)₄. It was found that the same is true for other phthalocyanines, viz. copper, manganese, iron(II) and vanadyl phthalocyanine-tetrasodiumsulfonates. In all these cases, addition of ionene caused a shift of the Q-band (600 - 700 nm) absorptions to shorter wavelengths, indicating a decrease in the amount of monomer complex present and an increase in dimer (aggregate) content. Therefore, it can be stated that ionenes enhance phthalocyanine aggregation independent of the central metal ion.

In order to find out if ionenes generally induce aggregation of compounds with aggregational ability, ionene was investigated in combination with congo red (CR). This dye is known to associate strongly in aqueous solution⁷⁴ and was therefore expected to behave similar to the cobalt catalyst, although its structure is completely different.



congo red (CR)

In Fig. 4.4 the spectra are shown, recorded for congo red solutions containing different amounts of ionene. It clearly shows, that the addition of ionene to the dye causes a decrease of absorbance over the total wavelength range, which indicates that interaction between polymer and dye takes place. The peak at 498 nm, that is associated with the presence of monomeric dye species, decreases more strongly than the absorption maximum of the dimers

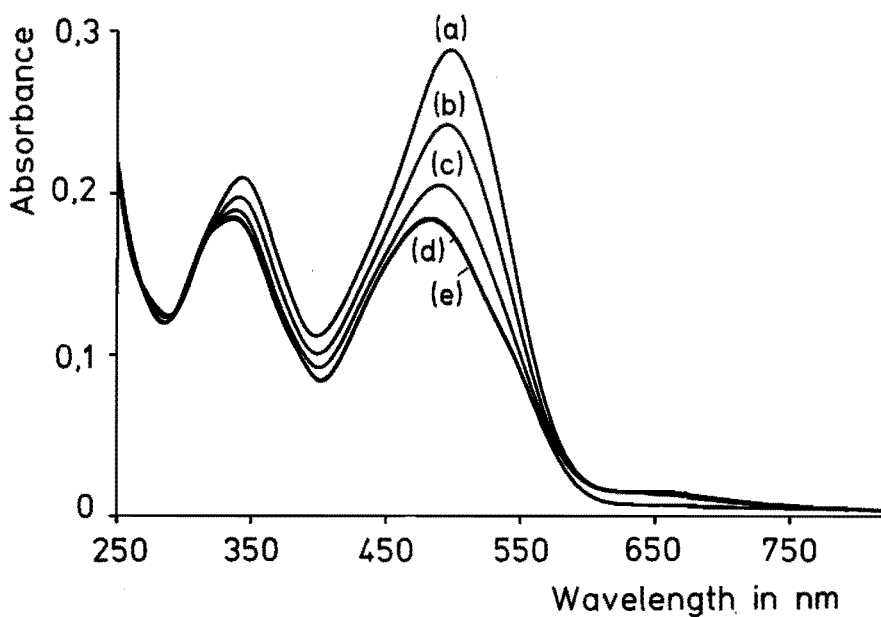


Fig. 4.4 Spectra of congo red (CR)/ionene solutions: $N^+/CR = 0$ (a), 0.5 (b), 1 (c), 2 (d) and 100 (e). [CR] was kept constant at $10^{-5} \text{ mol dm}^{-3}$, pH = 7.

(aggregates) at 344 nm. Thus, again it can be concluded that the ionene enhances aggregate formation.

The congo red spectrum gradually changes upon ionene addition until a ratio of $N^+ : CR = 2:1$ is reached, where the charges on the polyelectrolyte are just matching those on the dye. Further addition of ionene has no effect on the spectrum (Fig. 4.4, lines d and e: the spectrum of the solution with $N^+/CR = 100$ coincides with the one for $N^+/CR = 2$), which strongly indicates the formation of a stoichiometric polymer/dye complex. Completely analogous results have been described for the cobalt catalyst system (section 4.1) and were also found for the other metal phthalocyanines. In these cases complexation occurred at $N^+ : Mt = 4:1$ ($Mt = Co, Cu, Mn, Fe$ and VO), in accordance with the matching charges on the components. Apparently, stoichiometric complexation is not restricted to the catalyst system, but

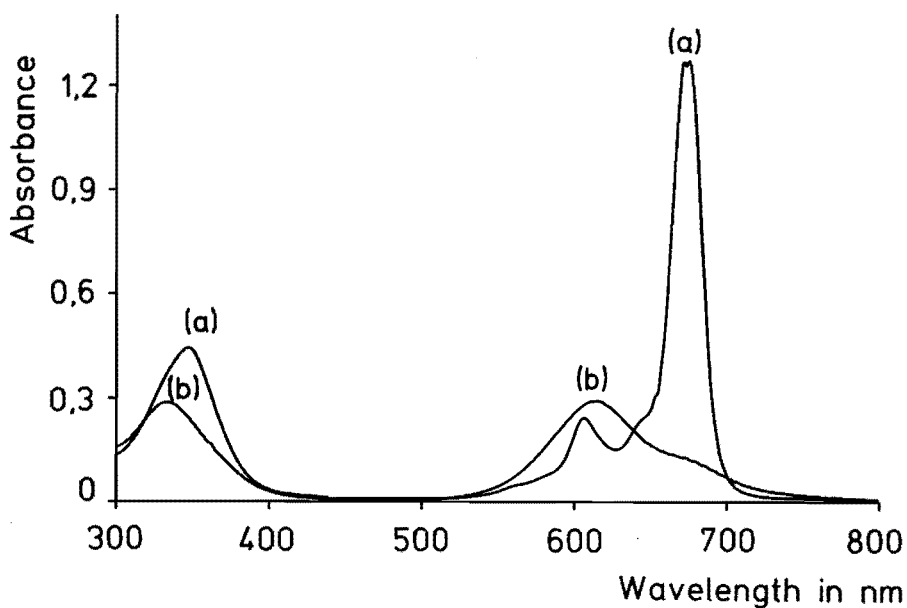


Fig. 4.5 Spectra of $CuPc(NaSO_3)_4$ in 50/50 DMF/water in the absence (a) and in the presence of ionene (b). $[Cu] = 8 \cdot 10^{-6} \text{ mol dm}^{-3}$, $[N^+] = 10^{-2} \text{ mol dm}^{-3}$.

generally occurs when ionene is combined with anionically charged compounds with a propensity to aggregation.

It should be mentioned here that all aggregated complexes appeared to be highly stable. In polymer-free systems the phthalocyanine aggregates are known to dissociate into monomeric species upon addition of e.g. dimethylformamide (DMF)⁷⁵, but when this solvent was added to a solution also containing ionene, the aggregates remained. This effect is illustrated in Fig. 4.5, depicting spectra obtained for CuPc(NaSO₃)₄ in a 50/50 DMF/water mixture, in the absence (a) and presence (b) of 2,4-ionene. Spectrum a shows the characteristics of the purely monomeric complex, spectrum b corresponds with the dimer (aggregate) form.

4.2.2 Turbidimetry

In order to study the role of aggregation in the ionene/dye interaction, it was desired to compare the above-mentioned systems with combinations of ionenes with other anionic species, viz. complexes known not to aggregate in aqueous solution, e.g. Fe(CN)₆^{x-} (x = 3 or 4). Since such compounds can not be studied spectrophotometrically due to low molar absorptivities, a more suitable technique was sought.

Polymer-metal complexes as concerned here, that are primarily based on electrostatic interaction, are often electroneutral. As a consequence, such complexes are usually less soluble in polar solvents like water, resulting in precipitation or formation of colloidal systems. Turbidity measurements can therefore be a powerful tool in tracing this type of complexation, provided that the concentrations of the compounds are chosen within the appropriate range.

Indeed, the formation of the catalyst complex could easily be demonstrated in this way, as can be seen in Fig. 4.6. This figure shows that optimum turbidity is reached at the complexing ratio of N⁺/Co = 4, which is in excellent agreement with the results of the above described experiments.

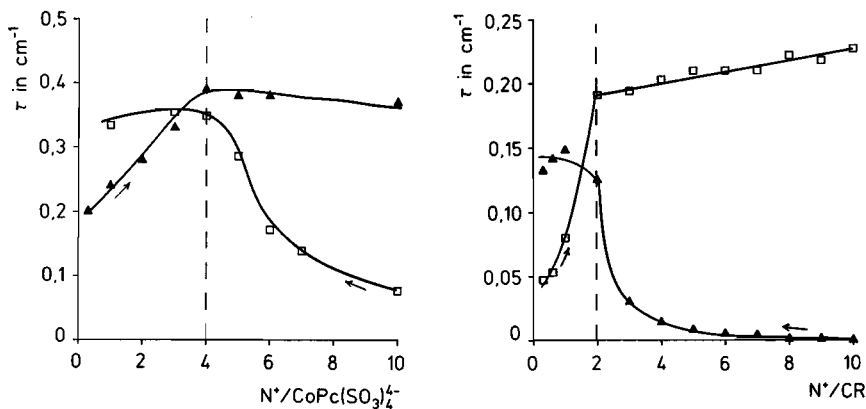


Fig. 4.6 Dependence of turbidity on the $\text{N}^+/\text{CoPc}(\text{SO}_3)_4^{4-}$ -ratio; \square : $[\text{N}^+]$ was kept constant at $10^{-3} \text{ mol dm}^{-3}$, $[\text{Co}]$ was increased; \blacktriangle : $[\text{Co}]$ was kept constant at $2 \cdot 10^{-4} \text{ mol dm}^{-3}$, $[\text{N}^+]$ was increased.

Fig. 4.7 Turbidity versus $\text{N}^+/\text{congo red}(\text{CR})$ -ratio; \square : $[\text{CR}]$ was kept constant at $10^{-3} \text{ mol dm}^{-3}$, $[\text{N}^+]$ was increased; \blacktriangle : $[\text{N}^+]$ was kept constant at $10^{-3} \text{ mol dm}^{-3}$, $[\text{CR}]$ was increased.

Furthermore, it is obvious that the complex is highly stable: once it has been formed, disturbing the stoichiometry by adding either component has no effect on the turbidity, indicating that no resolubilization occurs. This implies that when a solution of the catalyst system is needed, one should mix the components carefully and in the right order, i.e. the compound desired in excess must be taken as the one, to which the other is added dropwise (otherwise a precipitate may be formed irreversibly). Of course, this precaution is not necessary at low concentrations, where the complex is completely soluble.

Analogous results were obtained for the congo red/ionene system, as demonstrated in Fig. 4.7. In this case, the stable complex, that could not be resolubilized either, was formed at a ratio of $\text{N}^+/\text{CR} = 2$, again in accordance with the matching opposite charges.

Finally, the model compounds $\text{Fe}(\text{CN})_6^{x-}$ (with $x = 3$ and 4) were examined turbidimetrically. The results, depicted in Fig. 4.8, indicate that these compounds can also form stoichiometric complexes with ionenes. Also in this case, the charges are matching, since optimum turbidity is observed at $\text{N}^+/\text{Fe}(\text{CN})_6^{x-} = 3$ and 4 for $x = 3$ and 4 , respectively. Nevertheless, an important difference with the dye systems remains: unlike the catalyst and the congo red species, these model complexes resolubilize easily upon addition of either constituent, as appears from the symmetry of the curves. This behaviour unambiguously indicates that these complexes are less stable than those of the dye systems, suggesting a less strong interaction between the $\text{Fe}(\text{CN})_6^{x-}$ anions and the polyelectrolyte.

It is postulated that this difference is a consequence of the fact that the hexacyanoferrates can only be present in their monomeric form, whereas the

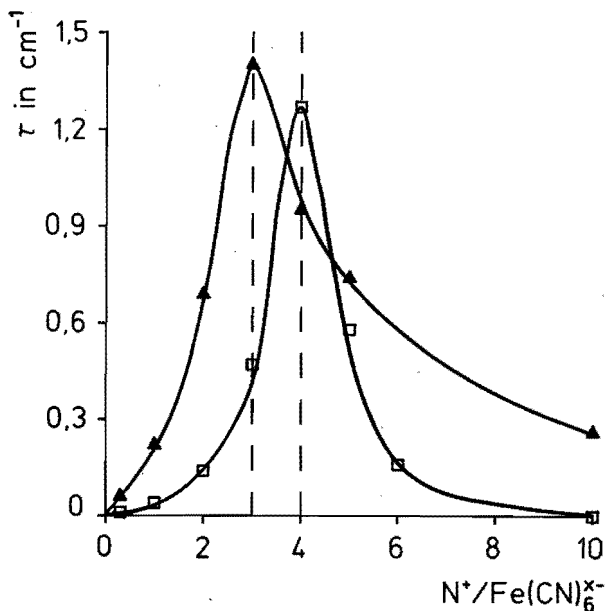


Fig. 4.8 Effect of varying the $\text{N}^+/\text{Fe}(\text{CN})_6^{x-}$ -ratio on the turbidity of the solution; ◻: $x = 4$, ▲: $x = 3$.

$[\text{Fe}(\text{CN})_6^{x-}]$ was kept constant at $10^{-3} \text{ mol dm}^{-3}$, $[\text{N}^+]$ was varied.

dye compounds form dimers and higher aggregates. In the previous section, this aggregation was demonstrated spectrophotometrically and it was shown to be strongly enhanced by the presence of ionene. In turn, turbidimetry shows that aggregate formation enhances the electrostatic interaction between ionene and these anions. Considering reported aggregation numbers of 45 for congo red⁷⁶⁾ and up to 20 for CuPc(NaSO₃)₄⁶⁹⁾ (both in polymer-free, salt containing solutions), implying entities carrying charges of -80 to -90, this interaction enhancement seems plausible. These unusually high charges should indeed lead to very stable complexes. Even the formation of ionomeric "crosslinks" between polymer chains is most likely to occur, which was investigated by viscometric measurements, described below.

4.2.3 Viscometry

Viscometry is a useful technique to study interactions between polymers and additives, like salts or metal complexes, because interactions usually are accompanied by changes in polymer coil dimensions. Therefore, viscometry was applied to the CoPc(SO₃)₄⁴⁻/ionene catalyst system, to obtain additional proof of the proposed complex formation. Furthermore, the ionene was examined in combination with Fe(CN)₆⁴⁻, an entity only interacting electrostatically. This would make it possible to determine whether the catalyst complexation can be completely explained in terms of electrostatic interactions or whether other secondary binding forces are involved. The results are shown in Fig. 4.9.

As can be seen, in both systems the apparent reduced viscosity strongly decreases as the metal complex content is raised. This effect was expected to occur, since the added anions will shield off the positive charges on the polymer chains, resulting in contraction of the polymer coils. A similar effect was mentioned by Brouwer et al.⁷⁷⁾, who studied analogous systems with poly(vinylamine) instead of ionene.

In their experiments, the results for the model compound Fe(CN)₆⁴⁻ practically coincided with those obtained for the catalyst, indicating similar

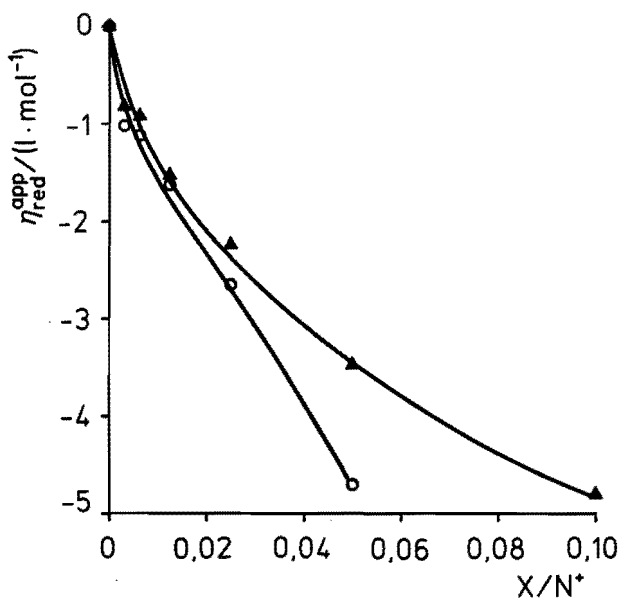


Fig. 4.9 Apparent reduced viscosity as a function of metal complex/ionene-ratio (X/N^+), with $X = Fe(CN)_6^{4-}$ (\blacktriangle) and $X = CoPc(SO_3)_4^{4-}$ (\circ). $[N^+] = 10^{-2} \text{ mol dm}^{-3}$, temp. = $25.00 \pm 0.05 \text{ }^\circ\text{C}$.

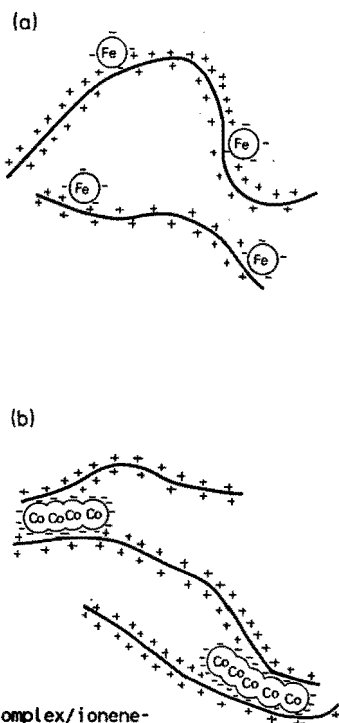


Fig. 4.10 Schematic representation of proposed interaction structures of $Fe(CN)_6^{4-}$ /ionene (a) and $CoPc(SO_3)_4^{4-}$ /ionene (b) complexes.

interactions between each of the two metal complexes and the polymer (PVAm).

However, the measurements of the ionene system discussed here, reveal that $CoPc(SO_3)_4^{4-}$ gives rise to a much stronger viscosity decrease than $Fe(CN)_6^{4-}$, especially for $Co/N^+ > 0.02$. According to Brouwer⁷⁷, such an additional viscosity decrease can be explained by assuming the occurrence of intra- or intermolecular chelate formation. Since ionenes contain no groups allowing coordinative interaction, this chelation should, in the present case, be interpreted as the formation of ionomeric "crosslinks" between the cationic polymer chains by means of bridging cobalt complex anions. Such an effect

becomes even more likely, when considering the aggregation of the phthalocyanine, leading to entities that carry multiple negative charges, thus facilitating this type of "crosslinking". Because the hexacyanoferrate does not show aggregation, interchain interactions are expected to occur much less in that case. On these grounds, interaction structures are proposed as schematically given in Fig. 4.10. Non-aggregating compounds are believed to exhibit predominantly intrachain or reversible interchain interactions with ionene (Fig. 4.10a), whereas systems containing the catalyst or congo red may show also irreversible interchain interactions ("crosslinks") (b).

In the previous sections, it has been demonstrated that optimum $\text{CoPc}(\text{NaSO}_3)_4$ /ionene complexation, occurring at $\text{Co}/\text{N}^+ = 0.25$, is accompanied by maximum aggregation. Thus, the viscosity should decrease upon addition of $\text{CoPc}(\text{NaSO}_3)_4$ until this ratio is reached and should then remain constant. Unfortunately, this interesting experiment, that might once more verify the concept of stoichiometric interaction, could not be carried out, because some precipitation of the complex occurred at the concentrations needed (i.e. $[\text{Co}] \geq 10^{-3}$ mol/l and $[\text{N}^+] = 10^{-2}$ mol/l).

4.3 Polysoap-type ionenes

4.3.1 Ionene-induced deaggregation of $\text{CoPc}(\text{NaSO}_3)_4$

From the preceding sections, it can be concluded that a wide variety of ionenes has a propensity to promote dimerization rather than to isolate the monomeric cobalt species, since even at $\text{N}^+/\text{Co} = 10^5$ no monomers can be detected.

However, 2,10-, 2,12- and 3,3 C_{12} -ionene do show a site isolation effect at high N^+/Co -ratios. This effect is illustrated in Fig. 4.11 for 2,10-ionene. It clearly demonstrates that at low ionene concentrations aggregation is enhanced analogously to the other ionene systems, but with a large excess of

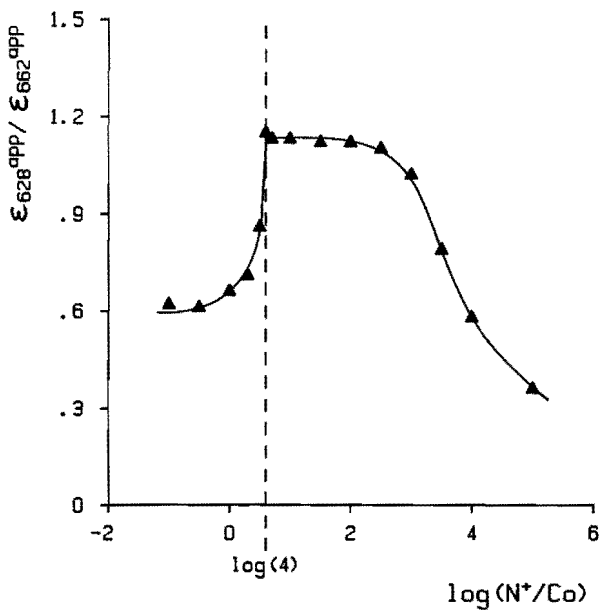


Fig. 4.11 Ratio of absorbances at 628 and 662 nm as a function of the N^+/Co -ratio for 2,10-ionene. Aqueous solutions, $[Co] = 2 \cdot 10^{-6} \text{ mol dm}^{-3}$.

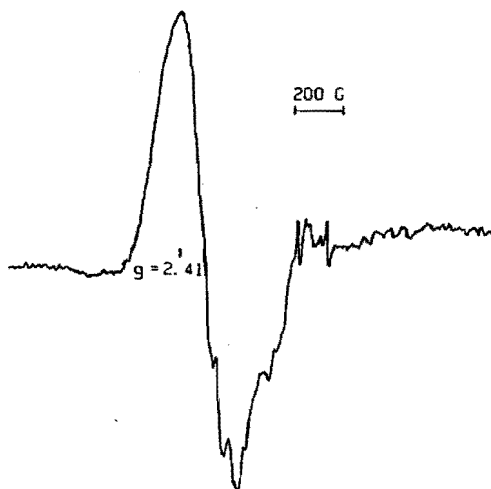


Fig. 4.12 ESR-spectrum of monomeric $Co(II)Pc(NaSO_3)_4$ as stabilized by 2,10-ionene. $[Co] = 10^{-3} \text{ mol dm}^{-3}$, $[N^+] = 0.15 \text{ mol dm}^{-3}$, liquid N_2 temp.

2,10-ionene ($N^+/Co \geq 10^3$) the equilibrium is shifted back to the monomer side, as can be concluded from the decrease of A_{628}/A_{662} . At $N^+/Co = 10^5$, the monomer concentration is even higher than it was at the same cobalt concentration without any ionene present. The presence of the monomeric complex could also be demonstrated by EPR spectroscopy (see Fig. 4.12).

It must be noted that the distinct behaviour of 2,10- and 2,12-ionene, as compared with the other ionenes studied, can not be explained by the difference in charge densities: although 6,6-ionene has the same average charge density as 2,10-ionene, it does not show any site isolation effect in the investigated concentration range. Apparently, the effect of site isolation is due to some other property of the 2,10- and 2,12-ionenes; most probably the hydrophobic character⁷⁸⁾ of the C_{10} - and C_{12} -chain segments plays a role. Characterization of this hydrophobicity will be discussed in section 4.3.2.

Hydrophobic effects may also underlie another phenomenon observed. At a constant N^+/Co -ratio of 2000, dilution of the catalyst solution caused an increase in the relative amount of dimeric complex: the absorptivity at 628 nm increased while at 662 nm it decreased; for example, at $[N^+] = 8 \cdot 10^{-2}$ M $A_{628}/A_{662} = 0.70$ whereas at $[N^+] = 5 \cdot 10^{-3}$ M this ratio was found to be 0.93. Thus, in this respect the system behaves opposite to the polymer-free system. The same behaviour was found for 2,12- and 3,3 C_{12} -ionene.

This effect is looked upon as an indication of the existence of micelle-like structures inducing the monomerisation^{79,80)} of the phthalocyanine. Upon dilution (at constant N^+/Co) the micelles will be broken down resulting in a molecular solution that will behave more like the other (hydrophilic) ionene-systems. Therefore, further diluting a 2,10-ionene solution at low $[N^+]$ level should lead to identical results as were obtained for the polyelectrolyte-type ionenes. Indeed, in these cases, no change of absorptivity with polymer concentration was observed, indicating a constant degree of aggregation. The constancy of absorptivity at 628 nm for 6,6-ionene and for 2,10-ionene at $N^+/Co = 10$ (low $[N^+]$, i.e. no micellar structures) is presented in Fig. 4.13.

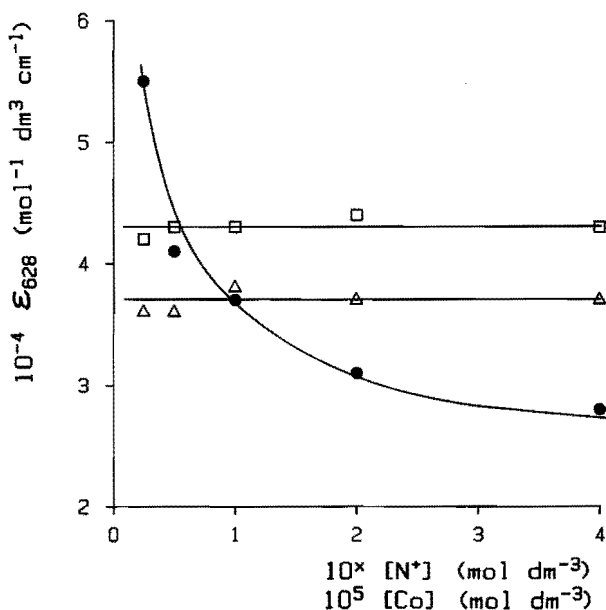


Fig. 4.13 Dependence of the absorptivity at 628 nm on the catalyst concentration. Aqueous solutions of (□): 6,6-ionene, $N^+/Co = 1000$, $x = 2$; (●): 2,10-ionene, $N^+/Co = 1000$, $x = 2$; (△): 2,10-ionene, $N^+/Co = 10$, $x = 4$.

By comparison, the changing absorptivity for the 2,10-ionene at $N^+/Co = 1000$ (high $[N^+]$, i.e. micellar structures) is shown in the same figure.

4.3.2 Characterization of 2,10-ionene hydrophobicity

Three of the investigated ionenes, viz. 2,10-, 2,12- and 3,3C₁₂-ionene, were found to exhibit soap-like behaviour (foam formation, monomerization^{79,80}) of the CoPc(NaSO₃)₄ complex (see section 4.3.1)), deviating from the behaviour of the polyelectrolyte-type ionenes described in the preceding sections. For 3,3C₁₂-ionene this was expected on the basis of ref.⁸¹). However, according to literature⁷⁸), for x,y-ionenes a minimum number of 14 methyl groups between adjacent ammonium groups is required to obtain a polysoap. Therefore, the behaviour of 2,10- and 2,12-ionene was rather unexpected and the soap-like

character of 2,10-ionene was further investigated, in particular in order to determine if it can be described in terms of a critical micelle concentration (cmc).

A usual method to determine the cmc, is measuring the surface tension of solutions containing varying amounts of the soap. The results of this method, applied to the 2,10-ionene system, are depicted in Fig. 4.14. It clearly shows that, indeed, micelles or similar associate structures are formed and the cmc appears to be about $0.06 \text{ mol dm}^{-3} \text{ N}^+$: the surface tension gradually decreases until $[\text{N}^+] \approx 0.06 \text{ mol dm}^{-3}$, after which it remains constant.

This cmc value was confirmed by another, independent, method, in which the shift of λ_{max} (δ_{MO}) in the spectrum of the dye compound methyl orange (MO) was measured as a function of 2,10-ionene concentration. It is known⁸²⁾ that λ_{max} of this dye strongly depends on the local polarity of the solvent and

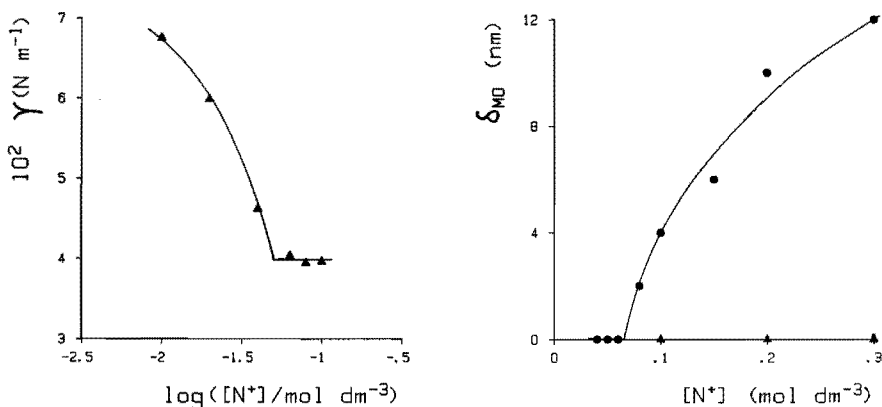


Fig. 4.14 Surface tension, γ , in dependence of 2,10-ionene concentration in aqueous solution; temp. = 20.0 °C.

Fig. 4.15 Blue shift of λ_{max} for methylorange (MO) as a function of the concentration of 2,10-ionene (●) and 2,4-ionene (▲) in aqueous solution; $[\text{MO}] = 3 \cdot 10^{-5} \text{ mol dm}^{-3}$, temp. = 25.0 °C, λ_{max} (without ionene) = 468 nm.

that MO dissolves preferably in an apolar environment. This phenomenon also takes place in 2,10-ionene solutions, as is illustrated in Fig. 4.15, revealing that for $[N^+] \geq 0.08 \text{ mol dm}^{-3}$ the 2,10-ionene creates a micellar (apolar) environment for the dye (δ_{MO} increases). For comparison, the results of the same experiment with 2,4-ionene are included in the figure as well. Obviously, in that experiment no shift and thus no micellization could be observed.

Thus, it can be concluded from both cmc determination methods, that 2,10-ionene indeed acts soap-like, having a cmc of $0.07 \pm 0.01 \text{ mol dm}^{-3}$, which agrees very well with the value reported for its monomeric analogue, decyltrimethylammoniumbromide⁸³).

With respect to the catalytic experiments with 2,10-ionene (see chapter 5), it must be noted that usually ionene-concentrations are used ($[N^+] = 10^{-3} \text{ mol dm}^{-3}$) far below the above-mentioned cmc. However, under catalytic reaction conditions the cmc may well be lower, due to the presence of e.g. the catalyst complex, thiolate anions and buffer components. In fact, it was established by surface tension measurements, that the cmc is lowered to $0.01 \text{ mol dm}^{-3} N^+$ when $2 \cdot 10^{-5} \text{ mol dm}^{-3} \text{ CoPc}(\text{NaSO}_3)_4$ is added to the 2,10-ionene.

4.4 Conclusions

From the previous sections, the following conclusions may be drawn. Turbidimetric and spectrophotometric investigations revealed that ionenes can form complexes with negatively charged compounds. The stoichiometry of these complexes corresponds to the ratio at which positive and negative charges are just matching. Thus, it can be concluded that complexation is achieved by electrostatic interaction.

However, to stabilize the complexes, some additional binding forces appear to be needed. In ionene/dye systems, e.g. containing phthalocyanine or congo red, these forces appear to be intermolecular interactions between dye molecules by π -overlap, resulting in aggregated species. Aggregation was

spectrophotometrically shown to be enhanced by polyelectrolyte-type ionenes. It involves concentration of negative charges (increase of charge density), thus leading to a stronger interaction with the ionene. Viscometric results even suggested the formation of ionomeric "crosslinks" in the ionenes, as a consequence of this aggregation effect.

Polysoap-type ionenes, like 2,10-, 2,12- and 3,3C₁₂-ionene, were observed to have the ability to monomerize the CoPc(NaSO₃)₄ complex due to the formation of micelle-like structures. Since presumably the degree of aggregation of the catalyst complex has a large influence on its reactivity, both ionene types had to be further investigated. First, the effects of substrates on the monomeric or aggregated structures were studied, the results of which are presented in chapter 5.

5.1 Interaction of O_2 with the catalyst

Both for the polymer-free⁴⁵⁾ as well as for the PVAm-bound⁵²⁾ catalyst it has been argued that the formation of dioxygen-bridged $\text{CoPc}(\text{NaSO}_3)_4$ dimers, induced by alkali addition, inactivates the catalyst. Therefore, it was assumed that an important function of the polymer would be the cobalt site isolation. For polysoap-type ionenes like 2,10-ionene, this was indeed found to be the case, as was discussed in section 4.3.1. In accordance with this

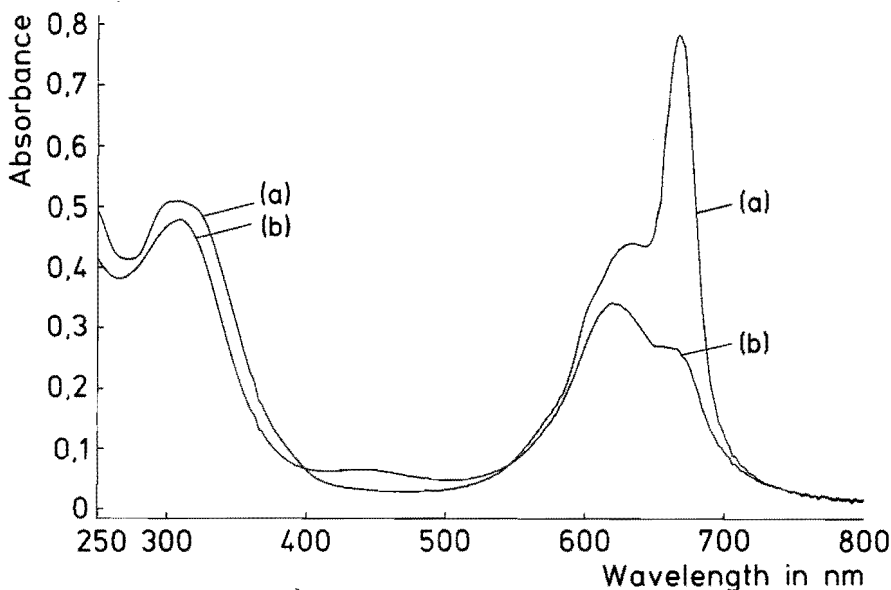


Fig. 5.1 Spectra of $10^{-5} \text{ mol dm}^{-3}$ $\text{CoPc}(\text{NaSO}_3)_4$ -solutions at $\text{pH} = 12.5$ under dioxygen atmosphere; (a) without additives, (b) in the presence of 2,4-ionene, $[\text{N}^+] = 10^{-3} \text{ mol dm}^{-3}$.

monomerization, upon admittance of O₂ (at high pH) no μ -peroxo adduct was observed to be formed, but only the spectrum of the (probably Co(III)-) monomeric complex was obtained, having maximum absorbance at 664-666 nm (λ_{max} of the dimeric adduct is 672-674 nm).

From the foregoing chapter, however, it is evident that in the case of CoPc(NaSO₃)₄ combined with polyelectrolyte-type ionenes, like 2,4-ionene, no site isolation occurs, at least not under normal reaction conditions (usually [Co] = 2 · 10⁻⁷ mol dm⁻³ and [N⁺] = 10⁻³ mol dm⁻³). Nevertheless, as was established spectrophotometrically (Figure 5.1), formation of the dioxygen adduct appears to be suppressed by these ionenes. Only in very basic solutions (pH \geq 13) the corresponding absorbance maximum at 672 nm was observed, but even then the adduct could easily be removed from the solution by bubbling through nitrogen for about 15 min.

Substantially different results were obtained in the absence of ionenes, using simple salts instead. In that case, even in a solution at pH 11 the dioxygen adduct was found to be formed and in addition the adduct appeared to be much more stable (at pH = 13, after 2 hours of bubbling through nitrogen, the peak at 672 nm had still not completely disappeared)⁸⁴). Since it was observed that simple salts do not give rise to stoichiometric complexation with the phthalocyanine, whereas ionenes do, it seems likely that the difference in behaviour toward dioxygen reflects the difference in interaction with the cobalt complex. Presumably, the stronger interaction of ionenes with CoPc(NaSO₃)₄ makes dioxygen adduct formation unfavourable.

This seems to be in contradiction with the very high thiol oxidation activities reported for the ionene systems⁵⁴) (with turnover numbers of approx. 3000 s⁻¹), since obviously dioxygen is needed during the catalytic cycle. However, both facts still can be in agreement, provided that the redox reaction step involving dioxygen, takes place by a so-called outersphere mechanism. Such a mechanism, viz. oxidation of the cobalt centre mediated by the abstraction of an electron from the phthalocyanine ring and thus without

direct metal-oxidant interaction, was recently suggested by Geiger et al.⁸⁵⁾ for CoPc(NaSO₃)₄ oxidized by Ce⁴⁺, Cl₂⁻ or Br₂⁻. One-electron oxidation of the ring by dioxygen was mentioned by Ogata et al.⁸⁶⁾, who studied CoPc in organic solvents.

Alternatively, it is possible that dioxygen adduct formation takes place after complexation of thiol with the catalyst complex. Also in the presence of thiol, however, no μ -peroxo complex could be detected. It can not be ruled out that a different type of dioxygen-containing complex is formed with spectral characteristics closely resembling that of the dioxygen-free complex.

5.2 Interaction of thiol with the catalyst

5.2.1 Effects of thiol on aggregation

The investigations described in chapter 4, made clear that aggregation of Co(II)Pc(NaSO₃)₄ can be easily controlled by addition of certain ionenes and by choosing appropriate concentrations of the components.

To obtain insight in the role of the aggregates during the catalytic conversion of thiols, catalyst systems with different degrees of aggregation were now studied in the presence of 2-mercaptoethanol (under anaerobic conditions). These experiments were primarily focused on elucidating whether thiolate anions can break up the aggregates (by forming coordinative bonds with cobalt via its two axial positions and/or by changing the valency of the central cobalt ion).

First, an excess of 2,10-ionene was used in order to determine the visible light spectrum of the interaction product of the monomeric catalyst and the thiol. This spectrum is presented in Fig. 5.2a and is typical of monomeric one-electron-reduced cobalt phthalocyanine. It was established that complete reduction of the cobalt was achieved, since the EPR-signal of the Co(II) complex was totally lost. Fig. 5.2a shows main absorption bands at 316

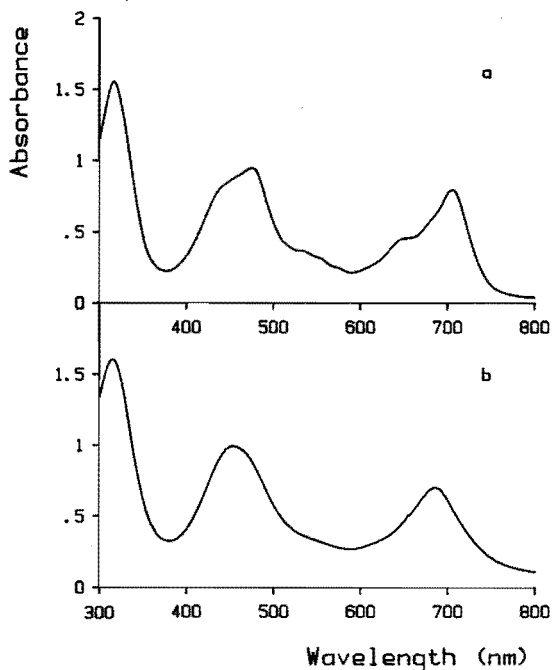


Fig. 5.2 Spectra of $\text{CoPc}(\text{NaSO}_3)_4$ in water in the presence of thiol and ionene under anaerobic conditions; $[\text{Co}] = 4 \cdot 10^{-5} \text{ mol dm}^{-3}$, $[\text{RSH}] = 4.8 \cdot 10^{-2} \text{ mol dm}^{-3}$.

(a) monomeric $[\text{Co}(\text{I})\text{Pc}(\text{NaSO}_3)_4]^-$, 2,10-ionene, $\text{N}^+/\text{Co} = 3000$, $\text{pH} = 9$;

(b) aggregated $[\text{Co}(\text{I})\text{Pc}(\text{NaSO}_3)_4]^-$, 2,4-ionene, $\text{N}^+/\text{Co} = 3000$, $\text{pH} = 9$.

nm (Soret-band), 476 nm (metal to ligand charge transfer, MLCT) and 706 nm (Q-band) and shoulders around 440 and 650 nm, which is in very good agreement with literature^{42,80,87}.

The same procedure using 2,4-ionene led to a different spectrum, shown in Fig. 5.2b. Here, both the MLCT- and Q-bands have been shifted to shorter wavelengths - 454 and 684 nm - and the fine structure has disappeared. Similar effects are observed for the Co(II) species upon its aggregation, which

suggests the assignment of the spectrum of Fig. 5.2b to aggregated¹ $[\text{Co(I)Pc}(\text{NaSO}_3)_4]_n^{n-}$. This is in good agreement with the findings of Kozlyak et al.⁸⁰⁾, who analogously claim to be able to control Co(II)- and Co(I)-phthalocyanine aggregation by the addition of cationic soaps (monomerization) or (poly)salts (aggregation). (The similarity between their results with CTAB and those with 2,10-ionene presented here is striking and again indicative of the soap-like character of the 2,10-ionene system.)

The 2,xyl- and 6,2NØ-ionenes, that were previously reported to stabilize the Co(II) complex in its purely dimeric form (section 4.1.3), in the presence of thiol gave spectra very similar to that of the 2,4-ionene system, but with $\lambda_{\text{max}} = 460$ and 688 nm. These absorption maxima are ascribed to purely dimeric $[\text{Co(I)Pc}(\text{NaSO}_3)_4]_2^{2-}$.

The polymer-free catalyst was also studied in the presence of thiol. Its spectrum also appeared to be very similar to that of the 2,4-ionene containing system (Fig. 5.2b), indicating the presence of mainly the aggregated Co(I) species under these conditions. In the case of this polymer-free system, the equilibrium could be reversibly shifted to the monomer side (resulting in a spectrum identical to Fig. 5.2a) by heating the solution to 85 °C (see Fig. 5.3). Addition of e.g. DMF or ethanol led to monomerization as well, in analogy with the observations for the Co(II) compound (see section 4.2.1).

When the 2,4-ionene containing system was heated to 85 °C, no dissociation of aggregates could be observed. Neither was this found upon addition of ethanol. Thus, 2,4-ionene strongly stabilizes aggregates, in the

¹Nevin et al.⁸⁸⁾, who reduced the cobalt complex electrochemically, also observed the spectrum of Fig. 5.2b and ascribed it to the monomeric form. However, their assignment is not well-argued and absence of aggregates under their conditions, viz. a high cobalt concentration ($5 \cdot 10^{-4} \text{ mol dm}^{-3}$) and a very high ionic strength (0.9 mol dm^{-3}), seems very unlikely.

Co(I) form as well as in the Co(II) form. The other polyelectrolyte-type ionenes show similar behaviour, although the low charge density 6,6-ionene stabilizes the aggregates to a lesser extent, as was concluded from Co(I) monomerization at 65 °C.

It was established that all ionenes (polyelectrolyte- and polysoap-type) enhance the degree of cobalt reduction, which could be deduced from the higher ratio of the intensities of the MLCT- and Q-bands, respectively, for the ionene systems as compared with the polymer-free system. Especially at low thiolate anion concentrations the difference was obvious. This supports the view⁵⁴⁾ that ionenes, due to their cationic charge, strongly increase the local concentration of thiolate anions (the reductive species).

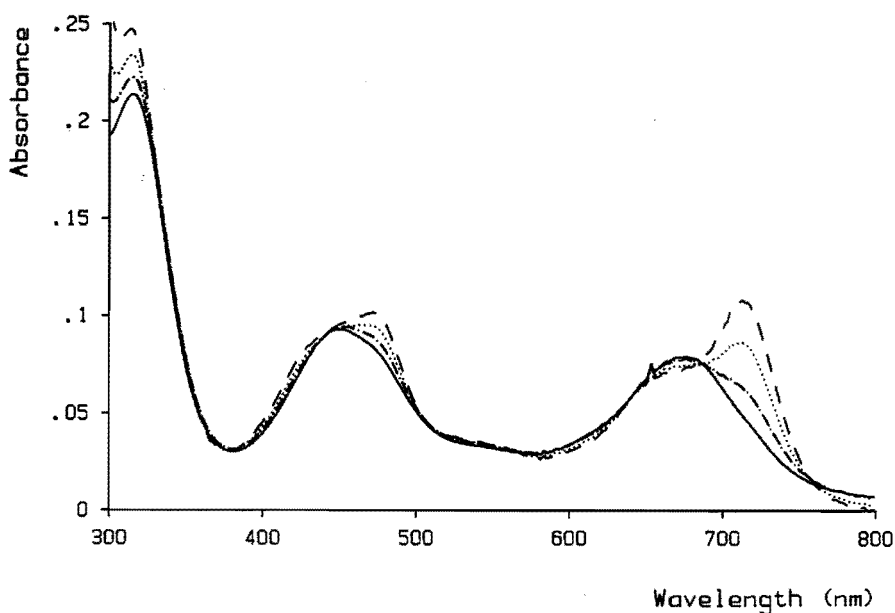


Fig. 5.3 Effect of varying temperature on the spectrum of aqueous $\text{CoPc}(\text{NaSO}_3)_4$ in the presence of 2-mercaptoethanol; spectra at 25 (—), 45 (-.-.), 65 (...) and 85 °C (---).
 $[\text{Co}] = 4 \cdot 10^{-6} \text{ mol dm}^{-3}$, $[\text{RSH}] = 4.8 \cdot 10^{-2} \text{ mol dm}^{-3}$, $\text{pH} = 9$, under N_2 .

5.2.2 Concentration effects on the degree of Co(I) aggregation

The reduced catalyst systems were further investigated in dependence of the N^+/Co -ratio and of the concentration of thiolate anions, $[RS^-]$, that was varied by changing the pH or the thiol content of the solution.

For 2,10-ionene it was expected that at $4 < N^+/Co < 10^3$ the aggregated Co(I) species would be observed, in analogy with the results for the unreduced system (see Fig. 4.11). Indeed, the presence of aggregates in this region could be demonstrated, although invariably monomeric species appeared to be present as well. Only below an N^+/Co -ratio of 5, no monomeric species were observed. The degree of aggregation depended mainly on the concentration of thiolate anions: increasing $[RS^-]$ resulted in a decrease of the amount of aggregates present, even at N^+/Co -ratios where Co(II) dimers were stable. Therefore, it is clear that thiolate ions act as axial ligands of the cobalt phthalocyanine molecules, thus disrupting their dimeric structure, in 2,10-ionene systems.

Another factor that influenced aggregation was the 2,10-ionene concentration rather than the N^+/Co -ratio. At $[N^+] > \text{approx. } 10^{-4} \text{ mol dm}^{-3}$ the system was measurably deaggregating. It is assumed that this deaggregation is induced by micelle formation.

At $N^+ : [Co(I)Pc(SO_3)_4]^{5-} = 5 : 1$ precipitation occurred due to charge compensation, however, the precipitate redissolved upon addition of more ionene. Similar behaviour was found for 2,4-ionene, but this system was more colloidal in character, as appeared from the high turbidity.

The 2,4-ionene was expected to enhance the degree of aggregation, reaching a maximum value at $N^+/Co = 5$ and remaining constant for higher ratios. However, at $N^+/Co = 5$ an additional effect (apart from colloid formation) took place, as illustrated by the spectrum in Fig. 5.4, which complicated the interpretation of the results. As can be seen, all absorption maxima were shifted to longer wavelengths. The process occurred at a very low rate and equilibrium was only reached after about 1 hour, resulting in

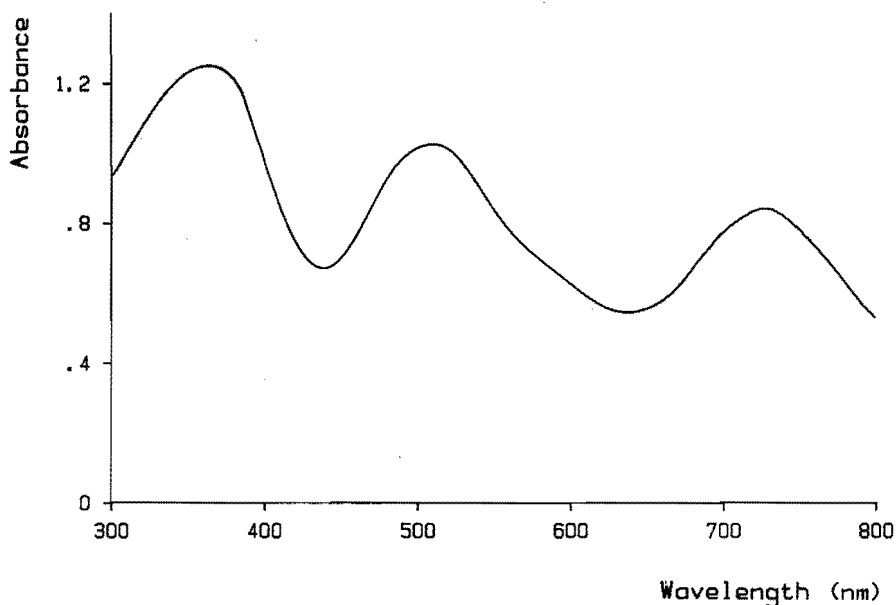


Fig. 5.4 Spectrum of aqueous $\text{CoPc}(\text{NaSO}_3)_4$ in the presence of thiol and 2,4-ionene at $\text{N}^+/\text{Co} = 5$; $[\text{Co}] = 4 \cdot 10^{-5} \text{ mol dm}^{-3}$, $[\text{RSH}] = 4.8 \cdot 10^{-2} \text{ mol dm}^{-3}$, $\text{pH} = 9$, equilibration time 1 hour.

absorption maxima at 364, 506 and 736 nm. The spectrum is difficult to assign, especially the band at 364 nm, since values in this region have only been reported for oxidized forms^{89,90)} of the cobalt complex which are probably not formed in the presence of thiol, i.e. under reducing conditions. More likely, a doubly reduced species is formed (the phthalocyanine ring being reduced as well as the cobalt centre), since an excess of thiol was being used. Indeed, when the applied concentration of thiolate anions was smaller than twice the cobalt concentration, the phenomenon was not observed. However, the spectrum obtained differs considerably from the spectrum for $[\text{Co}(\text{I})\text{Pc}^-(\text{NaSO}_3)_4]^{2-}$ reported by Nevin et al.⁸⁸⁾. The discrepancy may be due to the presence of different ligands. The presence of a dimeric species with mixed valence ($[\text{Co}(\text{II}) - \text{Co}(\text{I})]$) can not be ruled out either, since delocalization of electrons over the aggregates may occur. In this respect, it is interesting to

note that the compound exhibiting the spectrum of Fig. 5.4 was not formed in the non-aggregating 2,10-ionene system. It was thought, that EPR measurements would give more insight into the structure of the compound. However, due to precipitation this experiment could not be carried out.

Upon further addition of 2,4-ionene ($N^+/Co > 5$), the spectrum of aggregated Co(I) was restored and the Q-band was shifted to even shorter wavelength (about 650 nm), presumably indicating an even higher degree of aggregation. At large excesses of ionene ($N^+/Co > 100$) this band shifted back to 686 nm, but no evidence was found for the existence of monomeric Co(I) up to $N^+/Co = 10^4$, which was in agreement with expectations.

5.3 Relation between structure and catalytic activity: the catalytic site

5.3.1 Catalytic activity measurements: effect of varying N^+/Co

The catalytic activity of several ionenes was determined under standard conditions. As can be seen from Table 5.1, the activity of 2,10-ionene was extremely low as compared with the other ionenes. The difference is too large to be explained by a charge density effect. On the other hand, it strongly

Table 5.1 Catalytic activities of several ionenes^a.

ionene	σ^b	activity (mol RSH (mol Co) ⁻¹ s ⁻¹)
2,4	1.44	2550
2,6	1.15	2040
2,8	0.96	1680
6,6	0.82	1420
2,10 ^c	0.82	40

^a Conditions: pH = 9.0, $[RSH]_0 = 0.071 \text{ mol dm}^{-3}$, $[N^+] = 10^{-3} \text{ mol dm}^{-3}$, $[Co] = 2 \cdot 10^{-7} \text{ mol dm}^{-3}$

^b linear charge density parameter⁵⁴⁾

^c $[Co] = 4 \cdot 10^{-6} \text{ mol dm}^{-3}$ instead of $2 \cdot 10^{-7} \text{ mol dm}^{-3}$ where the activity was too low to be measured

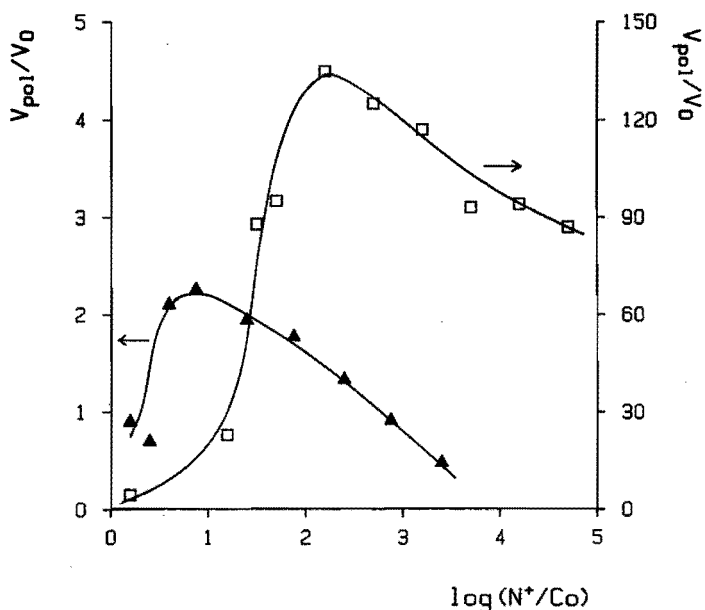


Fig. 5.5 Effect of varying the N^+/Co -ratio on the thiol oxidation rate of ionene-systems relative to the rate of the polymer-free catalyst; $V_0 = 30 \text{ mol RSH/mol Co.s}$, $\text{pH} = 9.0 - 9.1$, $[RSH]_0 = 0.071 \text{ mol dm}^{-3}$. (\square) 2,4-ionene, $[Co] = 2 \cdot 10^{-7} \text{ mol dm}^{-3}$; (\blacktriangle) 2,10-ionene, $[Co] = 4 \cdot 10^{-6} \text{ mol dm}^{-3}$.

suggests that the dimeric (aggregated) cobalt complex is the catalytically active species, since all tested ionene systems contain predominantly dimers except the much less active 2,10-ionene system.

The results obtained by varying the N^+/Co -ratio (see below) and the catalyst concentration (discussed in the next section) of 2,4- and 2,10-ionene systems provided more supporting evidence to this hypothesis.

In Fig. 5.5 thiol oxidation rates for the 2,4- and 2,10-ionene systems are depicted as a function of N^+/Co -ratio, with the rates expressed relative to the rate measured for the polymer-free catalyst. It is evident that, while the 2,4-ionene largely enhances the reaction rate (up to more than 120-fold), the 2,10-ionene exhibits an activity of the same order of magnitude as the

polymer-free system. Both polymer catalysts show an optimum in activity, the 2,4-ionene at $N^+/Co = \text{approx. } 200$ and the 2,10-ionene at $N^+/Co = 5-10$. Both curves will be explained below on the basis of the ability of the ionenes to locally increase the concentration of thiolate anions and the hypothesis that dimers (aggregates) are the catalytically active sites.

According to section 5.2, aggregates will be present in both systems at $N^+/Co(I) < 5$. Since there is an excess of phthalocyanine in this region, the charge on the ionenes will be completely compensated and enrichment of the catalyst domains with thiolate anions will not take place. The activities in this region should therefore be comparable to the activity of the polymer-free catalyst, which was indeed found.

Increasing the N^+/Co -ratio will lead to an increase in $[RS^-]_{\text{local}}$, having a positive effect on the reaction rate. In the case of 2,10-ionene, however, this effect is partly undone by the rate lowering due to the dissociation of the aggregates. At relatively low N^+/Co -ratios, or more precisely: at low $[N^+]$ where presumably only a small number of micelles is present, the thiolate concentration effect dominates over the deaggregation and a (small) rate-enhancement with respect to the polymer-free case is found. However, at high N^+/Co , deaggregation prevails and the relative reaction rate decreases below a value of 1.

For the 2,4-ionene, no Co(I) deaggregation was observed and at $N^+/Co < 100$ aggregation even appeared to be enhanced (shift of λ_{max} from 684 to 650 nm), while also the stability of the aggregates was increased. Together with the increased local thiolate anion concentration, this apparently results in a highly efficient catalyst. Since thiolate enrichment may be expected to be of similar importance in the 2,4- and 2,10-ionene systems (see also chapter 7), it can be concluded that aggregation mainly determines the high activity of the 2,4-ionene catalyst.

Above $N^+/Co = 200$ also the activity of the 2,4-ionene was found to decrease again, which may be caused by the following two effects. First, by

spectroscopy it was demonstrated that the degree of Co(I) aggregation slightly decreases in this region, indicated by a shift of the Q-band to longer wavelength. If the reaction rate is related to the degree of catalyst aggregation, this explains at least partly the observed activity decrease. The observation that the 2,xyl- and 6,2NØ-ionene catalysts, containing only dimers and no higher aggregates, have lower activities than the 2,4-ionene also supports this explanation. In addition, it seems plausible that in this N^+/Co region also $[RS^-]_{local}$ is somewhat lowered; in other words, when large excesses of ionene are applied, many RS^- -rich domains will not contain the cobalt complex and thus be ineffective. In this way, the efficiency of the catalyst will decrease, as was indeed established. Nevertheless, it must be noted that even at N^+/Co -ratios as high as $5 \cdot 10^4$ still 65% of the optimum activity is retained.

5.3.2 Dependence of catalytic activities on catalyst concentration

Fig. 5.6 shows the results of thiol oxidation rate measurements as a

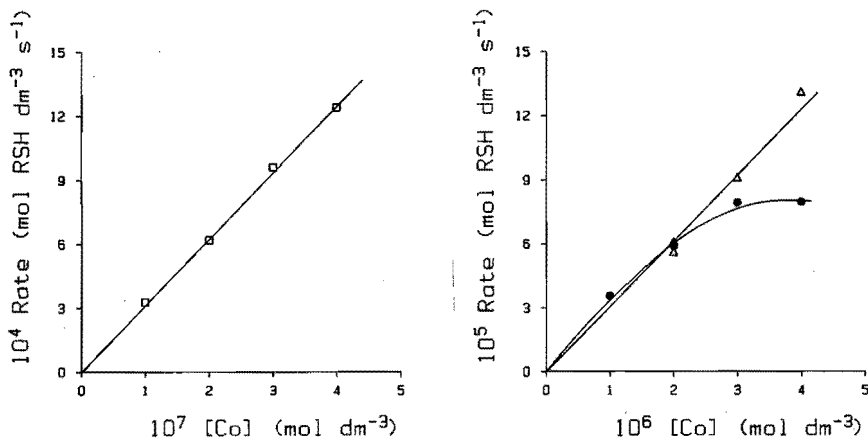


Fig. 5.6 Dependence of the thiol oxidation rate on the catalyst concentration;

pH = 9.2, $[RSH]_0 = 0.043 \text{ mol dm}^{-3}$.

a: 2,4-ionene, $N^+/Co = 2000$.

b: 2,10-ionene, (Δ) $N^+/Co = 10$, (\bullet) $N^+/Co = 2000$.

function of catalyst concentration, where N^+/Co was kept constant. The 2,4-ionene displays a linear relationship, in full agreement with the Michaelis-Menten kinetic model that has been published earlier³⁹⁾ (see also chapter 6). It is also in accordance with the theory of aggregates being the active species, provided that the degree of aggregation over the concentration range studied is constant, i.e. that the number of coordination sites is constant. In Fig. 4.13 it has been shown that this condition is indeed being fulfilled.

For the 2,10-ionene, it was demonstrated that at high $[N^+]$ the amount of aggregate is decreased (see sections 5.2.2 and 4.3.1). Therefore, the activity is no longer proportional to the catalyst concentration when N^+/Co is kept at a high value. On the other hand, when N^+/Co is kept sufficiently low (in such a way that $[N^+] < 10^{-4}$ mol dm⁻³), no deviation of linearity is observed, as also can be seen in Fig. 5.6b.

All kinetic data in dependence of type and concentration of ionene are thus consistent with the postulate that aggregates are the catalytically active species. Moreover, additional evidence is presented in Fig. 5.7, in which the results of catalytic experiments in ethanol/water mixtures are presented. Addition of alcohols to a solution of $CoPc(NaSO_3)_4$ or its reduced form favours the formation of the monomeric species⁶⁷⁾, whereas in the presence of 2,4-ionene the aggregates remain (see chapter 4.2.1). The curves of the activities versus ethanol content show a pattern that parallels the occurrence of the aggregates in these solvent mixtures: the polymer-free system exhibits a considerable loss of activity (about 75% at 25% ethanol content), while the loss in the ionene system is only small (about 10% at 25% ethanol). The minor activity decrease in the latter case may well be due to solvational effects.

Therefore, it is proposed that the catalytic species in the phthalocyanine-catalyzed thiol oxidation is the dimerized (or even higher aggregated) cobalt complex. This is in good agreement with the results of Beelen et al.⁹¹⁾, who observed a large rate increase when the (polymer-free) negatively charged

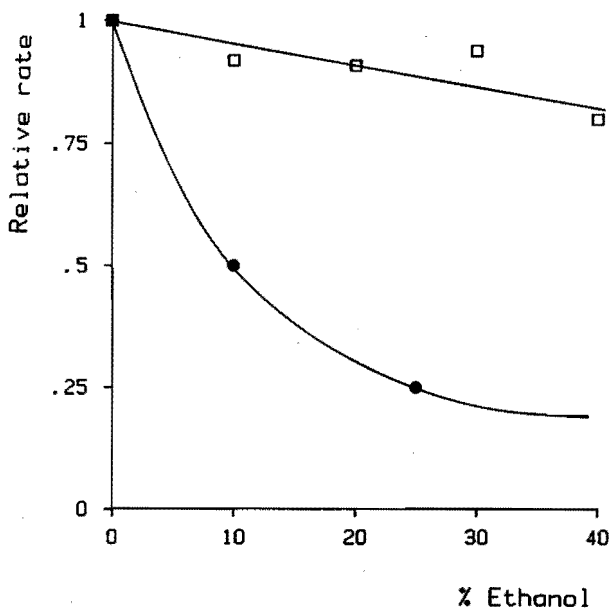


Fig. 5.7 Effect of ethanol on thiol oxidation rate. Rate expressed relative to the value in 100% water; $[Co] = 2 \cdot 10^{-7} \text{ mol dm}^{-3}$, $\text{pH} = 9.2 - 9.5$, $[RSH]_0 = 0.14 \text{ mol dm}^{-3}$. (●) polymer-free system; (□) with 2,4-ionene, $[N^+] = 10^{-3} \text{ mol dm}^{-3}$.

tetra-sulfo catalyst complex was combined with an equimolar amount of its positively charged tetra-ammonium counterpart, in which case the occurrence of dimers is evident.

A summary of the occurrence of aggregates in the various systems described in this and the previous chapter is presented in Table 5.2.

5.4 Conclusions and final remarks

In the previous sections, it was shown that $CoPc(NaSO_3)_4$ aggregates, as stabilized by polyelectrolyte-type ionenes, persist in the presence of thiol or dioxygen. With only dioxygen, no interaction with the catalyst could be observed since no μ -peroxo complex was formed (unless the pH was raised above

Table 5.2 Occurrence of phthalocyanine aggregates in various systems^a.

	CoPc(NaSO ₃) ₄					
	<u>unreduced</u>			<u>reduced (+ RSH)</u>		
	water 25 °C	alcohol	high temp.	water 25 °C	alcohol	high temp.
polymer-free	+/-	-	-	+	-	-
polysoap-type ionene						
c << "cmc"	+	+/-	+	+/-	-	--
c > "cmc"	+/-	-	-	--	--	--
polyelectrolyte type ionene	++	++	++	++	++	++

^a -- = no aggregates, - = little aggregates, +/- = aggregates and monomers in comparable amounts, + = mainly aggregates, ++ = only aggregates present

13). Interaction with thiol, however, appeared to occur, resulting in reduction of the cobalt complex.

Polysoap-type ionenes, monomerizing the phthalocyanine, did not show μ -peroxo complex formation with dioxygen either. In the presence of thiol, these complexes were also reduced and were even monomerized at concentrations where the unreduced CoPc(NaSO₃)₄ was aggregated.

The occurrence of aggregates was always found to be paralleled by high activities in catalytic thiol oxidation experiments. On these grounds, it was concluded that in the ionene-promoted process the aggregated cobalt complex is the catalytic site.

The question remains, why aggregates would be catalytically more active than the monomeric complex. Probably, mainly two effects are involved. In the first place, the ionene-containing aggregates were found to be very stable, e.g. against high temperatures and against complex formation with ligands like alcohols or dioxygen. The latter compound can give rise to the μ -peroxo

complex that is known to deactivate the catalyst⁴⁵⁾. Prevention of formation of this complex therefore enhances the reaction rate. However, as the polysoap-type ionenes, in spite of their monomerizing ability, also prevented formation of the dioxygen-bridged dimer complex, this explanation is not satisfactory.

Furthermore, the redox properties of the aggregates are presumably more favourable than those of the monomeric species. This was also suggested by Nevin et al.⁹²⁾, who demonstrated that dinuclear and tetranuclear phthalocyanines reduce dioxygen more efficiently than the mononuclear compound. They attributed this increased activity to electronic coupling between the phthalocyanine rings. Redox properties in relation to degree of aggregation will be further discussed in chapter 7.

6 KINETIC MODELING OF THE IONENE-PROMOTED THIOL AUTOXIDATION

6.1 Introduction

In the preceding chapter, it was demonstrated that polyelectrolyte-type ionenes, like 2,4-ionene, have a positive effect on the oxidation of thiols by stabilizing the phthalocyanine catalyst in its highly active, aggregated form. More detailed information about the mechanism of the polymer-promoted process was desired, in order to be able to design the most effective catalyst system. Therefore, the kinetics of the process were studied, aimed at elucidating the polymer effects on individual reaction steps rather than on overall reaction rate.

Kinetic investigations were performed under carefully controlled conditions, since e.g. pH and ionic strength were known to substantially affect reaction rate⁵⁴). Independent variation of such process parameters provided detailed mechanistic information and will be discussed in chapter 7.

Here, the general form of kinetics and mechanism are discussed, as well as substrate inhibition and side-reactions.

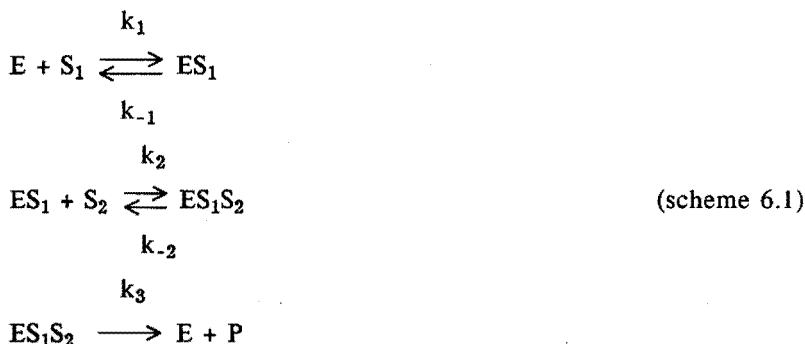
6.2 The 2-substrate Michaelis-Menten model

6.2.1 Initial rate as a function of substrate concentrations

At a pH of 8.30 and an ionic strength of 0.1 mol dm^{-3} , the initial rate of oxidation of 2-mercaptoethanol was measured as a function of dioxygen and thiolate anion concentration. Thiolate anion rather than thiol concentration was taken as the variable, because the anions are considered^{38,54}) to be the reactive species.

In Figs. 6.1 and 6.2 the observed dependencies of initial rate on both

[O₂] and [RS⁻] are presented. The curves reveal saturation kinetics in both substrates, suggesting that the process can be described by a two-substrate Michaelis-Menten model⁹³, according to scheme 6.1:



where E = CoPc(NaSO₃)₄, S₁ and S₂ are the two substrates and P is the product. If the reaction rate is given by eq. 6.1

$$v_f = d[P]/dt = k_3 [ES_1S_2] \quad (6.1)$$

and steady-state kinetics are assumed in both ES₁ and ES₁S₂, it can be derived that⁹³)

$$v_f = \frac{C_1 [E]_{tot}}{1 + C_2/[S_2] + C_3/[S_1] + C_2C_4/[S_1][S_2]} \quad (6.2)$$

with C₁ = k₃, C₂ = (k₋₂ + k₃)/k₂, C₃ = k₃/k₁ and C₄ = k₋₁/k₁.

It is customary to express the specific rate (r) as the consumption of thiol (instead of the formation of product) per mole catalyst per second⁴⁷). Since the reaction of thiols with dioxygen generally proceeds according to the stoichiometry of scheme 6.2,

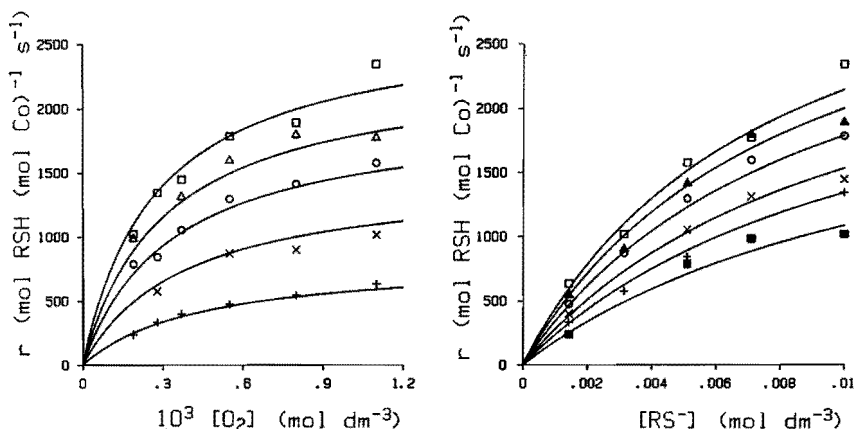
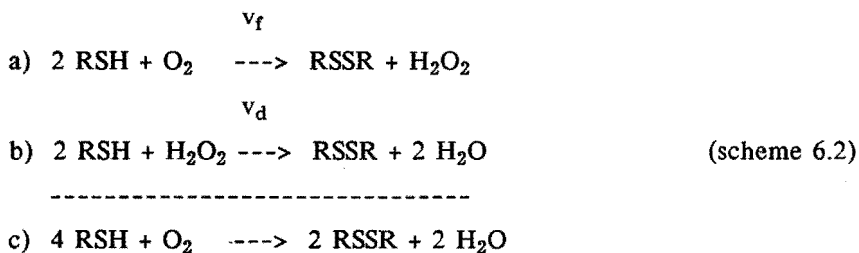


Fig. 6.1 Initial reaction rate as a function of dioxygen concentration at initial thiolate anion concentrations of $0.00143 \text{ mol dm}^{-3}$ (+), $0.00314 \text{ mol dm}^{-3}$ (x), $0.0051 \text{ mol dm}^{-3}$ (O), $0.0071 \text{ mol dm}^{-3}$ (Δ) and $0.010 \text{ mol dm}^{-3}$ (\square). Drawn lines calculated according to eq. 6.2. Temp. = $25.0 \pm 0.5 \text{ }^\circ\text{C}$, $I = 0.1 \text{ mol dm}^{-3}$, $\text{pH} = 8.30 \pm 0.05$.

Fig. 6.2 Initial reaction rate as a function of thiolate anion concentration at dioxygen concentrations of $1.9 \cdot 10^{-4} \text{ mol dm}^{-3}$ (\blacksquare), $2.8 \cdot 10^{-4} \text{ mol dm}^{-3}$ (+), $3.7 \cdot 10^{-4} \text{ mol dm}^{-3}$ (x), $5.5 \cdot 10^{-4} \text{ mol dm}^{-3}$ (O), $8.0 \cdot 10^{-4} \text{ mol dm}^{-3}$ (\blacktriangle) and $1.1 \cdot 10^{-3} \text{ mol dm}^{-3}$ (\square). Drawn lines calculated according to eq. 6.2. Conditions as in Fig. 6.1.



where reaction b) is considered as a fast consecutive reaction⁵¹ (so that k_3 only refers to the catalytic step a)), the expression for r becomes:

$$r = - 1/[E]_{tot} * d[RSH]/dt = 4 v_f/[E]_{tot} \quad (6.3)$$

The measured kinetic data (data points of Figs. 6.1 and 6.2) were fitted to this equation by means of a non-linear least squares calculation, resulting in the drawn curves of Figs. 6.1 and 6.2. The constants found were: $C_1 = 1000 \pm 100 \text{ s}^{-1}$, $C_2 = 1.5 \pm 0.3 \cdot 10^{-4} \text{ mol dm}^{-3}$, $C_3 = 4.0 \pm 0.2 \cdot 10^{-3} \text{ mol dm}^{-3}$ and $C_4 = 1.4 \pm 0.4 \cdot 10^{-2} \text{ mol dm}^{-3}$. The good agreement between experiments and calculation can be seen from Table 6.1, in which the measured and calculated rates are shown. The average difference between measured and calculated activities is 4.5%. From these data it can be concluded that the kinetics of the thiol oxidation, catalyzed by $\text{CoPc}(\text{NaSO}_3)_4$ in the presence of 2,4-ionene, follow the two-substrate Michaelis-Menten model. This model is also in accordance with the previously mentioned (chapter 5.3.2) first order in Co concentration.

On the basis of formula 6.2 and 6.3, it can not be determined which substrate reacts first with the catalyst (scheme 6.1). However, in the system here discussed no dioxygen adducts could be detected in the absence of thiol (section 5.1). Therefore, it is assumed that prior to dioxygen coordination thiol must coordinate. Following the above-mentioned considerations, S_1 is designated to the thiolate anion and S_2 to dioxygen. Thus, the equilibrium constant for thiol coordination ($k_1/k_{-1} = 1/C_4$) is equal to $70 \text{ dm}^3 \text{ mol}^{-1}$, which is in good agreement with the findings of Kozlyak et al.⁴³⁾ for cysteine. The thiol turn-over number ($4 k_3$) equals 4000 s^{-1} , which is a very high (enzyme-like) number for this kind of reactions.

Of course scheme 6.1 is an oversimplification of any correct reaction mechanism because the valency of the cobalt in the catalyst changes during the reaction and radicals may occur as intermediates⁴⁵⁾. These individual reaction steps will be considered in chapter 7.

Table 6.1 Measured and calculated activities at 25 °C; I = 0.1 mol dm⁻³, pH = 8.3, 10⁻³ mol dm⁻³ 2,4-ionene.

10 ³ [RS ⁻] ₀ (mol dm ⁻³)	10 ³ [O ₂] ₀ (mol dm ⁻³)	r _{obs} ^a	r _{calc} ^a	delta (%)
1.07	1.1	634	602	5.0
1.07	0.8	545	545	0.0
1.07	0.55	475	467	1.7
1.07	0.37	400	382	4.6
1.07	0.28	333	322	3.3
1.07	0.19	238	250	-5.1
2.36	1.1	1018	1097	-7.7
2.36	0.8	901	1003	-11.3
2.36	0.55	871	871	0.0
2.36	0.28	577	616	-6.8
4.08	1.1	1578	1548	2.0
4.08	0.8	1414	1426	-0.8
4.08	0.55	1296	1254	3.3
4.08	0.37	1054	1055	-0.1
4.08	0.28	844	909	-7.7
4.08	0.19	788	722	8.4
5.68	1.1	1775	1838	-3.5
5.68	0.8	1797	1703	5.2
5.68	0.55	1598	1510	5.6
5.68	0.37	1314	1282	2.4
5.68	0.19	985	892	9.4
8.0	1.1	2347	2133	9.1
8.0	0.8	1893	1989	-5.1
8.0	0.55	1788	1778	0.6
8.0	0.37	1450	1524	-5.1
8.0	0.28	1345	1333	0.9
8.0	0.19	1021	1079	-5.7

^a r expressed in units of mole thiol per mole catalyst per second; r_{obs}: observed initial rate, r_{calc}: initial rate calculated according to formula 6.2

6.2.2 Dioxygen consumption rate curves

Because during the whole conversion the pH is maintained constant and the catalyst is not broken down during the reaction⁵⁴⁾, the rate of dioxygen consumption over the whole conversion contains kinetic information related to eqs. 6.2 and 6.3. Assuming that the concentration of thiol is low, then the

rate of dioxygen consumption varies linearly with the thiol concentration:

$$r = k [\text{RSH}] = k e^{-kt} [\text{RSH}]_0 \quad (6.4)$$

with $k = 4C_1/(C_3 + C_2C_4/[\text{O}_2])$.

Therefore, the dioxygen consumption should decrease according to an exponential decay curve. For comparison, the dioxygen uptake rate curves for an unbuffered and a buffered system are shown in Fig. 6.3a and 6.3b. In Fig. 6.3b also the exponential curve is drawn which is fitted through the last part of the curve. From this fit a value for k of $4.1 \cdot 10^{-2} \text{ s}^{-1}$ is found which gives, at an initial thiol concentration of $0.014 \text{ mol dm}^{-3}$, a dioxygen consumption rate of $19 \text{ ml O}_2 \text{ min}^{-1}$, a value which relates well to the dioxygen consumption rate at the maximum of the curve ($15 \text{ ml O}_2 \text{ min}^{-1}$).

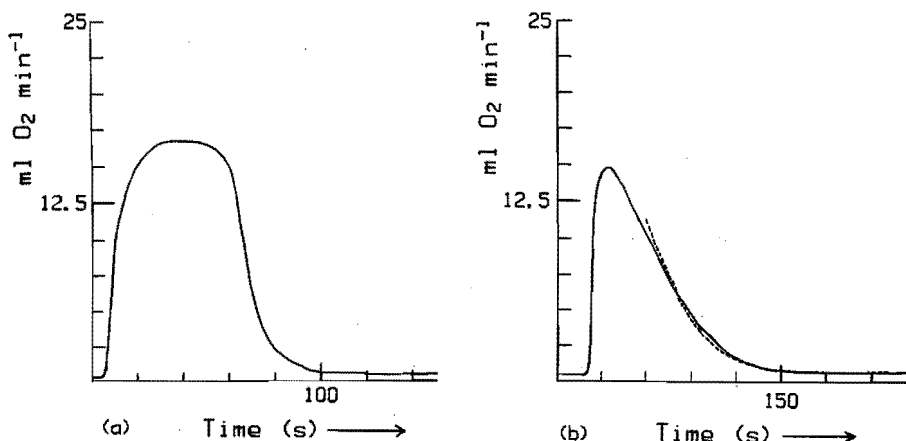


Fig. 6.3 Dioxygen uptake rate versus time at low thiol concentration;

temp. = 25 °C, $[\text{RSH}] = 0.014 \text{ mol dm}^{-3}$.

(a) Unbuffered system; $I \approx 0 \text{ mol dm}^{-3}$, initial pH = 8.3, $[\text{Co}] = 2 \cdot 10^{-7} \text{ mol dm}^{-3}$, $[\text{O}_2] = 0.0011 \text{ mol dm}^{-3}$

(b) Buffered system; $I = 0.1 \text{ mol dm}^{-3}$, pH = 8.3, $[\text{Co}] = 1.1 \cdot 10^{-6} \text{ mol dm}^{-3}$, $[\text{O}_2] = 3.7 \cdot 10^{-4} \text{ mol dm}^{-3}$

The dotted line represents the exponential fit according to eq. 6.4.

At higher thiol concentrations the dioxygen consumption rate curve can no longer be described in this way. There, the saturation kinetics in thiol must be taken into account (Fig. 6.4). In that case eq. 6.2 can be used to predict the dioxygen consumption rate curve by numerically calculating the thiol concentrations in small time steps. In Fig. 6.4 a calculated curve is depicted which describes the experimental dioxygen consumption rate curve rather well.

At lower thiol concentrations, differences occur between calculated and observed dioxygen consumption rate curves. The total dioxygen consumption for complete conversion, i.e. the integral of the dioxygen uptake curve, in this case was found to be higher than calculated. This indicates that the reaction stoichiometry of scheme 6.2 is complicated, probably by hydrogen peroxide formation. Indeed, H_2O_2 could be detected in the reaction mixtures, accounting for the excess of dioxygen consumed. In general, only small amounts of peroxide could be detected. However, at low thiol concentrations the relative amount of hydrogen peroxide increased. This explains why at low thiol concentrations the exponential fit through the dioxygen consumption rate curve

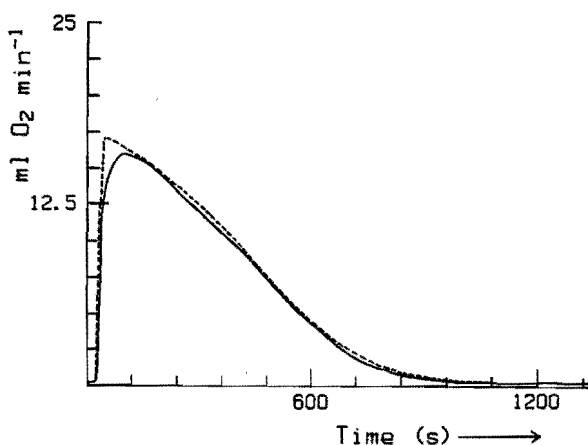


Fig. 6.4 Dioxygen uptake rate versus time at high thiol concentration. $[\text{RSH}] = 0.2 \text{ mol dm}^{-3}$, $[\text{O}_2] = 5.5 \cdot 10^{-4} \text{ mol dm}^{-3}$, $[\text{Co}] = 2 \cdot 10^{-7} \text{ mol dm}^{-3}$, other conditions as in Fig. 6.1. The dotted line represents the fit according to eq. 6.2.

Table 6.2 Comparison of measured and calculated reaction rates at high thiol concentration^a.

[O ₂] (mol dm ⁻³)	r _{obs}	r _{calc}	delta (%)
0.00110	2780	2750	1.1
0.00081	2530	2590	-2.4
0.00055	2050	2360	-15
0.00037	1670	2060	-23
0.00019	760	1510	-99

^a [RSH]₀ = 0.2 mol dm⁻³

gave a larger rate constant than expected from the initial rate (Fig. 6.3b).

The reactions involving H₂O₂ will be further discussed in section 6.3.

6.2.3 Coordination of thiol to the catalyst: substrate inhibition

At high [RSH]₀ (> 0.1 mol dm⁻³) and low [O₂] (< 0.00055 mol dm⁻³), it was found that deviations from the Michaelis-Menten kinetics occurred, leading to initial reaction rates lower than the expected values (see Table 6.2). As the deviation was larger when [O₂] was lower, it was thought that this phenomenon is the result of substrate inhibition, due to occupation of dioxygen coordination sites by excess thiolate anions. A strong indication of the occurrence of this effect was found by means of stopped-flow measurements.

The stopped-flow technique is a powerful tool in studying reaction steps with rate constants up to 10³ s⁻¹, like metal-ligand coordination steps. If the mechanism proposed in section 6.2.1 is valid, the rate constant for the coordination of the first thiolate anion to the catalyst complex is approx. 2 · 10⁵ dm³ mol⁻¹ s⁻¹ (= k₃/C₃) and thus, this reaction is not detectable by stopped-flow measurements (unless very low concentrations are applied). Indeed, upon fast mixing of dioxygen-free solutions of catalyst ([Co] = 2 · 10⁻⁵ mol dm⁻³, [N⁺] = 10⁻³ mol dm⁻³) and thiol ([RSH] = 0.01 to 0.12 mol dm⁻³, pH 8.3), the absorptivity at 450 nm observed at t = 0 was already much higher than expected for CoPc(NaSO₃)₄/ionene, indicating a reaction had taken place

at a time scale faster than detectable. Nevertheless, a consecutive reaction could be observed, its rate constant depending on thiol concentration according to eq. 6.5, when assuming first order behaviour in $\text{CoPc}(\text{NaSO}_3)_4$. (Two other consecutive reactions, probably redox steps, were observed as well, being independent of thiol concentration.)

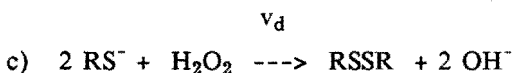
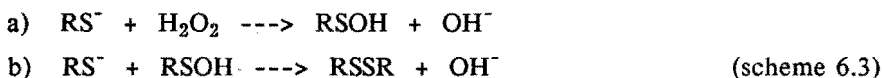
$$k_{\text{obsd}} = k_1 [\text{RSH}] + k_{-1} \quad (6.5)$$

The observed rate constant increased from 3.3 s^{-1} at $0.014 \text{ mol dm}^{-3}$ thiol to 10.9 s^{-1} at $0.112 \text{ mol dm}^{-3}$ thiol. From these data an equilibrium constant of $35 \text{ dm}^3 \text{ mol}^{-1}$ was estimated for this second thiol coordination equilibrium and rate constants were calculated to be: $k_1 = 77 \text{ dm}^3 \text{ mol}^{-1} \text{ s}^{-1}$ and $k_{-1} = 2.2 \text{ s}^{-1}$. Although these values are rather low, dioxygen interaction with the catalyst complex may be hindered when large thiol and low dioxygen concentrations are applied.

6.3 Side-reactions: accumulation of H_2O_2

6.3.1 Hydrogen peroxide decomposition

From scheme 6.2, it is clear that accumulation of hydrogen peroxide can occur when its formation via step a) proceeds at a higher rate than its decomposition via b). Therefore, kinetic data of both processes are desired, in order to be able to predict the peroxide accumulation and the accompanying deviation from the overall reaction stoichiometry.



First, the second reaction step, b), will be discussed, which has been described⁹⁴⁻⁹⁷⁾ to follow an S_N2-type mechanism according to scheme 6.3. Barton et al.⁹⁴⁾ investigated the kinetics of the conversion of cysteine and cysteamine according to this process. They found a rate dependence that was first order in both H₂O₂ and thiolate anion. The reaction rate constants, calculated according to

$$v_d = - d[\text{H}_2\text{O}_2]/dt = k [\text{RS}^-] [\text{H}_2\text{O}_2] \quad (6.6)$$

were reported to be 10 and 12.4 dm³ mol⁻¹ s⁻¹ for cysteamine and cysteine, respectively. The same kinetic relationship was also mentioned for the conversion of n-propylthiol in a study of Giles et al.^{96,97)}. They reported a rate constant of 7 dm³ mol⁻¹ s⁻¹ (at 25 °C).

Since 2-mercaptoethanol is the substrate used in the kinetic study described here, the kinetics of the reaction of scheme 6.3 for this thiol were examined. The rate of the process was determined spectrophotometrically in dependence of thiol and H₂O₂ concentration, while also the effects of CoPc(NaSO₃)₄ and 2,4-ionene were studied.

The following results were obtained:

- at pH-values above 9, the reaction rate was too high to study the kinetics of the process by the spectrophotometric method;
- for pH \leq 9, the reaction appeared to be first order in H₂O₂ and thiolate anion;
- the rate constant according to equation 6.6 was found to be 4.3 ± 0.8 dm³ mol⁻¹ s⁻¹ when an excess of thiol was used and 12 ± 3 dm³ mol⁻¹ s⁻¹ with an excess of hydrogen peroxide; the result obtained with excess of peroxide is thought to be less reliable, since under these conditions a secondary reaction, probably photo-oxidation of the thiol (ref.⁶³⁾, part 1, ch. 10 and part 2, ch. 17), was observed, seriously disturbing the kinetic measurements; in Fig. 6.5 the effect of the secondary process is

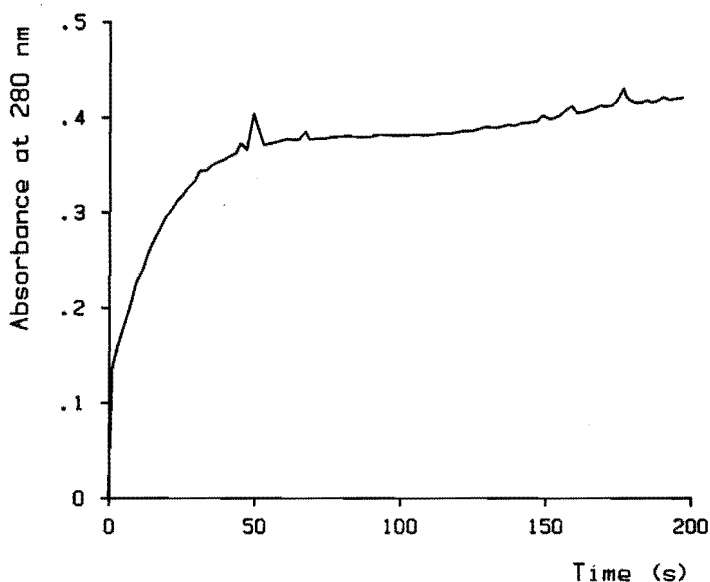


Fig. 6.5 Variation in absorbance at 280 nm with time, during the reaction of an excess of H_2O_2 with 2-mercaptoethanol.

Conditions: nitrogen atmosphere, $[\text{H}_2\text{O}_2]_0 = 0.11 \text{ mol dm}^{-3}$, $[\text{RSH}]_0 = 4.7 \times 10^{-3} \text{ mol dm}^{-3}$, $\text{pH} = 8.0$.

illustrated;

- addition of Co phthalocyanine and/or ionene had no detectable effect on reaction rate.

Especially the latter finding is very important: since the rate of formation of the peroxide (step a), scheme 6.2) depends on both the cobalt and the ionene concentration whereas its decomposition rate (scheme 6.3 or step b) in scheme 6.2) apparently does not, the amount of accumulated hydrogen peroxide will thus depend on these quantities. Moreover, accumulation will, of course, depend on the initial concentrations of thiol and dioxygen.

6.3.2 Simulation of hydrogen peroxide accumulation

In the preceding section it was shown that the kinetics of step b) of scheme 2 can be described by equation 6.6 with $k \approx 4 \text{ dm}^3 \text{ mol}^{-1} \text{ s}^{-1}$. For step

a) it has been demonstrated (section 6.2.1) that the kinetics follow the 2-substrate Michaelis-Menten model ($v_f = d[\text{H}_2\text{O}_2]/dt$, see eq. 6.2).

Thus, for a given initial concentration of thiol and given concentrations of dioxygen and $\text{CoPc}(\text{NaSO}_3)_4$ and with values for C_1 - C_4 at the applied pH, the accumulation of hydrogen peroxide can be calculated by combining both kinetic relationships. Using the values for C_1 - C_4 determined at pH 8.30 and following the numeric calculation procedure described in chapter 3, the following results were obtained.

Increase of the cobalt concentration leads to an increase in peroxide accumulation, as depicted in Fig. 6.6. This is the consequence of the fact that the H_2O_2 formation (step 6.2a) is accelerated by the catalyst, whereas

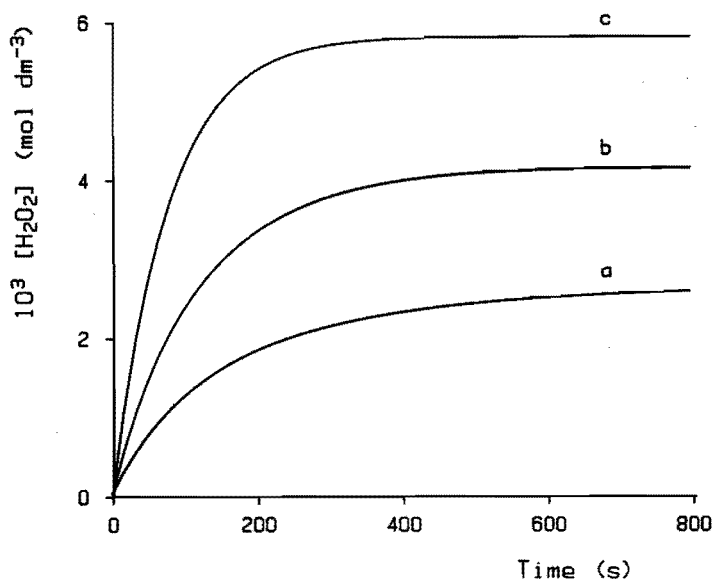


Fig. 6.6 Effect of varying the $\text{CoPc}(\text{NaSO}_3)_4$ -concentration on the simulated H_2O_2 -accumulation curves. Simulations based on eqs. 6.6 and 6.2, with $k = 4 \text{ dm}^3 \text{ mol}^{-1} \text{ s}^{-1}$, $C_1 = 10^3 \text{ s}^{-1}$, $C_2 = 1.5 \cdot 10^{-4} \text{ dm}^3 \text{ mol}^{-1}$, $C_3 = 4 \cdot 10^{-3} \text{ dm}^3 \text{ mol}^{-1}$ and $C_4 = 1.4 \cdot 10^{-2} \text{ dm}^3 \text{ mol}^{-1}$. Conditions: $[\text{O}_2] = 0.00055 \text{ mol dm}^{-3}$, $[\text{RSH}]_0 = 0.02 \text{ mol dm}^{-3}$, $\text{pH} = 8.3$; $[\text{Co}] = 10^{-7}$ (a), $2 \cdot 10^{-7}$ (b) and $4 \cdot 10^{-7} \text{ mol dm}^{-3}$ (c).

the decomposition rate (step 6.2b) is not affected.

Analogously, increase of the dioxygen concentration also causes enhancement of peroxide accumulation.

Variation of the initial thiol concentration results in two types of H_2O_2 accumulation curves, as can be seen in Fig. 6.7a and b. At low $[\text{RSH}]_0$ ($< 0.04 \text{ mol dm}^{-3}$), the curve shows characteristics of pseudo-first-order kinetics and increase of the thiol concentration in this region leads to an increase in peroxide accumulation. However, at high $[\text{RSH}]_0$ the shape of the curve changes: first, the hydrogen peroxide concentration rapidly increases (with an initial rate that is independent of thiol concentration); then, when a certain level is reached which is lower as $[\text{RSH}]_0$ is higher, the amount of accumulated H_2O_2 remains almost constant for a period; finally, the hydrogen peroxide concentration starts to increase again but at a relatively low rate.

These complicated accumulation profiles are due to the fact that the kinetics of the formation of H_2O_2 (step 6.2a, eq. 6.2) change from zeroth to first order in thiolate anion as thiol concentration decreases. The H_2O_2 - "plateau" at high thiol concentration and low conversion indicates that a steady state is reached, i.e. v_f equals v_d in this region.

6.3.3 Accumulation measurements

To verify if the kinetic theory described above is correct, H_2O_2 accumulation curves were measured in dependence of thiol, dioxygen and cobalt concentration, by analyzing samples of the reaction mixtures during the catalytic conversion of thiol.

It was found that, especially for low initial thiol concentrations, these experimental curves were in very good agreement with the simulated profiles; typical examples are shown in Fig. 6.8a and b.

For high $[\text{RSH}]_0$ at low conversions, the measured amounts of peroxide were often too low, compared with the calculated values. This was found to be a result of inadequate mixing of the samples with the concentrated acid that was

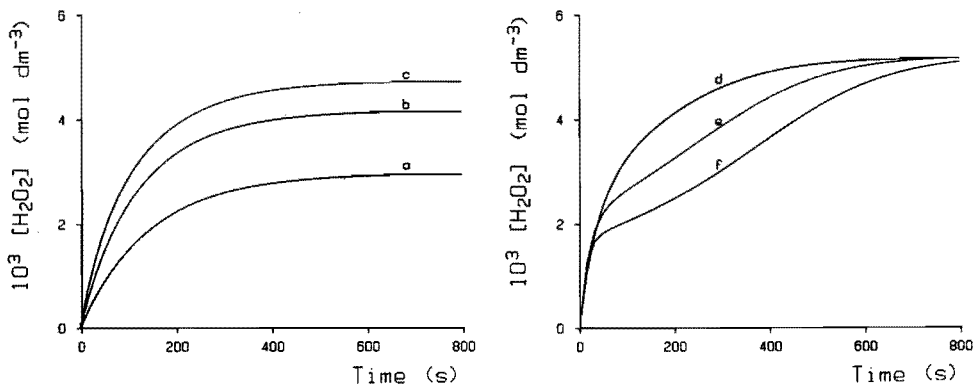


Fig. 6.7 Effect of varying the initial thiol concentration on the simulated H_2O_2 -accumulation curves. Kinetic parameters as in Fig. 6.6.
 Conditions: $[\text{O}_2] = 0.00055 \text{ mol dm}^{-3}$, $[\text{Co}] = 2 \cdot 10^{-7} \text{ mol dm}^{-3}$, $\text{pH} = 8.3$.
 a) Low $[\text{RSH}]_0$: 0.01 (a), 0.02 (b) and 0.03 mol dm^{-3} (c).
 b) High $[\text{RSH}]_0$: 0.06 (d), 0.12 (e) and 0.18 mol dm^{-3} (f).

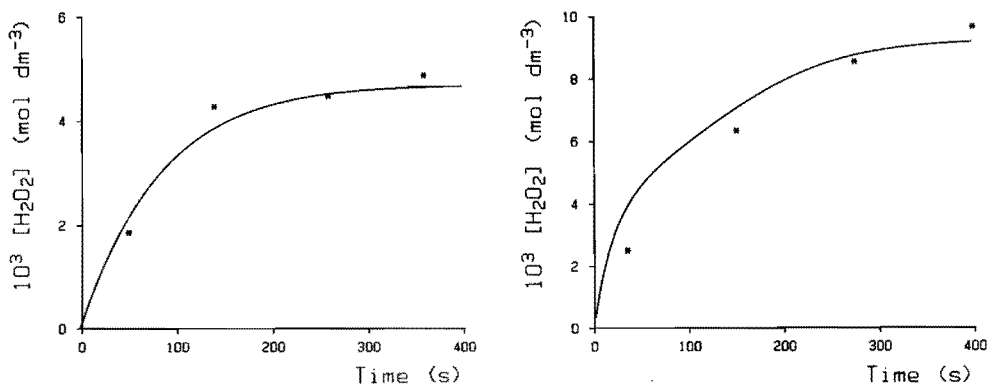


Fig. 6.8 Comparison of experimentally determined (*) and simulated (drawn line) H_2O_2 -accumulation curves. Kinetic parameters as in Fig. 6.6.
 Conditions: $[\text{O}_2] = 0.00055 \text{ mol dm}^{-3}$, $[\text{Co}] = 4 \cdot 10^{-7} \text{ mol dm}^{-3}$, $\text{pH} = 8.3$; $[\text{RSH}]_0 = 0.0142$ (a) and $0.114 \text{ mol dm}^{-3}$ (b).

added in order to quench further reaction (see experimental section). At the moment the sample is taken out of the reactor, the dioxygen concentration is immediately decreased to zero, stopping the H_2O_2 formation process. However, as long as the sample is not sufficiently mixed with the hydrochloric acid, the decomposition reaction of peroxide still continues, at a relatively high rate due to the high thiol concentration. Therefore, the amount of H_2O_2 that is measured, will be too low. Nevertheless, the shape of the obtained experimental curves is very similar to the shape of the calculated ones. It can thus be concluded that the kinetic model satisfactorily describes the H_2O_2 accumulation process.

6.3.4 Influence of H_2O_2 accumulation on catalytic measurements

In our laboratory, the kinetics of catalytic thiol conversion are studied by measuring the dioxygen uptake rate curves. Since the overall stoichiometry of reaction 6.2c will no longer be valid when peroxide is accumulated, the effects of accumulation on dioxygen flow curves had to be studied. Fig. 6.9 shows three of these curves, one experimentally determined (a), the other two simulated, (b) without and (c) with a correction for H_2O_2 accumulation.

At the start of the reaction both simulations deviate from the experimental curve due to the experimental procedure (see section 3.2.6).

Curve 6.9b represents a calculation based on the assumption that no H_2O_2 is accumulated so that the stoichiometry of $\text{RSH} : \text{O}_2 = 4 : 1$ is maintained during the whole process. It is evident that, at high conversions, the experimental curve (6.9a) shows a considerable deviation from this model curve, as was expected. This illustrates very well that, in general, kinetic studies are to be based on initial rates, where the effect of by-products is not yet detectable.

However, in this process it is now possible to obtain more kinetic data from one flow curve, since the complete curve can be analyzed by means of the kinetic model including peroxide accumulation effects. Fig. 6.9 shows that the

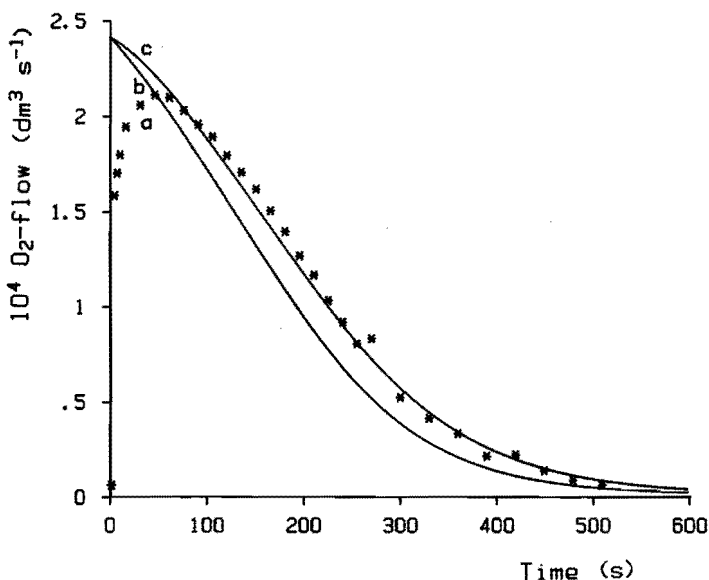


Fig. 6.9 Dioxygen uptake rate curves as experimentally determined (a) and simulated (b, c). Simulation b is based on eq. 6.2 and a constant stoichiometry of $\text{RSH} : \text{O}_2 = 4 : 1$, simulation c is based on eqs. 6.6 and 6.2. Kinetic parameters as in Fig. 6.6.

Conditions: $[\text{O}_2] = 0.0011 \text{ mol dm}^{-3}$, $[\text{Co}] = 2 \cdot 10^{-7} \text{ mol dm}^{-3}$, $[\text{RSH}]_0 = 0.071 \text{ mol dm}^{-3}$, $\text{pH} = 8.3$.

calculated curve according to this model (6.9c) is in good agreement with the experimental result (6.9a).

6.4 Conclusions

Analysis of initial rate dependence on dioxygen and thiolate anion concentrations revealed that the kinetics of the oxidation of 2-mercapto-ethanol as catalyzed by $\text{CoPc}(\text{NaSO}_3)_4/\text{ionene}$ can be very well described by a two-substrate Michaelis-Menten model.

Only at high thiol concentrations in combination with low dioxygen pressures, serious deviations from this model were observed, probably as a

result of occupation of dioxygen binding sites by excess thiolate anions. Stopped-flow measurements indicated that coordination of two thiol ligands to the catalyst complex indeed is possible.

In order to be able to describe complete dioxygen uptake rate curves for the catalytic oxidation of thiol, it appeared necessary to include the H_2O_2 accumulation process in the kinetic equations. Formation of the peroxide could be described by the Michaelis-Menten rate equation (6.2), whereas the H_2O_2 decomposition reaction followed kinetics that were first order in both H_2O_2 and thiolate anion (eq. 6.6). Accumulation curves and dioxygen uptake rate curves could be very well predicted on the basis of these kinetic equations.

The knowledge on hydrogen peroxide accumulation was applied in performing the investigations of the next chapter. Complete dioxygen flow curves were then used for kinetic analyses, the data being corrected for accumulated H_2O_2 .

7 EFFECTS OF VARYING REACTION CONDITIONS ON THE KINETIC PARAMETERS; MECHANISTIC CONSIDERATIONS

7.1 General features

7.1.1 pH variation

pH-Effects on catalytic activity were measured for several dioxygen and thiol concentrations, so that it was possible to determine how each kinetic parameter is affected by changing the pH (Table 7.1). Also the effect on the overall activity was established, as illustrated in Fig. 7.1.

Keeping [RSH] constant (Fig. 7.1a), the catalytic activity showed an optimum around pH 9.5. The activity increase up to a pH of 9.5 was due to the increasing degree of thiol dissociation, as is evident from the pH independence at constant [RS⁻] in this region (Fig. 7.1b). This effect is also reflected in the fact that k_1 is practically independent of pH. (Table 7.1).

Above pH 9.5, activity decreases both at constant thiol and thiolate anion concentration. This rate decrease is mainly due to a decreasing

Table 7.1 Effects of pH on kinetic parameters^{a,b}.

pH	$10^{-5}k_1$	$10^{-2}k_{-1}$	$10^{-2}K_1$	$10^{-6}k_2^{\text{min } c}$	$10^{-3}K_2^{\text{min } c}$	$10^{-2}k_3$
7.9	3	50	0.5	13	14	9
8.3	3	40	0.7	7	7	10
8.85	1.1	6	2	3	3	10
9.5	5	7	7	3	3	10
10.5	2	1.4	17	2	3	9
11.5	1.3	1.1	11	1.9	3	8
12.3	1.3	0.6	20	1.7	3	5
13	4	1.2	30	1.6	5	3

^a 2,4-ionene, thiol: 2-mercaptoethanol

^b k_1 and k_2^{min} in $\text{dm}^3 \text{mol}^{-1} \text{s}^{-1}$, k_{-1} and k_3 in s^{-1} , K_1 and K_2^{min} in $\text{dm}^3 \text{mol}^{-1}$

^c $k_2^{\text{min}} = k_3/C_2$ ($k_{-2} \ll k_3$), $K_2^{\text{min}} = 1/C_2$ ($k_{-2} \gg k_3$)

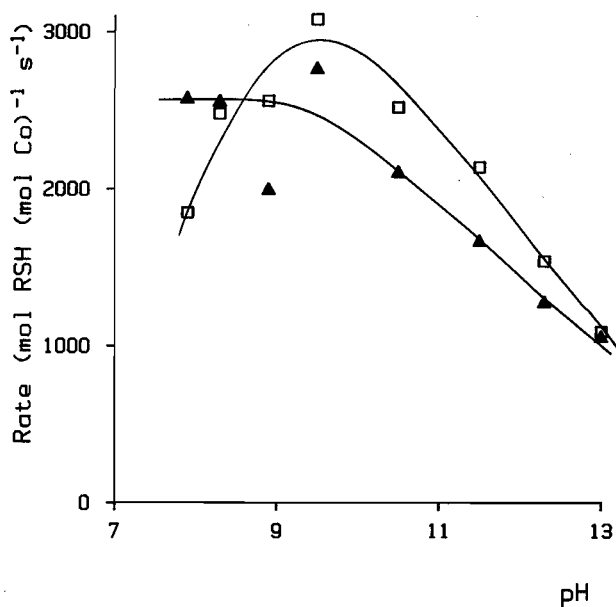


Fig. 7.1 Effect of pH on overall reaction rate at constant thiol concentration (a) and constant thiolate anion concentration (b).
 a) $[O_2] = 0.0011 \text{ mol dm}^{-3}$, $[RSH] = 0.14 \text{ mol dm}^{-3}$ (□)
 b) $[O_2] = 0.0011 \text{ mol dm}^{-3}$, $[RS^-] = 0.014 \text{ mol dm}^{-3}$ (▲)
 Other reaction conditions: $[N^+] = 10^{-3} \text{ mol dm}^{-3}$, 2,4-ionene was used, thiol: 2-mercaptoethanol.

efficiency of the product formation step, i.e. to a decrease in rate constant k_3 (Table 7.1). In section 7.2.2, the variation of kinetic parameters with pH will be further discussed.

7.1.2 Ionene variation

Based on the results reported previously by Brouwer et al.⁵⁴, it was expected that variation of the ionene charge density would lead to a parallel variation in overall activity, due to changes in local thiolate anion concentration.

Indeed, it was found that the activity increases with increasing charge density (Fig. 7.2). Within the series of x,y-ionenes, where x and y were varied between 2 and 6, the observed relationship was linear. The 2,xyl-ionene, containing aromatic groups in the polymer backbone, showed a lower activity than was expected on the basis of its calculated linear charge density. This is probably due to the fact that the 2,xyl-ionene chains have a longer persistence length and, thus, a lower coil density than the flexible x,y-ionene chains, leading to a lower electrostatic potential (see section 7.2.3).

It was established which reaction rate constants are responsible for the observed variations in overall activity. As can be seen in Table 7.2,

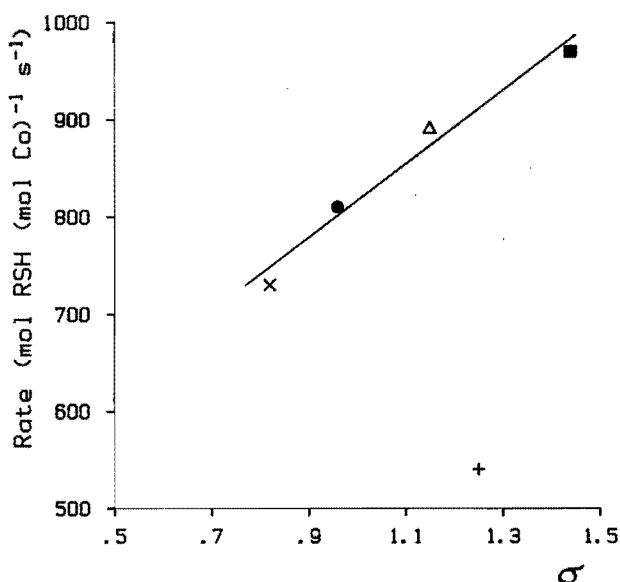


Fig. 7.2 Dependence of reaction rate on the linear charge density parameter, σ , of several ionenes; ■: 2,4-ionene, △: 2,6-ionene, ●: 6,4-ionene, x: 6,6-ionene, +: 2,xyl-ionene.

$[\text{O}_2] = 0.00055 \text{ mol dm}^{-3}$, $[\text{RSH}] = 0.017 \text{ mol dm}^{-3}$, $\text{pH} = 8.9$, $[\text{N}^+] = 10^{-3} \text{ mol dm}^{-3}$, thiol: 2-mercaptoethanol.

Table 7.2 Kinetic parameters for several ionenes^a.

ionene ^b	$10^{-5}k_1$	$10^{-2}k_{-1}$	$10^{-2}K_1$	$10^{-6}k_2^{\min}$	$10^{-3}K_2^{\min}$	$10^{-2}k_3$
2,4	1.1	6	2	3	3	10
2,6	1.3	2	7	1.4	1.4	10
6,4	1.5	2	8	1.0	1.1	9
6,6	1.1	1.3	8	1.0	1.1	9
2,xyl	0.6	0.2	30	0.8	0.8	10

^a conditions: pH = 8.85, thiol: 2-mercaptoethanol

^b linear charge density parameters: 2,4-ionene: 1.44, 2,6-ionene: 1.15, 6,4-ionene: 0.96, 6,6-ionene: 0.82, 2,xyl-ionene: 1.25

^c for dimensions and definitions of k_2^{\min} and K_2^{\min} : see Table 7.1

surprisingly k_1 , in fact an apparent rate constant also accounting for differences in local $[RS^-]$, remained almost constant within the x,y-ionene series. Thus, it must be concluded that the local thiolate anion concentration is not the determining factor in the different activities of these ionenes (presumably, variations in linear charge density are compensated by variations in coil dimensions). On the other hand, it was calculated that the decrease of activity on going from 2,4- to 6,6-ionene was predominantly caused by a (small) increase of C_2 (decrease of k_2 or K_2). For 2,xyl-ionene, the low value of k_1 and the high C_2 -value appeared to contribute to its low activity. In all cases, the effects of k_1 and C_2 were partly compensated by changes in k_{-1} . These effects will be discussed in more detail in section 7.2.4.

7.1.3 Thiol variation

By varying the R-group of RSH, it is also possible to obtain mechanistic information. Especially the charge on the R-group seemed an interesting parameter in the polyelectrolyte catalytic system. It was expected that thiols carrying a highly negative charge would be relatively more concentrated within the polymer coil domains and the oxidation of these thiols would therefore be

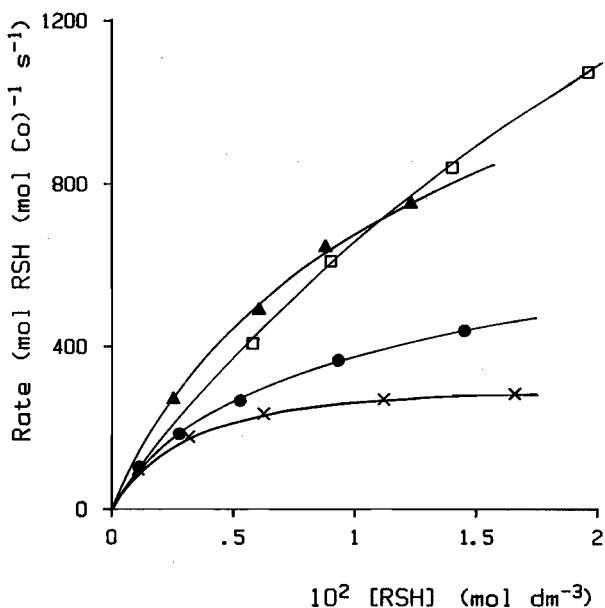


Fig. 7.3 Reaction rate versus thiol concentration for the oxidation of 2-mercaptoethanol R^0SH (□), aminoethanethiol R^+SH (▲), cysteine $R^\pm SH$ (●) and mercaptoacetic acid R^-SH (x).
 $[O_2] = 0.00055 \text{ mol dm}^{-3}$, $pH = 8.9$, $[N^+] = 10^{-3} \text{ mol dm}^{-3}$, 2,4-ionene was used.

enhanced. To verify this assumption, the following thiols were used in catalytic experiments and compared with the previously investigated mercaptoethanol ($R^0 = -CH_2CH_2OH$): mercaptoacetic acid ($R^- = -CH_2COO^-$), cysteine ($R^\pm = -CH_2CH(COO^-)NH_3^+$) and aminoethanethiol ($R^+ = -CH_2CH_2NH_3^+$).

Fig. 7.3 shows the activities for these thiols at $pH = 8.9$ and constant dioxygen concentration. It clearly shows, that, in contrast to what was expected, aminoethanethiol and mercaptoethanol are being oxidized at a higher rate than the thiols carrying negatively charged R-groups, although the values for k_1 (Table 7.3) indicate that the latter compounds are indeed more concentrated locally than the uncharged or positively charged thiols. The activity differences are mainly caused by different k_3 -values (Table 7.3) and

Table 7.3 Kinetic parameters for several thiols^a.

thiol ^b	$10^{-5}k_1$	$10^{-2}k_{-1}$	$10^{-2}K_1$	$10^{-6}k_2^{\text{min}}$	$10^{-3}k_2^{\text{min}}$	$10^{-2}k_3$
R^-SH	11	3	30	0.8	8	1.0
R^0SH	1.1	6	2	3	3	10
$R^\pm SH$	0.5	1.5	3	1.4	7	2
R^+SH	0.4	0.6	7	2	3	6

^a conditions: 2,4-ionene, pH = 8.85 at which the degrees of thiol dissociation, $[RS^-]/[RSH]$, are 0.05 for R^-SH , 0.26 for R^0SH , 0.58 for $R^\pm SH$ and 0.86 for R^+SH

^b R^-SH = mercaptoacetic acid, R^0SH = mercaptoethanol, $R^\pm SH$ = cysteine, R^+SH = aminoethanethiol

^c for dimensions and definitions of k_2^{min} and K_2^{min} : see Table 7.1

will be further discussed in section 7.2.5.

7.2 Effects on individual kinetic parameters; reaction mechanism

7.2.1 Postulation of mechanism

With the aid of the dependence of the kinetic parameters on pH (Table 7.1), ionene charge density (Table 7.2) and type of thiol (Table 7.3; all data are summarized in Table 7.4), the reaction mechanism of the ionene-promoted catalytic thiol oxidation was evaluated in detail.

The model of scheme 6.1 formed the basis of this evaluation. However, it was taken into account that this scheme is only a simplified representation of the process because each presented reaction step in reality consists of more than one step, viz. coordination and electron transfer (redox) steps.

Furthermore, an alternative mechanism was considered, in which the first kinetically perceptible reaction step is the interaction of dioxygen with the RS^- -Co-complex. Formation of that complex was then regarded as a saturated pre-equilibrium, whereas the addition of the second thiolate anion (necessary

Table 7.4 Summary of effects of reaction conditions on kinetic parameters and overall reaction rate^a.

	k_1	k_{-1}	K_1	k_2 or k_2	k_3	rate ^b
pH						
7.9 --> 10	0	-	+	-	0	+ ^c
10 --> 13	0	0	0	0	[-]	-
ionene						
2,xyl --> x,y	[+]	+	-	+	0	+
6,6 --> 2,4	0	+	-	[+]	0	+
R (RSH)						
$R^- \rightarrow R^0$	-	+ ^d	- ^d	+	[+]	+
$R^0 \rightarrow R^+$	[-]	- ^d	+ ^d	-/0	[-]	-

^a - = decrease, + = increase, 0 = constant; the symbols [+] and [-] denote the rate constants contributing most to the observed differences in overall reaction rate

^b keeping all other conditions constant

^c [RSH] is constant; if [RS⁻] is constant, then the rate is also constant

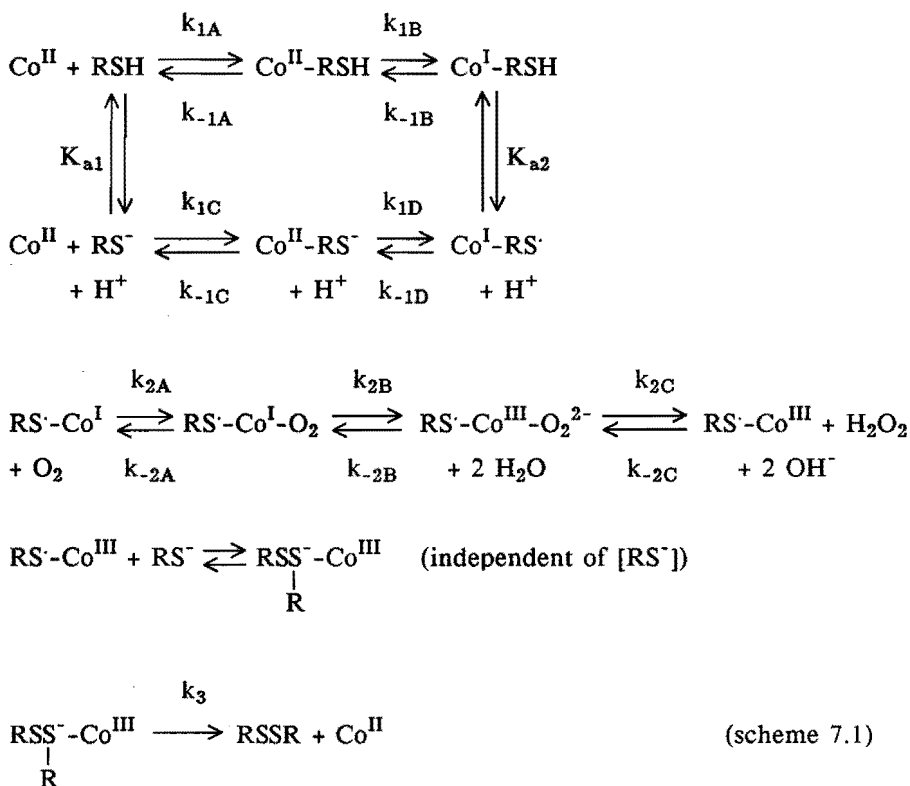
^d at constant pH; expected at constant [RSH]/[RS⁻]: k_{-1} +, K_1 -

to form RSSR) was assumed to be responsible for the observed Michaelis-Menten kinetics in thiol. In the mechanism of scheme 6.1, the rate of the addition of the second thiolate anion is assumed to be independent of thiol concentration. Both these mechanisms are in agreement with the observation that the catalytic thiol oxidation does not show second order kinetics in thiol.

A third possible mechanism, in which the first reaction is the addition of dioxygen to CoPc(NaSO₃)₄, was rejected since it has been demonstrated spectroscopically that no interaction occurs between dioxygen and the ionene-bound metal complex (see section 5.1).

On the basis of all kinetic data obtained, the mechanism of scheme 6.1 appeared to be the most probable reaction pathway. In scheme 7.1, where Co

represents $\text{CoPc}(\text{NaSO}_3)_4$, a more detailed description can now be given, which is proposed as the mechanism for the ionene-promoted process. Further argumentation for the choice of this mechanism, based on various experimental observations, follows below.



7.2.2 pH-effects

The value of k_1 appeared to be very sensitive to small changes in thiol concentration caused by small variations in H_2O_2 -accumulation (see section 3.3) and therefore k_1 could not be determined very accurately. Nevertheless, it could be concluded that this rate constant does not change significantly

within the pH-range investigated (7.9-13) and has a value of $2.6 \pm 1.4 \cdot 10^5 \text{ dm}^3 \text{ mol}^{-1} \text{ s}^{-1}$. The constancy of k_1 is in good agreement with the fact that the reactivity of the thiol molecule is negligible as compared to that of the thiolate anion^{38,54} ($k_{1A}, k_{1B} \ll k_{1C}, k_{1D}$), which was implemented in the kinetic equation 6.2.

The largest pH effect was found for k_{-1} , although its effect on the overall reaction rate was calculated to be rather small. It was found, that k_{-1} decreases on going from pH 7.9 to about 10, while at still higher pH values k_{-1} remained constant. This suggests the involvement of an acid/base-equilibrium in this reaction step with a pK_a around 9. Since mercaptoethanol has a pK_a of 9.3 under reaction conditions, this thiol, coupled to the catalyst, seemed a likely candidate for this equilibrium. Therefore, an attempt was made to describe the pH dependence of k_{-1} by assuming two parallel Co-thiol dissociation routes for both the protonated and unprotonated thiol form, as presented in scheme 7.1.

The following set of equations corresponds to this model:

$$k_{-1} = (1-\alpha) k_{-1}^{\text{RSH}} + \alpha k_{-1}^{\text{RS}^-} \quad (7.1)$$

$$\alpha = 1/(10^{pK_{a2}-pH} + 1) \quad (7.2)$$

where k_{-1}^{RSH} (a combination of k_{-1A} and k_{-1B}) and $k_{-1}^{\text{RS}^-}$ (k_{-1C} and k_{-1D}) are the rate constants for the dissociation of the Co-RSH-complex and the Co-RS⁻-complex, respectively, and K_{a2} is the apparent acid dissociation constant of the Co-RSH-complex (either in the Co^{II} or in the Co^I state). With $k_{-1}^{\text{RSH}} = 6 \cdot 10^3 \text{ s}^{-1}$, $k_{-1}^{\text{RS}^-} = 10^2 \text{ s}^{-1}$ and $pK_{a2} = 8.4$, a good fit of the experimentally determined k_{-1} -values was obtained, as can be seen in Fig. 7.4. Apparently, the acidity of the thiol is increased upon its binding to the phthalocyanine complex. The fact that the RSH complex reacts at a much higher rate than the deprotonated form, probably results from the electron withdrawing property of RSH which will cause weakening of the Co-RSH bond.

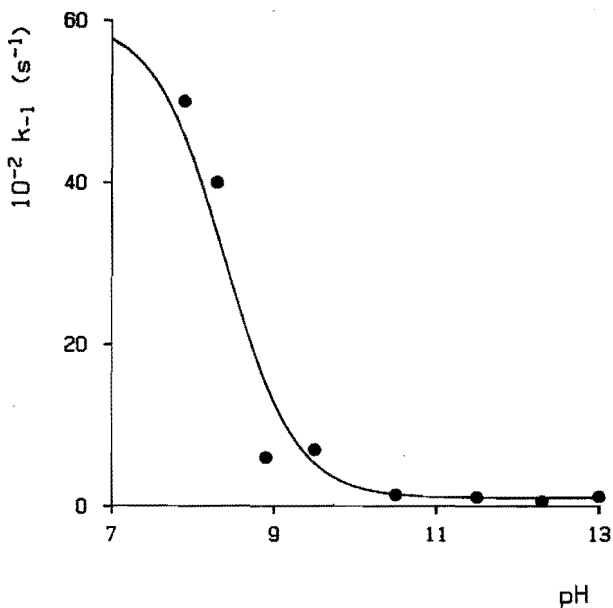


Fig. 7.4 Rate constant k_{-1} as a function of pH.

Data points obtained from fitting the kinetic results to eq. 6.2, drawn curve calculated according to eqs. 7.1 and 7.2, assuming $k_{-1}^{\text{RSH}} = 6000 \text{ s}^{-1}$, $k_{-1}^{\text{RS}^-} = 100 \text{ s}^{-1}$ and $\text{p}K_{\text{a}2} = 8.4$.

Concerning the dioxygen addition to the $\text{Co}^{\text{I}}\text{-RS}^-$ -complex, also a small pH-dependence was observed. However, it is difficult to draw conclusions from this, because k_{-2} can not be determined and therefore it remains unknown whether a kinetic effect is measured (if $k_{-2} \ll k_3$ then $k_2 = k_3/C_2$, see equation 6.2) or a thermodynamic effect (if $k_{-2} \gg k_3$ then $K_2 = 1/C_2$). Thus, either k_2 or K_2 decreases with increasing pH until $\text{pH} \approx 8.5$, after which constant values are reached ($k_2 = 2.2 \pm 0.6 \cdot 10^6 \text{ dm}^3 \text{ mol}^{-1} \text{ s}^{-1}$ and $K_2 = 3.3 \pm 0.8 \cdot 10^3 \text{ dm}^3 \text{ mol}^{-1}$). Presumably, the acid dissociation of water plays a role in this pH dependence since the effect is largest around pH 7. Moreover, it seems very likely that the presence of OH^- hinders the formation of peroxide as shown in scheme 7.1.

Finally, the rate constant of the product formation step, k_3 , appeared to be constant for $7.9 \leq \text{pH} \leq 11$. At high pH, however, k_3 was observed to

decrease. This may be due to one of the following effects: (1) OH^- stabilizes (inactivates) the ternary reaction intermediate or (2) large amounts of hydroxide ions induce the formation of (small amounts of) the inactive μ -peroxo Co complex^{45,68,84} (see also section 5.1), thus lowering the efficiency of the catalyst.

7.2.3 Varying the type of ionene: conformational and structural effects

Before discussing the dependence of the kinetic parameters on the type of ionene, the effects of varying the ionene structure on chain conformation and catalyst structure have to be considered. As the alkyl and xylyl segments were regarded as chemically inert, direct effects of ionene structure elements on reaction kinetics have not been taken into account.

With respect to chain conformation, it is clear that 2,xyl-ionene differs considerably from the x,y-ionenes, since the latter compounds consist of flexible chains, whereas 2,xyl-ionene contains aromatic groups in the polymer backbone, keeping the $\text{N}^+ - \text{N}^+$ distances more or less fixed. Therefore, the x,y-ionenes will exhibit higher coil densities than the 2,xyl-ionene, accompanied by higher electrostatic potentials, leading to stronger enhancement of the thiolate anion concentration within the polymer coil domains ($[\text{RS}^-]_{\text{local}}$). This will be shown to affect thiol oxidation kinetics.

Within the x,y-ionene series, differences in electrostatic potential will probably be rather small, since the variation in linear charge density will be (at least partly) compensated by changes in coil dimensions: while the 2,4-ionene chains will be largely expanded due to repulsion between the closely spaced positive charges, the chains of e.g. 6,6-ionene may be more contracted since the repulsion will be less along the longer alkyl segments. Therefore, only minor differences in $[\text{RS}^-]_{\text{local}}$ within this ionene series are expected.

Apart from the effect on thiolate enrichment within the polymer domains, the ionene charge density, or more precisely the electrostatic potential, may also affect another quantity, viz. the degree of aggregation of the cobalt

catalyst. The importance of this phenomenon has been discussed in chapter 5, in which it was demonstrated that the aggregated phthalocyanine complex is far more active in the catalytic thiol autoxidation than its monomeric form (section 5.3).

For the ionenes discussed here, the degree of aggregation was spectroscopically studied (see sections 4.1.2, 4.1.3 and 5.2.1), revealing that the 2,xyl-ionene system contains only dimers, whereas the x,y-ionenes contain higher aggregates. In the next section, it will be demonstrated that the degree of phthalocyanine aggregation is an important factor influencing reaction kinetics.

It would have been interesting to include 2,10-ionene in these kinetic investigations, since this ionene stabilizes the catalyst complex in its monomeric form (chapter 5). However, the activity of this system was too low to allow determination of the kinetic parameters with sufficient accuracy. Moreover, the kinetic behaviour of this system was observed to be complicated by a deviation from first-order kinetics in Co (section 5.3.2).

7.2.4 Effects of the type of ionene on kinetic parameters

Looking at Table 7.2, it is evident that k_1 is not very sensitive to charge density changes. Between the x,y-ionenes ($k_1 = 1.3 \pm 0.2 \cdot 10^5 \text{ dm}^3 \text{ mol}^{-1} \text{ s}^{-1}$) and 2,xyl-ionene the observed difference in this rate constant is only a factor of 2. Nevertheless, this relatively small decrease of k_1 was calculated to be the most important factor determining the lower overall activity of the 2,xyl-ionene. The lowering of k_1 is probably a result of the lowered local thiolate anion concentration due to the decreased charge density. Within the x,y-ionene series, k_1 , and thus $[\text{RS}^-]_{\text{local}}$, appears to be constant, indicating that differences in linear charge density are indeed (at least partly) compensated by coil dimensions, as was discussed above.

The value of k_1 varies considerably (Table 7.2); even within the x,y-ionene series the observed variation is significant. If this variation was

caused by a shift in electrostatic potential leading to a shift in the K_{a2} equilibrium, one would expect an increase of k_{-1} with decreasing charge density: as was stated in the discussion on pH effects (section 7.2.2), $k_{-1}^{RSH} \gg k_{-1}^{RS^-}$ and a system with low charge density, where $[RSH]_{local}$ is relatively high, should therefore exhibit a high value for k_{-1} . Instead, it was found that k_{-1} strongly decreases on going from 2,4- to 2,xyl-ionene (by a factor of 30 !).

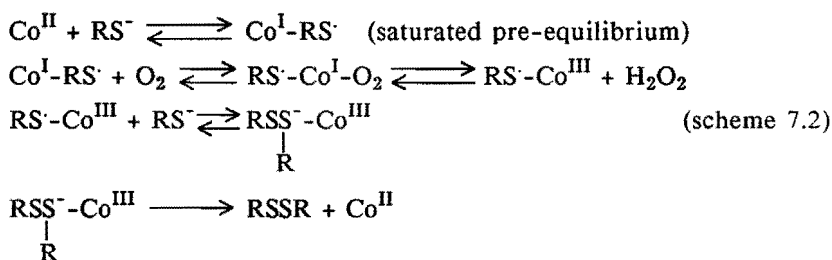
A possible explanation for this phenomenon can be found in the variation of the degree of cobalt aggregation on varying the type of ionene. In the 2,xyl-ionene system only dimers occur, while the x,y-ionenes stabilize higher aggregates. If transfer of electrons from Co^I to RS^{\cdot} (k_{-1B} or k_{-1D}) is facilitated by an increase in the degree of aggregation, this would account for the observed variation in k_{-1} . It would also be in good agreement with the results of Nevin et al.⁹²⁾, who found that tetranuclear phthalocyanine complexes are more efficient reductors than the analogous mononuclear or dinuclear complexes. It must be noted, that this argumentation implies a variation of the degree of aggregation even within the x,y-ionene series, which appeared impossible to prove spectroscopically. Nevertheless, it is postulated that the observed charge density effect on k_{-1} is a result of the dependency of k_{-1B} and/or k_{-1D} on the degree of aggregation of the cobalt catalyst.

Based on the foregoing, it is obvious that reaction step 2B (scheme 7.1) must also show a dependence of reaction rate on charge density, because an analogous electron transfer is involved as was discussed above. Indeed, an increase in C_2 (decrease in k_2 or K_2) with decreasing charge density was recorded, but the effect was very small. This may be due to one of the following reasons: (1) the redox step (2B) is much faster than the coordination of dioxygen to the catalyst complex (2A), so that the rate of the latter step determines the observed k_2 value; (2) if $k_3 \ll k_{-2}$ only a thermodynamic effect is measured and a change in charge density probably

affects k_{2B} and k_{-2B} equally. On the basis of the present results it is impossible to discriminate between these possibilities.

The rate constant for product formation, k_3 , was found to be constant for all ionenes investigated. This implies that neither local concentration effects, nor aggregate-facilitated Co oxidation play a role during this step. This is consistent with the proposed mechanism of scheme 7.1, where peroxide formation takes place in step 2 and the second thiolate anion addition is assumed to be kinetically not detectable.

The constancy of k_3 was also the main reason why the alternative mechanism, based on the assumption that the first kinetically perceptible step is the addition of dioxygen, was rejected. If, according to that mechanism, peroxide formation would take place before the formation of disulfide, the reaction scheme would become:



This scheme corresponds to a so-called ping-pong mechanism⁹⁸⁾ which is described by a kinetic equation of the form of formula 7.3:

$$v = \frac{a [\text{Co}]}{1 + b/[\text{O}_2] + c/[\text{RS}^-]} \quad (7.3)$$

However, the obtained kinetic data presented in this thesis can not be fitted to this equation satisfactorily. Thus, it can be concluded that scheme 7.2

does not provide an appropriate representation of the catalytic process.

7.2.5 Effects of varying the type of thiol

Variation of the R-group of RSH leads to large variations in overall reaction rate and kinetic parameters (esp. k_1 and k_3), as was demonstrated in Fig. 7.3 and Table 7.3. The value of k_1 increases with increasing negative charge on the thiolate anion. This is in accordance with expectation, since negatively charged species will be attracted more by the positively charged ionene than species carrying no net charge and will thus be more concentrated within the polymer domains (in the vicinity of the polymer-bound catalyst complex).

The behaviour of k_{-1} is much more complicated; this rate constant increases in the order: $R^+SH < R^\pm SH < R^-SH < R^0SH$. Probably, this is due to different degrees of thiol dissociation at the applied pH. Considering the pH-effects, it was discussed above that $k_{-1}^{RS^-} \ll k_{-1}^{RSH}$. Therefore, the obtained value of k_{-1} for aminoethanethiol will be relatively small ($\approx k_{-1}^{RS^-}$), because this thiol is dissociated to a large extent at pH 8.9. On the other hand, the thiol-group of mercaptoacetic acid is hardly dissociated at this pH and thus, k_{-1} will be relatively large ($\approx k_{-1}^{RSH}$). On these grounds, it is estimated that, at a constant $[RSH]/[RS^-]$ -ratio, k_{-1} will increase in the following order: $R^-SH \ll R^\pm SH < R^0SH < R^+SH$. This order was expected and can be easily understood, since electron transfer to RS^\cdot (k_{-1B} or k_{-1D}) will be more difficult when the R-group is negatively charged (electron donating).

The effect of changing the type of thiol on C_2 (k_2 or K_2) is rather small, leading to the conclusion that electron donating or withdrawing properties of the thiols are not very important in this reaction step. This means, that the electron transfer step (k_{2B}) is not the determining factor in the observed rate effect. Therefore, either a thermodynamic effect is being measured or k_{2A} is determining the value of k_2 , which was also concluded on the basis of the charge density effects (vide supra).

Finally, k_3 appeared to depend strongly on the type of thiol. Very low values were found for mercaptoacetic acid and cysteine (10 and 5 times lower than for mercaptoethanol, respectively). This may be due to the position of the (saturated) equilibrium preceding the product formation step 3. Since the Co-bound thiol ligands in question are already carrying negatively charged groups ($R^-S^-Co^{III}$), it is likely that addition of a second thiolate anion will be relatively unfavourable because of repulsion. On the other hand, a positively charged R-group may exert an electron withdrawing effect and thus retard the electron transfer from RSS^-R to Co^{III} , lowering k_3 . This explains the observed order of increase for k_3 : $R^-SH < R^\pm SH \ll R^+SH < R^0SH$.

7.3 Conclusions

Summarizing all kinetic data (see Table 7.4) and the discussion above, it can be concluded that:

- the efficient oxidation of thiols requires a high thiolate anion concentration in the vicinity of the cobalt catalyst ($[RS^-]_{local}$), since $k_1^{RSH} \ll k_1^{RS^-}$. The local thiolate concentration can be increased by increasing the pH and the negative charge on the R-group of the thiol. Furthermore, $[RS^-]_{local}$ is enhanced by a high electrostatic potential on the ionene, which is, however, not directly related to the linear charge density of the polymer. Therefore, the differences in activity of the x,y-ionenes can not be explained on the basis of differences in thiolate enrichment.
- a low charge density of the ionene, leading to a low degree of phthalocyanine aggregation, gives rise to a decreasing efficiency for electron transfer from Co to substrates. Presumably, the degree of aggregation varies even within the x,y-ionene series, accounting for the different activities observed.
- the dissociation of the Co^I-RS^- -complex (k_{-1}) appears to be affected by

the above-mentioned aggregation effect. This reaction step is acid catalyzed, as became evident from the dependence of k_{-1} on pH and $pK_a(\text{thiol})$.

- the overall reaction rate is largely dependent on k_3 , that decreases upon increasing the pH above 11, or when the R-group of the thiol is more negatively charged.

The observed dependencies of the kinetic parameters on pH, the type of ionene and the type of thiol, can be combined with the general kinetic characteristics of the polymer-promoted catalytic system (two-substrate Michaelis-Menten model) to give a reaction mechanism of the form of scheme 7.1.

8 POLYELECTROLYTE-PROMOTED CATALYTIC OXIDATION OF A HYDROPHOBIC THIOL

8.1 Introduction

In the previous chapters, an elaborate study was presented on structural and kinetic aspects of the polyelectrolyte-promoted autoxidation of thiols using $\text{CoPc}(\text{NaSO}_3)_4$ as a catalyst. In order to obtain mechanistic information, a well-defined homogeneous system was investigated. Thus, 2-mercaptoethanol was chosen as a model substrate, since it is well soluble in the reaction medium (water), as is the corresponding disulfide.

However, it is also very interesting to study whether hydrophobic thiols can be oxidized by using this type of catalyst systems and, if possible, to determine how the mechanism of the process is affected by the thiol hydrophobicity.

Brouwer et al.⁹⁹⁾ reported previously, that the oxidation of 1-dodecane-thiol is indeed enhanced by ionenes. Nevertheless, the efficiency of the process was found to be rather poor as compared with that of 2-mercaptoethanol (the maximum observed rate was lower by a factor of about 10). Furthermore, the kinetic data were treated as for a homogeneous system, which may not be completely justified.

Therefore, this hydrophobic thiol oxidation has now been investigated in more detail and reaction conditions have been further optimized. In this chapter, the possibilities and limitations of ionenes in the catalytic conversion of dodecanethiol are discussed, as well as the mechanism of this process in comparison with its homogeneous counterpart.

8.2 Results and discussion

8.2.1 Reaction procedure

When an oxidation experiment with 1-dodecanethiol is performed according to the method developed for mercaptoethanol (see section 3.2.6), a dioxygen uptake rate curve is obtained as depicted in Fig. 8.1a. It clearly demonstrates that, after the reaction has started, the reaction rate slowly increases, although the amount of thiol present is, of course, decreasing. Only when about 35% of the thiol is converted, the rate starts to decrease again.

Apparently, optimum reaction conditions are reached after a relatively long period on reaction time scale, most probably as a result of slow mixing of the thiol with the catalyst system, since the reaction is started by adding the thiol to the dioxygen-saturated catalyst mixture. It can be expected that mixing of the hydrophobic substrate with the hydrophilic $\text{CoPc}(\text{NaSO}_3)_4/$

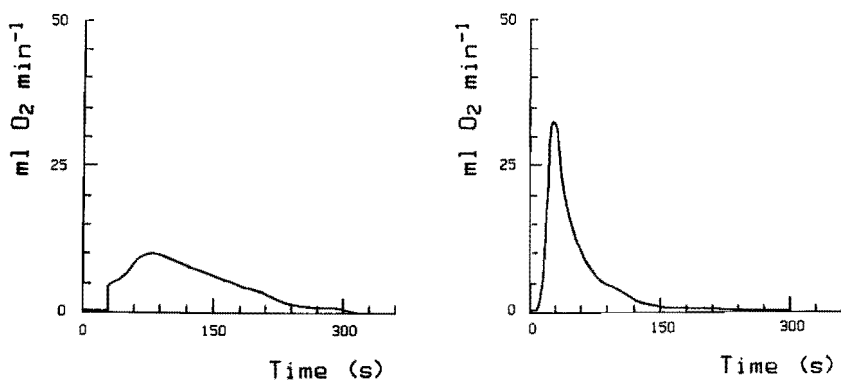


Fig. 8.1 Dioxygen uptake rate curves for the catalytic oxidation of 1-dodecanethiol according to different reaction procedures (see text).
Conditions: $\text{pH} = 13$, $[\text{RSH}]_0 = 0.021 \text{ mol dm}^{-3}$, $[\text{N}^+] = 10^{-3} \text{ mol dm}^{-3}$,
 $[\text{Co}] = 10^{-6} \text{ mol dm}^{-3}$, polymer promotor: 2,4-ionene ($M_n = 7400$).
a) Reaction started by thiol addition.
b) Reaction started by $\text{CoPc}(\text{NaSO}_3)_4$ addition.

/ionene system requires some time to reach equilibrium conditions.

In order to verify this assumption, the reaction procedure was somewhat adapted: first the ionene solution was mixed with the thiol and then the reaction was started by introducing the cobalt complex. The result of this procedure is illustrated in Fig. 8.1b. It is evident, that the maximum reaction rate is now reached almost immediately after starting the reaction, confirming the above-mentioned hypothesis. Since the thiol concentration at this point is still high, also the observed rate is higher than was found for the conventional reaction procedure.

Because the above described method leads to less complicated kinetic behaviour, further experiments were performed according to this method.

8.2.2 Thiol dispersion in the reaction medium

On the basis of the very low solubility of dodecanethiol in aqueous media ($3 \cdot 10^{-5} \text{ mol dm}^{-3}$ at $50 \text{ }^\circ\text{C}^{100}$), it was expected that a two-phase system would be formed upon mixing the thiol with the catalyst solution. Indeed, phase-separation was observed without stirring, especially at low ionene concentrations. At high ionene concentrations an emulsion-like system was obtained, suggesting that the 2,4-ionene exhibits some surface-active characteristics.

In such a two-phase system, where the substrate exists mainly in one phase and the catalyst in the other, reaction rate should depend largely on stirring speed, since this (at least partly) determines the contact surface between the two phases. However, reaction rate also depends on stirring speed because gas-phase dioxygen has to be sufficiently mixed with the reaction solution. To discriminate between these effects, the rate dependence on stirring speed was determined for both 2-mercaptoethanol and 1-dodecanethiol. The results are depicted in Fig. 8.2, which clearly shows that low stirring speeds lead to insufficient dioxygen transport to the reaction solution, limiting reaction rate. At 1500 rpm this problem is overcome, as can be

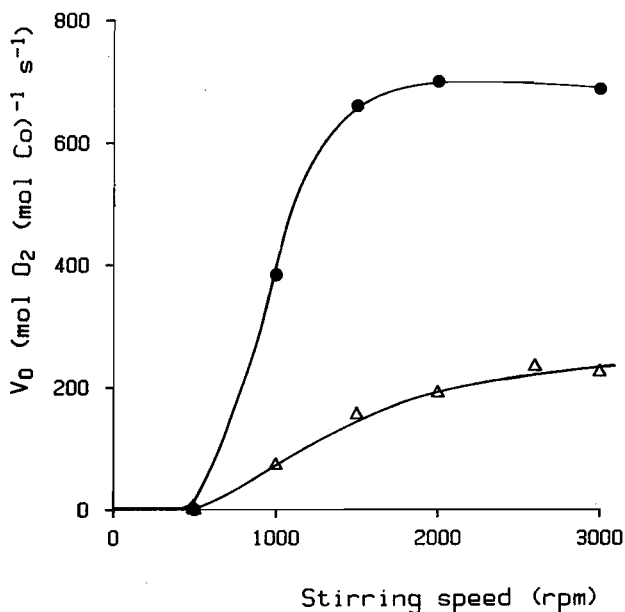


Fig. 8.2 Dependence of initial reaction rate, V_0 , on stirring speed in the 2,4-ionene-promoted oxidation of 2-mercaptoethanol (●) and 1-dodecanethiol (Δ).

Conditions ●: pH = 8, $[RSH]_0 = 0.19 \text{ mol dm}^{-3}$, $[N^+] = 10^{-3} \text{ mol dm}^{-3}$, $[Co] = 2 \cdot 10^{-7} \text{ mol dm}^{-3}$; Δ: pH = 13, $[RSH]_0 = 0.013 \text{ mol dm}^{-3}$, $[N^+] = 5 \cdot 10^{-4} \text{ mol dm}^{-3}$, $[Co] = 2 \cdot 10^{-7} \text{ mol dm}^{-3}$ (reaction started by $CoPc(NaSO_3)_4$ addition).

concluded from the constancy of reaction rate above this value for the mercaptoethanol system. On the other hand, dodecanethiol oxidation rate has not reached its maximum value even at a stirring speed of 2000 rpm (where $V_0 = 0.83 V_0^{\max}$), indicating that, indeed, the coexistence of two liquid phases enlarges the rate dependence on stirring speed.

Self-evidently, it is necessary to apply high stirring speeds in the dodecanethiol system to avoid mass-transport problems during kinetic measurements. Therefore, all further experiments were carried out at a stirring speed of 2600 min^{-1} .

8.2.3 Concentration effects on kinetics

The reaction rate was studied in dependence of substrate concentration and the concentrations of the catalyst components. Also the effect of varying pH was investigated.

On lowering the pH starting from pH 13, it was found that reaction rate decreased dramatically, reaching almost zero activity at pH < 10. This is in agreement with the fact that the thiolate anion is the reactive species, as was also established for mercaptoethanol (see chapter 7). Further experiments were therefore performed at pH 13.

Variation of the thiol concentration led to the behaviour depicted in Fig. 8.3. The kinetic order in thiol changed from 1 to 0 on increasing the amount of RSH and thus it seems that the process can be described by a Michaelis-Menten model, analogous to the mercaptoethanol oxidation (chapters

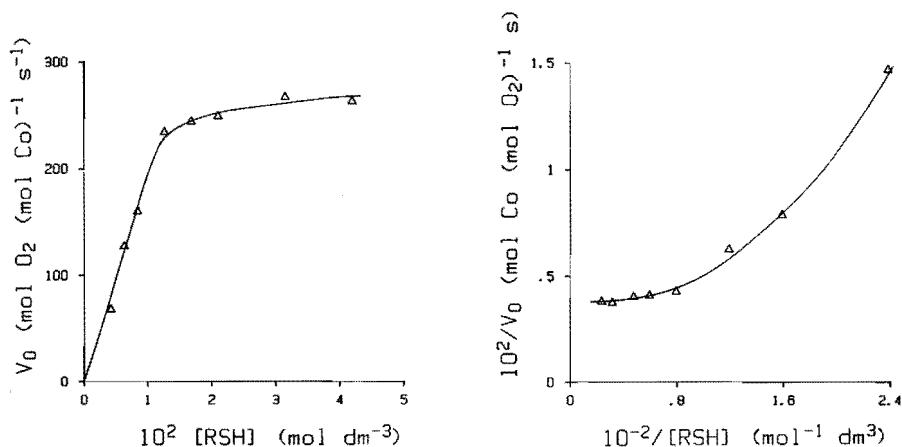


Fig. 8.3 a) Initial dodecanethiol oxidation rate as a function of the amount of thiol per unit reaction volume.

b) Lineweaver-Burk plot of the results of a).

Polymer promotor: 2,4-ionene ($M_n = 7400$), pH = 13, $[\text{N}^+] = 5 \cdot 10^{-4} \text{ mol dm}^{-3}$, $[\text{Co}] = 8 \cdot 10^{-7} \text{ mol dm}^{-3}$, reaction started by $\text{CoPc}(\text{NaSO}_3)_4$ addition.

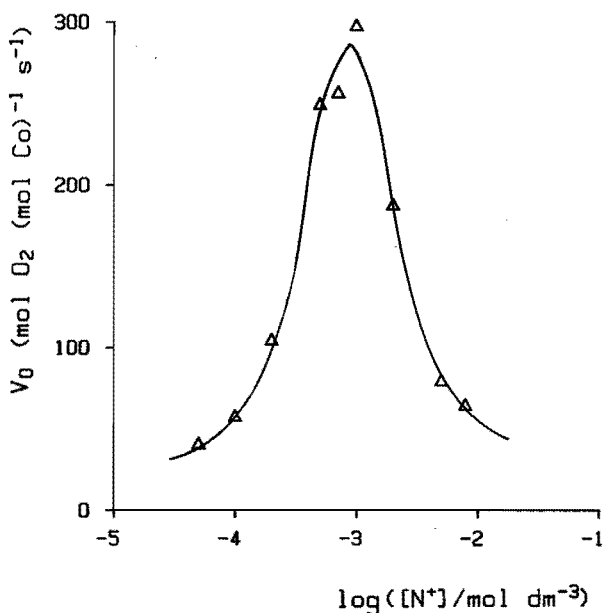


Fig. 8.4 Effect of varying the 2,4-ionene concentration on the initial dodecanethiol oxidation rate.

Conditions: $\text{pH} = 13$, $[\text{RSH}]_0 = 0.021 \text{ mol dm}^{-3}$, $[\text{Co}] = 8 \cdot 10^{-7} \text{ mol dm}^{-3}$
(reaction started by $\text{CoPc}(\text{NaSO}_3)_4$ addition).

6 and 7). However, a Lineweaver-Burk plot of the obtained results (Fig. 8.3b) clearly demonstrates that the Michaelis-Menten rate law is not obeyed ($1/V_0$ versus $1/[\text{RSH}]$ should be linear). This is likely to be due to the non-linear relationship between the amount of thiol present in the reaction mixture and the thiolate anion concentration in the vicinity of the catalyst.

This local thiolate anion concentration appeared to be highly dependent on the ionene concentration, as becomes evident from Fig. 8.4. Effective conversion of dodecanethiol was observed to be possible over only a small range of ionene concentrations: $10^{-4} \text{ mol dm}^{-3} < [\text{N}^+] < 10^{-2} \text{ mol dm}^{-3}$, with a sharp optimum at $[\text{N}^+] \approx 10^{-3} \text{ mol dm}^{-3}$. For the oxidation of mercaptoethanol the reported range was much larger and the optimum was less pronounced¹⁰¹. The results of Fig. 8.4 can be explained as follows.

The ionene interacts electrostatically with the thiolate anions that exist at the thiol-water interface. At low $[N^+]$, only a small part of the thiolate anions is in contact with the ionene that binds the cobalt catalyst complex, whereas the rest of the thiol remains separated in droplets from which only slow transport to the catalyst is possible. Therefore, the oxidation rate is rather low.

Upon increasing $[N^+]$, the contact surface between ionene and thiol (thiolate anion) is enhanced, resulting in an increased activity. At $[N^+] \approx 10^{-3} \text{ mol dm}^{-3}$, an optimum contact surface appears to be reached; an emulsion-like system is then obtained, where the ionene apparently stabilizes small thiol droplets (stabilization was not sufficient to allow determination of particle size).

Further addition of ionene only leads to an increase of the ionene concentration in the aqueous phase (instead of in the phase boundary layer). Part of the cobalt complex will probably be bound to this aqueous ionene fraction and, thus, will not be available for interaction with thiol.

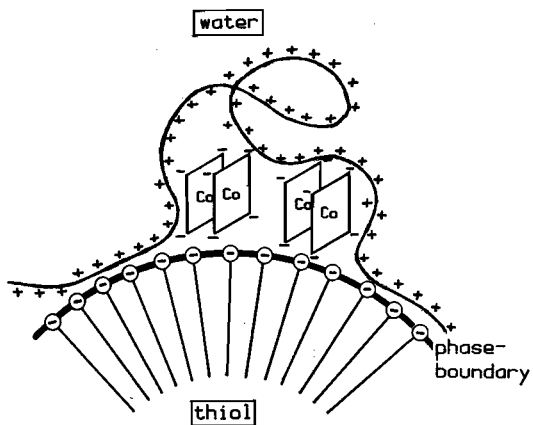


Fig. 8.5 Schematic representation of the phase-boundary interaction of the catalyst system with the hydrophobic substrate.

Therefore, the efficiency of the catalyst complex is lowered at high $[N^+]$ -values. The explanation is in agreement with the observation that the rate optimum is shifted to lower $[N^+]$ upon decreasing the cobalt concentration. This also explains why the initial rate is not linear with $[Co]$ as was expected for a Michaelis-Menten type process.

Summarizing the observed concentration effects, it can be stated that the kinetics of the process under study are highly complicated due to the two-phase character of the reaction mixture. The mechanism of the reaction seems to be best characterized as a phase-boundary mechanism, as schematically given in Fig.8.5.

8.2.4 Effect of varying the type of ionene

Since the contact surface between thiol and ionene appeared to be a very important factor determining the oxidation activity, attempts were made to improve this by building hydrophobic groups into the ionene, thus offering the possibility of hydrophobic interaction with the thiol. A more hydrophobic character of ionenes can be achieved by several methods: by introduction of longer alkyl-segments in the polymer backbone, as in 2,10-ionene (see section 4.3.2) (1); by replacement of ammonium-ion attached methyl groups by longer

Table 8.1 Effect of varying the type of ionene on the initial rate of dodecanethiol oxidation^a.

ionene	initial rate (mol O ₂ /mol Co.s)
2,4	250
2,10 ^b	17
3,3/C ₁₂ ^c	50
oleyl ^c	410

^a conditions: pH 13, $[RSH] = 0.021 \text{ mol dm}^{-3}$, $[Co] = 10^{-6} \text{ mol dm}^{-3}$, $[N^+] = 5 \cdot 10^{-4} \text{ mol dm}^{-3}$

^b $[N^+] = 10^{-5} \text{ mol dm}^{-3}$ (optimum)

^c $[Co] = 2 \cdot 10^{-7} \text{ mol dm}^{-3}$

side groups, as in 3,3C₁₂-ionene⁸¹) (2); or by coupling a hydrophobic moiety to one end of the ionene chains, as in oleyl-ionene (3) (structure: see p. 15).

The activities of these soap-like ionenes were measured and compared to that of 2,4-ionene (see Table 8.1). It was found that 2,10-ionene and 3,3C₁₂-ionene exhibit rather low activities, whereas oleyl-ionene was even somewhat more active than 2,4-ionene.

The 2,10- and 3,3C₁₂-ionenes were expected to be relatively inactive since they stabilize CoPc(NaSO₃)₄ in the, catalytically not very active, monomeric form (see chapter 5).

On the other hand, oleyl-ionene enhances aggregation of the phthalocyanine analogous to 2,4-ionene through its polyelectrolyte-type blocks, obviously without any interference of its soap-like blocks. This can be easily understood, since the oleyl segments, that might lead to interaction with the lipophilic substrate particles, are separated from the ionene segments that electrostatically bind the cobalt complex. Thus, the oleyl-ionene system is comparable to 2,4-ionene, as is also obvious from Fig. 8.6 where the effect of varying [N⁺] is shown. The general features of this curve are the same as that of Fig. 8.4, but the optimum activity is higher and above the optimum the rate decrease is less drastic. Presumably, these differences are the results of a better interaction between the thiol and the catalyst system.

From Table 8.1 and Fig. 8.6 it is evident, that dodecanethiol is oxidized most efficiently by a polymer containing a high charge density polyelectrolyte block (binding CoPc(NaSO₃)₄ in its active aggregated form and electrostatically interacting with RS⁻) and a separate hydrophobic block (leading to hydrophobic interaction with the substrate).

8.2.5 Side reaction, deactivation of the catalyst

It has been reported in chapter 6, that mainly one by-product may be

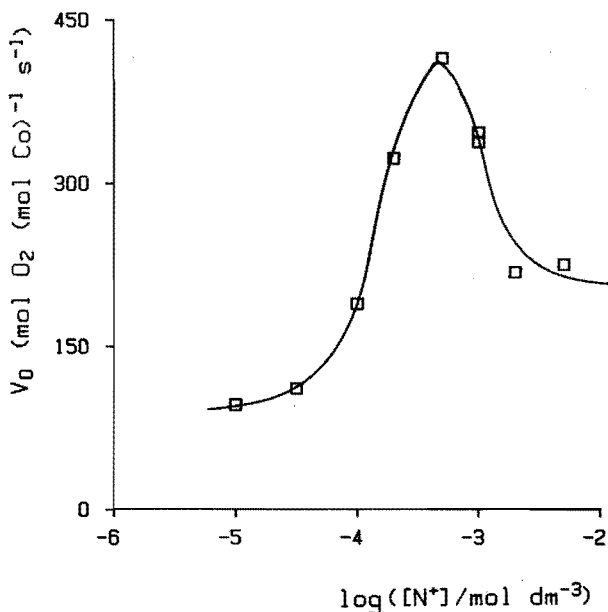
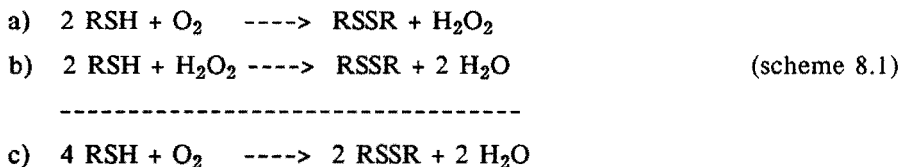


Fig. 8.6 Initial oxidation rate versus the oleyl-ionene concentration.
 Conditions as in Fig. 8.4, except $[Co] = 2 \cdot 10^{-7} \text{ mol dm}^{-3}$.

formed in the polymer-promoted thiol oxidation, viz. hydrogen peroxide, according to reaction a) in scheme 8.1.



The occurrence of this reaction in the present thiol oxidation system was investigated and, indeed, could be demonstrated. The amount of accumulated peroxide appeared to be higher than was found for mercaptoethanol under the same conditions. It was determined, that for dodecanethiol the amount of accumulated H_2O_2 equals the amount of dioxygen consumed during oxidation ($\text{H}_2\text{O}_2 : \text{O}_2 = 1 : 1$). This implies, that the thiol oxidation process completely

follows reaction step a) and step b) does not occur, whereas in the mercapto-ethanol oxidation step b) is a fast consecutive reaction (see chapter 6). This difference is caused by the fact that hydrogen peroxide and thiol exist in two different phases in the dodecanethiol system. It appears that H_2O_2 is immediately transported to the bulk of the aqueous phase after it has been formed, so that no interaction with RSH is possible. The accumulation of peroxide may be a serious problem in the catalytic thiol conversion, since H_2O_2 may cause breakdown of the $CoPc(NaSO_3)_4$ -complex¹⁰².

Another way in which catalytic activity may be lost is by entrainment of the catalyst during the precipitation of the insoluble disulfide. The occurrence of this process could be easily seen from the blue color of the disulfide. It could not be established whether the ionene coprecipitates as well. Nevertheless, it is clear that the cobalt phthalocyanine/ionene system is not an ideal system for the oxidation of dodecanethiol, since inactivation occurs rapidly.

However, the study of this system in combination with dodecanethiol has revealed two phenomena that may be of general importance:

- hydrophilic polymers, like 2,4-ionene, may efficiently interact with hydrophobic substrates on a purely electrostatic basis, leading to emulsion-like systems; thus, in this respect, polyelectrolytes, when combined with oppositely charged substrate moieties, may gain surface-active properties
- in order to improve such polymer-substrate interaction, preferably block-copolymers, consisting of a hydrophobic and a hydrophilic part, should be used, rather than random-type copolymers.

8.3 Conclusions

From the above presented results, it can be concluded that the ionene-promoted oxidation of a hydrophobic thiol proceeds at the boundary of thiol

and aqueous phase. Therefore, the order of addition of reactants and the stirring speed highly affect reaction rate. The coexistence of two phases also leads to kinetics that deviate from the Michaelis-Menten model. Furthermore, reaction of thiol with the produced hydrogen peroxide (scheme 8.1, step b) is prohibited.

The pH dependence of the process revealed that thiolate anions are necessary for efficient oxidation. This explains why ionenes, in spite of their hydrophilicity, enhance reaction rate: they electrostatically interact with the thiolate anions, probably according to the schematic representation of Fig. 8.5, and also interact with the cobalt catalyst. If one of these interactions is not optimal, reaction rate dramatically decreases and, therefore, only a very small ionene concentration range results in efficient thiol oxidation (Figs. 8.4 and 8.6). Interaction of ionene with the thiolate anions can be improved by coupling hydrophobic blocks to the ionene chains.

Finally, it was established that the investigated catalyst system is not suitable for practical application since deactivation of the catalyst occurs. A possible solution for this problem may be the use of other solvents, leading to a homogeneous reaction mixture.

The combination of the hydrophobic substrate and the hydrophilic catalyst appears to be an interesting system to study hydrophobic and electrostatic interactions in emulsion.

9.1 Polymeric effects in catalysis

In the preceding chapters, it has been made clear that polymers may exert significant effects on catalytic reactions. In the investigated ionene-promoted catalytic thiol oxidation, this most notably became manifest from the polymer-induced shift toward the (fast) reductive cycle of the reaction mechanism and the effective suppression of the (slow) oxidative cycle as observed in the polymer-free system (section 2.1). The remaining reductive cycle, schematically given in scheme 7.1 (see section 7.2), corresponds with saturation kinetics in dioxygen, instead of the negative order in dioxygen found for the polymer-free case.

The change in mechanism stems from the formation of the polymer-stabilized dimeric or aggregated form of the catalyst, in contrast with the (catalytically inactive) μ -peroxo complex occurring in the polymer-free system. Besides being resistant against μ -peroxo complex formation, these dimers are more active in electron transfer reaction steps than their monomeric counterparts, thus leading to extremely efficient catalyst systems.

It must be emphasized that this structural effect of the polymer appears to be more important than the expected concentrational effect, i.e. the enhancement of local thiolate anion concentration, as was demonstrated for the x,y-ionene series. This conclusion may have more general relevance and should be kept in mind when studying other polymer catalyst systems. Moreover, it demonstrates the importance of combining detailed kinetic investigations with spectroscopy or other structure-elucidating techniques.

It is interesting to note that the effect on the spatial arrangement of the $\text{CoPc}(\text{NaSO}_3)_4$ units could be achieved by using simple ionenes that, apart from their electrostatically interacting ammonium groups, contain no

structural elements that can give rise to specific interactions (e.g. hydrogen bonding, steric hindrance, etc.). Just induction of intermolecular interactions between phthalocyanine molecules was shown to be sufficient to largely affect reaction kinetics and mechanism.

9.2 Prerequisites for application of polymer catalysts in thiol oxidation

Based on the obtained insight in the polymer-promoted catalytic oxidation of thiols, some requirements can be formulated that have to be met when designing a polymer catalyst suitable for practical application.

Primarily, an efficient system should contain a catalyst binding part with high electrostatic potential in order to stabilize $\text{CoPc}(\text{SO}_3)_4^{4-}$ dimers or, preferably, higher aggregates. The content of cationic groups should be sufficiently high, allowing the X^+/Co -ratio to largely exceed a value of 4, resulting in local enhancement of the thiolate anion concentration. Soap-type polymeric components, particularly interesting in oxidizing hydrophobic thiols, may be included in the catalyst system, provided that these parts occur in segments separated from the cationic Co complex binding sites. Monomerization of the complex (occurring in "non-blocky" amphiphilic polycation systems) is then avoided.

In practical application, of course deactivation of the catalyst must be prevented as much as possible. Since high stirring speeds have to be applied, the materials should be mechanically highly stable. This may be an important problem in designing heterogenized catalyst systems. Presumably, the problem can then be overcome by using a specially designed reactor with e.g. low-shear stirring equipment.

Furthermore, the materials have to be chemically stable in alkaline media. In the oxidation of thiols like 2-mercaptoethanol, this may be not too difficult to achieve, since optimum reaction rates are obtained at only slightly basic pH-values (9 - 10). However, a pH of 13 (or even higher) is

preferred when oxidizing thiols like 1-dodecanethiol, which calls for a highly base-resistant catalyst.

Finally, catalyst deactivation may occur due to the destructive action of by-products, such as sulfonic acids and hydrogen peroxide¹⁰²). Fortunately, sulfonic acids are not being formed in ionene systems, but hydrogen peroxide is. To keep accumulation of this product low, reaction conditions should be chosen in such a way that reaction of H_2O_2 with thiol proceeds at a rate similar to the rate of its formation (section 6.3). Reaction rates can be controlled by choosing the appropriate concentrations of reactants.

In the case of aqueous oxidation of hydrophobic thiols, taking place via a phase-boundary mechanism, accumulation of peroxide can not be avoided because it is transported to the bulk of the aqueous phase, away from the thiol-water interface. Since in this thiol oxidation process the catalyst is also lost by coprecipitation with the water-insoluble disulfide, it is advised to perform this reaction in organic solvent/water mixtures, in which substrate and product are completely soluble.

Application of catalyst systems soluble in the reaction medium, has the disadvantage of difficult catalyst separation and reuse. Therefore, heterogenization must be considered. In designing immobilized systems, apart from the above-mentioned requirements, the high reaction rate has to be taken into account as well, since it can easily result in mass-transport problems. In order to avoid these problems, the best strategy seems to be the heterogenization of the polymer catalyst on small, non-porous particles, e.g. latex particles^{5,31}).

REFERENCES

- 1a. G.W. Parshall, R.E. Putscher, *J. Chem. Educ.* 63 (1986) 189
- b. G.W. Parshall, *Organometallics* 6 (1987) 687
2. G. van Koten, P. van Leeuwen, *Chemisch Mag.* (1988) 337
3. H.J. van de Berg, Ph. D. Thesis, Groningen State University, The Netherlands, 1989
- 4a. M. Hassanein, W.T. Ford, *Macromolecules* 21 (1988) 525
- b. H. Turk, W.T. Ford, *J. Org. Chem.* 53 (1988) 460
5. K.H. van Streun, R. Tennebroek, P. Piet, A.L. German, *Eur. Polym. J.*, submitted
6. N. Ise, in "Polyelectrolytes and their applications", A. Rembaum, E. Selegny (eds.), Reidel, Dordrecht, 1975.
7. R.H. Grubbs, C. Gibbons, L.C. Kroll, W.D. Bonds jr., C.H. Brubaker jr., *J. Am. Chem. Soc.* 95 (1973) 2373
8. W.O. Haag, D.D. Whitehurst, 2nd North Am. Meeting Cat. Soc., 1971, p. 2733
9. C.E. Koning, J.J.W. Eshuis, F.J. Viersen, G. Challa, *Reactive Polym.* 4 (1986) 293
10. C.U. Pittman jr., R.M. Hanes, *J. Am. Chem. Soc.* 98 (1976) 5402
11. e.g. B.M. Trost, E. Keinan, *J. Am. Chem. Soc.* 100 (1978) 7780
12. T. Kunitake, in "Polymer-supported reactions in organic synthesis", P. Hodge, D.C. Sherrington (eds.), Wiley, New York, 1980
13. K.M. Brown, *Hydrocarb. Processing* 52 (1973) 69
14. K.M. Brown, W.K.T. Gleim, P. Urban, *Oil & Gas J.* 57 (1959) 73
15. W.M. Douglas, U.S. Patent 4,088,569 (1978)
16. D.H.F. Carlson, T.A. Verachtert, J.E. Sobel, U.S. Patent 4,028,269 (1977)
17. M. Friedman, "The chemistry and biochemistry of the sulphhydryl group in amino-acids, peptides and proteins", Pergamon, Oxford, 1973

18. P.C. Jocelyn, "Biochemistry of the SH-group", Academic Press, New York, 1972, p. 94
19. D.W. Jacobsen, *Inorg. Chim. Acta* 79 (1983) 193
20. F. Nome, J.H. Fendler, *J. Chem. Soc., Dalton Trans.* (1976) 1212
21. J.L. Peel, *Biochem. J.* 88 (1963) 296
22. C.F. Cullis, J.D. Hopton, C.J. Swan, D.L. Trimm, *J. Appl. Chem.* 18 (1968) 335
23. C.J. Swan, D.L. Trimm, *J. Appl. Chem.* 18 (1968) 340
24. N.N. Kundo, N.P. Keier, G.V. Glazneva, E.K. Mamaeva, *Kin. Katal.* 8 (1967) 1325
25. I.G. Dance, R.C. Conrad, *Austr. J. Chem.* 30 (1977) 305
26. J. van Welzen, A.M. van Herk, A.L. German, *Makromol. Chem.* 188 (1987) 1923
27. J. van Welzen, A.M. van Herk, A.L. German, *Makromol. Chem.* 189 (1988) 587
28. J. van Welzen, A.M. van Herk, A.L. German, *Makromol. Chem.* (1989), in press
29. A.M. van Herk, A.H.J. Tullemans, J. van Welzen, A.L. German, *J. Mol. Catal.* 44 (1988) 269
30. J. van Welzen, A.M. van Herk, H. Kramer, A.L. German, *J. Mol. Catal.*, submitted
31. A.M. van Herk, K.H. van Streun, J. van Welzen, A.L. German, *British Polym. J.* 21 (1989) 125
32. J. van Welzen, A.M. van Herk, H. Kramer, T.G.L. Thijssen, A.L. German, *J. Mol. Catal.*, submitted
33. J. van Welzen, A.M. van Herk, A.L. German, *Makromol. Chem.*, submitted
34. N.N. Kundo, N.P. Keier, *Russ. J. Phys. Chem.* 42 (1968) 707
35. A.D. Simonov, N.P. Keier, N.N. Kundo, E.K. Mamaeva, G.V. Glazneva, *Kin. Catal.* 14 (1973) 864
36. D.J. Cookson, T.D. Smith, J.F. Boas, P.R. Hicks, J.R. Pilbrow, *J. Chem. Soc., Dalton Trans.* (1977) 189

37. J. Dolansky, D.M. Wagnerova, J. Veprek-Siska, Coll. Czech. Chem. Commun. 41 (1976) 2326
38. P.-S. Leung, M.R. Hoffmann, Environm. Sci. Technol. 22 (1988) 275
39. W.M. Brouwer, P. Piet, A.L. German, J. Mol. Catal. 22 (1984) 297
40. D.M. Wagnerova, E. Schwertnerova, J. Veprek-Siska, Coll. Czech. Chem. Commun. 39 (1974) 1980
41. D.M. Wagnerova, E. Schwertnerova, J. Veprek-Siska, Coll. Czech. Chem. Commun. 38 (1973) 756
42. E.I. Kozlyak, A.S. Erokhin, A.K. Yatsimirskii, I.V. Berezin, Bull. Acad. Sci. USSR, Div. Chem. Sci. 35 (1986) 741
43. E.I. Kozlyak, A.S. Erokhin, A.K. Yatsimirskii, React. Kin. Catal. Lett. 33 (1987) 113
44. M.R. Hoffmann, B.C. Lim, Environm. Sci. Technol. 13 (1979) 1406
45. J. Zwart, Ph. D. Thesis, Eindhoven University of Technology, The Netherlands, 1978
46. J.H. Schutten, Ph. D. Thesis, Eindhoven University of Technology, The Netherlands, 1981
47. W.M. Brouwer, Ph. D. Thesis, Eindhoven University of Technology, The Netherlands, 1984
48. A. Skorobogaty, T.D. Smith, J. Mol. Catal. 16 (1982) 131
49. L.D. Rollmann, J. Am. Chem. Soc. 97 (1975) 2132
50. J. Zwart, H.C. van der Weide, N. Bröker, C. Rummens, G.C.A. Schuit, A.L. German, J. Mol. Catal. 3 (1977-78) 151
51. J.H. Schutten, J. Zwart, J. Mol. Catal. 5 (1979) 109
52. J.H. Schutten, P. Piet, A.L. German, Makromol. Chem. 180 (1979) 2341
53. W.M. Brouwer, P. Piet, A.L. German, J. Mol. Catal. 29 (1985) 335
54. W.M. Brouwer, P. Piet, A.L. German, J. Mol. Catal. 31 (1985) 169
55. W.M. Brouwer, P. Piet, A.L. German. Polym. Bull. 8 (1982) 245
56. A. Rembaum, W. Baumgartner and E. Eisenberg, J. Polym. Sci. Lett. Ed. 6 (1968) 159

57. A.J. Sonessa, W. Cullen, P. Ander, *Macromolecules* 13 (1980) 195
58. S.P.S. Yen, D. Casson, A. Rembaum,, in "Water soluble polymers", N.M. Bikales (ed.), Plenum, New York, 1973
59. J.H. Weber and P.H. Busch, *Inorg. Chem.* 4 (1965) 469
60. A.C. Egerton, A.J. Everett, G.J. Minkoff, S. Rudrakanchana, K.C. Salooja, *Anal. Chim. Acta* 10 (1954) 422
61. S. Balt, J. Meuldijk, *Z. Naturforsch., Teil B* 34 (1979) 843
62. IUPAC Solubility Data Series, Oxygen and Ozone, Pergamon Press, 7 (1981) 141
63. S. Patai (ed.), "The Chemistry of the Thiol Group", John Wiley & Sons, London, 1974; part 1, ch. 8
64. R. Davies, *J. Chem. Soc.* (1938) 2093
65. D.F. Detar, "Computer Programs for Chemistry", vol. I, Benjamin, New York, 1969
66. Z.A. Schelly, R.D. Farina, E.M. Eyring, *J. Phys. Chem.* 74 (1970) 617
67. Y.-C. Yang, J.R. Ward, R.P. Seiders, *Inorg. Chem.* 24 (1985) 1765
68. L.C. Gruen, R.J. Blagrove, *Aust. J. Chem.* 26 (1973) 319
69. O. Kratky, H. Oelschlaeger, *J. Colloid Interfac. Sci.* 31 (1969) 490
70. D.F. Bradley, M.K. Wolf, *Proc. Natl. Acad. Sci. U.S.A.* 45 (1959) 944
71. H. Przywarska-Boniecka, K. Fried, *Ann. Soc. Chim. Pol.* 50 (1976) 43
72. A. Elzing, Ph. D. Thesis, Eindhoven University of Technology, The Netherlands, 1987, p. 61
73. T.S. Srivastava, J.L. Przyblinsky, A. Nath, *Inorg. Chem.* 13 (1974) 1562
74. I.D. Rattee, M.M. Breuer, "The Physical Chemistry of Dye Adsorption", Academic Press, London, 1974, chapter 4
75. J.A. de Bolfo, T.D. Smith, J.F. Boas, J.R. Pilbrow, *J. Chem. Soc., Faraday Trans. II* 72 (1976) 481
76. E.I. Valko, "Kolloidchemische Grundlagen der Textilveredlung", Springer Verlag, Berlin, 1937
77. W.M. Brouwer, P. Piet, A.L. German, *Polym. Commun.* 24 (1983) 216

78. V. Soldi, N. de Magalhães Erismann, F.H. Quina, *J. Am. Chem. Soc.* 110 (1988) 5137
79. J.R. Darwent, I. McCubbin, G. Porter, *J. Chem. Soc., Faraday Trans. 2* 78 (1982) 903
80. E.I. Kozlyak, A.S. Erokhin, A.K. Yatsimirskii, *Zh. Oshchei Khim.* 58 (1988) 76
81. E.G. Knapick, J.A. Hirsch, P. Ander, *Macromolecules* 18 (1985) 1015
82. R.L. Reeves, R.S. Kaiser, M.S. Maggio, E.A. Sylvestre, W.H. Lawton, *Can. J. Chem.* 51 (1973) 628
83. J.H. Fendler, E.J. Fendler, "Catalysis in micellar and macromolecular systems", Academic Press, New York, 1975, p. 20
84. compare also: J. Veprek-Siska, E. Schwertnerova, D.M. Wagnerova, *Chimia* 26 (1972) 75
85. D.K. Geiger, G. Ferraudi, K. Madden, J. Granifo, D.P. Rillema, *J. Phys. Chem.* 89 (1985) 3890
86. Y. Ogata, K. Marumo, T. Kwan, *Chem. Pharm. Bull.* 17 (1969) 1194
87. L.D. Rollmann, R.T. Iwamoto, *J. Am. Chem. Soc.* 90 (1968) 1455
88. W.A. Nevin, W. Liu, M. Melnik, A.B.P. Lever, *J. Electroanal. Chem.* 213 (1986) 217
89. W. Liu, M.R. Hempstead, W.A. Nevin, M. Melnik, A.B.P. Lever, C.C. Leznoff, *J. Chem. Soc. Dalton Trans.* (1987) 2511
90. J.F. Myers, G.W. Rayner Canham, A.B.P. Lever, *Inorg. Chem.* 14 (1975) 461
91. T.P.M. Beelen, internal report
92. W.A. Nevin, W. Liu, S. Greenberg, M.R. Hempstead, S.M. Marcuccio, M. Melnik, C.C. Leznoff, A.B.P. Lever, *Inorg. Chem.* 26 (1987) 891
93. C. Tanford, "Physical Chemistry of Macromolecules", Wiley, New York, 1961, p. 644
94. J.P. Barton, J.E. Packer, R.J. Sims, *J. Chem. Soc., Perkin II* (1973) 1547
95. F.A. Davis, P.L. Billmers, *J. Am. Chem. Soc.* 103 (1981) 7016
96. D.W. Giles, J.A. Cha, P.K. Lim, *Chem. Eng. Sci.* 41 (1986) 3129

97. P.K. Lim, D.W. Giles, J.A. Cha, Chem. Eng. Sci. 41 (1986) 3141
98. D. Piskiewicz, "Kinetics of chemical and enzyme-catalyzed reactions", Oxford University Press, New York, 1977, ch. 6
99. W.M. Brouwer, A.J.M.S. Robeerst, P. Piet, A.L. German in "Homogeneous and Heterogeneous Catalysis, Proceedings of the Fifth International Symposium on Relations between Homogeneous and Heterogeneous Catalysis, Novosibirsk, 1986", eds. Yu. Yermakov, V. Likholobov, VNU Science Press, Utrecht, 1986
100. I.M. Kolthoff, I.K. Miller, J. Am. Chem. Soc. 73 (1951) 5118
101. K.H. van Streun, P. Piet, A.L. German, Eur. Pol. J. 23 (1987) 941
102. J.H. Schutten, T.P.M. Beelen, J. Mol. Catal. 10 (1981) 85

SUMMARY

This thesis describes investigations on the effects of ionenes on the autoxidation of thiols catalyzed by tetrasulfonato-phthalocyaninacobalt(II) ($\text{CoPc}(\text{NaSO}_3)_4$). The study was aimed at elucidating the mechanism of the polymer-promoted process, especially with respect to the reaction steps affected by the polymer, in order to obtain insight in the (co-)catalytic role of the polymer.

Mechanistic information was gathered by means of spectroscopic and kinetic methods (chapter 3). The knowledge on the polymer-free process available from literature, is summarized in chapter 2 and forms the basis of the work presented.

First, the results of the spectroscopic investigations are discussed (chapters 4 and 5). In chapter 4, the interaction of several ionenes with the catalyst complex is described. It is demonstrated that ionenes can be classified in two categories: polyelectrolyte-type and polysoap-type ionenes.

Both types gave rise to stoichiometric complexation of the ionene and the Co-complex at the ratio of $\text{N}^+ : \text{Co} = 4 : 1$, where the charges on the ionene and the $\text{CoPc}(\text{SO}_3)_4^{4-}$ are just matching. This complexation was found to be due to purely electrostatic interaction, since experiments with model compounds like $\text{Fe}(\text{CN})_6^{4-}$ led to similar results.

In the polyelectrolyte-type systems, containing e.g. 2,4-ionene, this type of complexation appeared to be irreversible, the complex being stabilized up to N^+/Co -ratios of 10^6 due to strong aggregation of the phthalocyanine units. Other compounds with aggregational ability behaved analogously. On the other hand, with polysoap-type ionenes, like 2,10-ionene, above a certain ionene concentration micellization was found to occur, inducing monomerization of the catalyst.

The effects of substrates on the polymer catalyst complexes are discussed in chapter 5. In contrast with the polymer-free system, no interaction with dioxygen could be demonstrated. Especially with respect to the polyelectrolyte-type ionenes, this was rather surprising since formation of the dimeric μ -peroxo complex from the direct dimers (aggregates) was expected. However, this (catalytically inactive) species was only observed at very high pH-values (≥ 13).

Addition of 2-mercaptoethanol to the catalyst systems gave rise to reduction of the Co compound. The differences between polyelectrolyte- and polysoap-type ionenes observed, were analogous to those in the unreduced system, except that polysoap-induced Co^{I} monomerization occurred to an even higher extent than had been found for Co^{II} . From the parallel between catalytic activity and degree of catalyst aggregation, it was concluded that aggregates are the catalytic sites in the polymer catalyst systems, whereas the monomeric form can be regarded as relatively inactive.

In chapters 6 and 7, the results of the kinetic investigations are presented. Under carefully controlled conditions, initial rates were measured as a function of dioxygen and thiolate anion concentrations. The data obtained fitted very well a two-substrate Michaelis-Menten model (chapter 6). Only at

high thiol and low dioxygen concentrations deviations occurred, probably as a result of substrate inhibition.

In describing complete dioxygen uptake rate curves ($r \neq r_{\text{initial}}$), it appeared necessary to extend the kinetic model, taking into account the accumulation of hydrogen peroxide.

The kinetic parameters of the Michaelis-Menten rate equation were further studied in dependence of pH, type of ionene and type of thiol (**chapter 7**). The results obtained were combined, leading to a detailed reaction mechanism, consistent with all experimental data presently available. Considering the catalytic role of the polymer, it was concluded that it increases reaction rate by locally enhancing the thiolate anion concentration (in the vicinity of the polymer-bound catalyst) as well as by inducing a high degree of $\text{CoPc}(\text{SO}_3)_4^{4-}$ aggregation. The latter effect appears to improve the efficiency of electron transfer from catalyst to substrates.

Finally, in **chapter 8** a study is described of the ionene-promoted oxidation of a hydrophobic thiol, viz. 1-dodecanethiol. It was established that also in this case the role of the polymer is enhancement of the local thiolate anion concentration and stabilization of the aggregated phthalocyanine. However, the process was complicated due to the insolubility of the thiol in the (aqueous) reaction medium. The dependence of reaction rate on concentrations, reaction procedure and stirring speed revealed that the catalytic conversion should be described by a phase-boundary model, where the ionene, binding the catalyst, interacts with the thiolate anions existing at the boundary layer between thiol droplets and aqueous phase. This interaction, and as a consequence catalytic activity, could be improved by attaching a hydrophobic block to the (polyelectrolyte-type) ionene.

SAMENVATTING

Dit proefschrift beschrijft onderzoek naar de effecten van ionenes op de oxidatie van thiolen gekatalyseerd door kobalt(II)-ftalocyanine-tetranatrium-sulfonaat ($\text{CoPc}(\text{NaSO}_3)_4$). De studie had ten doel het mechanisme van het polymeer-gepromoteerde proces op te helderen, in het bijzonder met betrekking tot de reactie-stappen die beïnvloed worden door het polymeer, zodat inzicht verkregen zou worden in de (co-)katalytische rol van het polymeer.

Mechanistische informatie is verzameld met behulp van spectroscopische en kinetische methoden (hoofdstuk 3). De uit de literatuur beschikbare kennis van het polymeervrije proces, zoals is samengevat in hoofdstuk 2, vormt het uitgangspunt van het gepresenteerde werk.

Allereerst worden de resultaten van het spectroscopische onderzoek behandeld (hoofdstuk 4 en 5). In hoofdstuk 4 wordt de interactie van verschillende ionenes met het katalysatorcomplex beschreven. Er wordt aangetoond dat de ionenes kunnen worden ingedeeld in twee categorieën: polyelectroliet-achtige en polyzeep-achtige ionenes.

Beide typen gaven aanleiding tot complexering van het ionene met het Co-complex bij een verhouding van $\text{N}^+ : \text{Co} = 4 : 1$, waar de ladingen van het ionene en het $\text{CoPc}(\text{SO}_3)_4^{4-}$ elkaar juist compenseren. Deze complexering bleek het gevolg van puur electrostatische wisselwerking, aangezien vergelijkbare resultaten werden verkregen bij experimenten met modelverbindingen zoals $\text{Fe}(\text{CN})_6^{4-}$.

In de polyelectroliet-achtige systemen, bijv. 2,4-ionene, bleek deze complexering irreversibel te zijn; het complex werd gestabiliseerd tot N^+/Co -verhoudingen van 10^5 ten gevolge van sterke aggregatie van het ftalocyanine-complex. Andere verbindingen met mogelijkheid tot aggregatie vertoonden analoog gedrag. Anderzijds werd met polyzeepen zoals 2,10-ionene boven een bepaalde ionene-concentratie micelvorming waargenomen, wat monomerisatie van de katalysator induceerde.

De effecten van substraten op de polymere katalysatorcomplexen worden besproken in hoofdstuk 5. In tegenstelling tot in het polymeervrije systeem, kon geen interactie met zuurstof aangetoond worden. In het bijzonder met betrekking tot de polyelectroliet-achtige ionenes, was dit nogal verrassend, aangezien de vorming van het dimere μ -peroxo-complex uit het directe dimeer (aggregaat) verwacht werd. Echter, dit (katalytisch niet actieve) complex werd alleen waargenomen bij zeer hoge pH (≥ 13).

Toevoegen van 2-mercaptoethanol aan de katalysator-systemen leidde tot reductie van de Co-verbinding. De waargenomen verschillen tussen polyelectroliet- en polyzeep-achtige ionenes waren analoog aan die voor de ongereduceerde systemen, met dit verschil dat de polyzeep-geïnduceerde monomerisatie van het Co^I -complex zelfs nog in hogere mate optrad dan gevonden was voor Co^{II} . Uit het parallelle verloop van de katalytische activiteit en de aggregatiegraad van de katalysator werd geconcludeerd, dat aggregaten de katalytisch actieve plaatsen vormen in de polymere katalysatorsystemen, terwijl de monomere vorm te beschouwen is als relatief inactief.


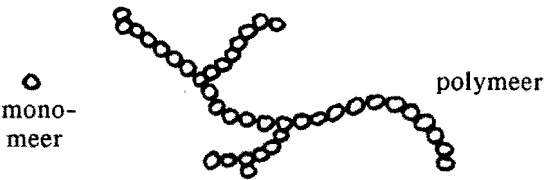

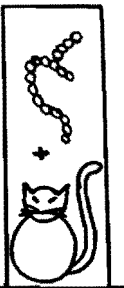

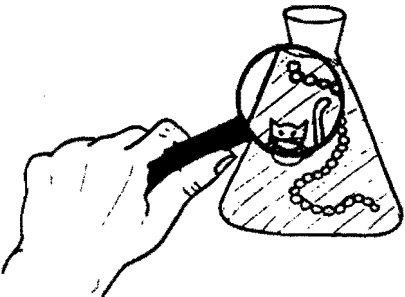
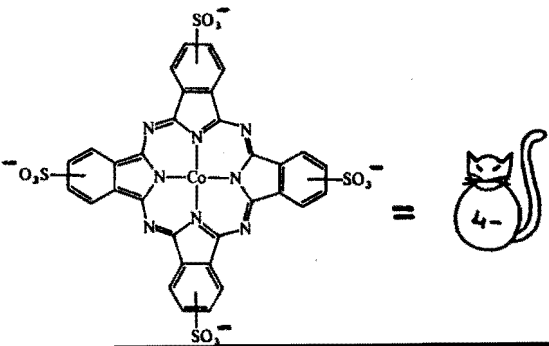
In de hoofdstukken 6 en 7 worden de resultaten van het kinetische onderzoek gepresenteerd. Onder zorgvuldig beheerste reactieomstandigheden werden initiële snelheden gemeten als functie van de zuurstof- en thioaat-anion-concentraties. De verkregen gegevens kwamen goed overeen met een twee-substrats Michaelis-Menten-model (hoofdstuk 6). Alleen bij hoge thiol- en lage zuurstof-concentraties traden afwijkingen op, waarschijnlijk ten gevolge van substraat-inhibitie.

Bij het beschrijven van complete zuurstof-opname-snelheidscurven ($r \neq r_{\text{initieel}}$) bleek het noodzakelijk, het kinetische model uit te breiden en rekening te houden met de accumulatie van waterstofperoxide.

De kinetische parameters in de Michaelis-Menten-snelheidsvergelijking werden verder onderzocht als functie van pH, type ionene en type thiol (hoofdstuk 7). De verkregen resultaten werden gecombineerd tot een gedetailleerd reactie-mechanisme, dat consistent is met alle beschikbare experimentele gegevens. Betreffende de katalytische rol van het polymeer werd geconcludeerd dat dit de reactiesnelheid verhoogt door zowel lokaal de thioaatanion-concentratie te verhogen (in de buurt van de polymeer-gebonden katalysator) als een hoge graad van $\text{CoPc}(\text{SO}_3)_4^{4-}$ -aggregatie te induceren. Laatstgenoemde effect blijkt de efficiëntie van electron-overdracht van katalysator naar substraten te verbeteren.

Tenslotte wordt in hoofdstuk 8 een studie beschreven van de ionene-gepromoteerde oxidatie van een hydrofoob thiol, nl. 1-dodecaanthiol. Vastgesteld werd dat ook in dit geval de rol van het polymeer bestaat in het verhogen van de lokale thioaatanion-concentratie en het stabiliseren van geaggregeerd ftalocyanine. Het proces werd echter gecompliceerd doordat het thiol onoplosbaar was in het reactiemedium (water). De afhankelijkheid van de reactiesnelheid van concentraties, reactie-procedure en roersnelheid, maakte duidelijk dat de katalytische omzetting beschreven moet worden met behulp van een fase-grensvlakmodel, waarin het ionene, dat de katalysator bindt, interactie heeft met de thioaatanionen die zich aan het grensvlak tussen water- en thiofase bevinden. Deze interactie, en daarmee samenhangend de katalytische activiteit, kon verbeterd worden door het (polyelectroliet-achtige) ionene te voorzien van een hydrofoob blok aan het ketenuiteinde.

SAMENVATTING VOOR LEKEN

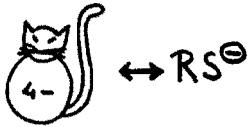
<p style="text-align: center;">Een kat(alsator)</p> <div style="text-align: center;">  </div> <p style="text-align: center;">versnelt reacties</p>	<p style="text-align: center;">Een polymeer....</p> <div style="text-align: center;">  </div>
<p style="text-align: center;">....helpt daar soms bij</p> <div style="display: flex; align-items: center;"> <div style="margin-right: 20px;"> <p style="writing-mode: vertical-rl; transform: rotate(180deg);">reactie-snelheid</p> <p style="text-align: center;">↑</p> </div> <div style="display: flex; justify-content: space-around; align-items: center;"> <div style="text-align: center;"> <p>zonder</p>  </div> <div style="text-align: center;">  </div> </div> </div>	<p style="text-align: center;">Vraag is:</p> <div style="text-align: center; font-size: 4em;">  </div> <p style="text-align: center;">WAAROM/HOE ?</p>
<p style="text-align: center;">Dat heb ik onderzocht voor...</p> <div style="text-align: center;">  </div>	<p style="text-align: center;">...een modelreactie:</p> $2 \text{RS}^{\ominus} \longrightarrow \text{RSSR}$ <div style="text-align: center;">  </div>

Belangrijkste resultaten:

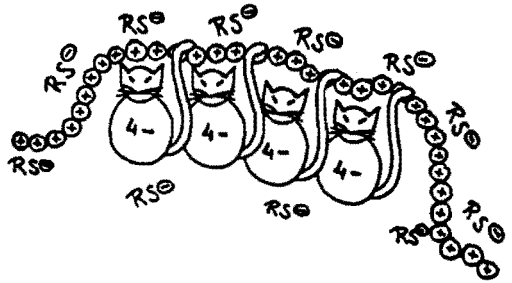
best werkende polymeer =



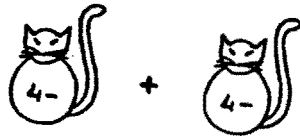
Hoge plus-lading polymeer



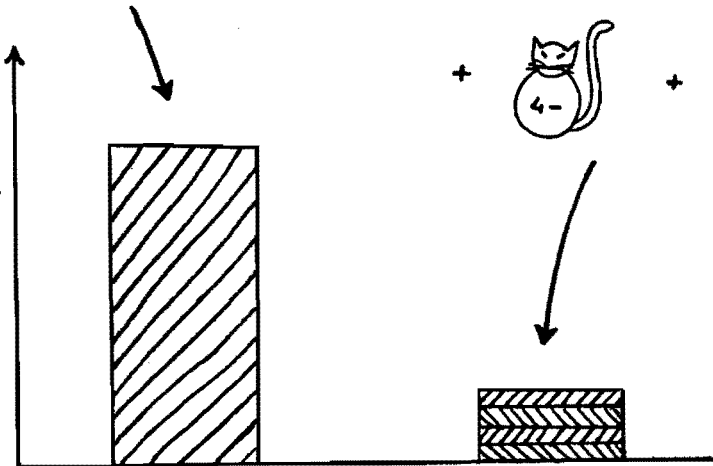
heft afstoting
min-ladingen op



Bovendien blijkt te gelden:



reactie-
snelheid



CURRICULUM VITAE

- 4 april 1961 geboren te Rotterdam
- 1979 eindexamen VWO; Chr. s.g. "Melanchthon" te Rotterdam
- 1982 kandidaatsexamen Sla (anorganische scheikunde);
Rijksuniversiteit Leiden
- 31 mei 1985 doctoraalexamen scheikunde, cum laude; Rijksuniversiteit Leiden
Hoofdvak: heterogene katalyse o.l.v. Prof. dr. V. Ponec
Bijvak 1: analytische chemie o.l.v. Prof. dr. A. Bult en
Dr. W.P. van Bennekom
Bijvak 2: lerarenopleiding o.l.v. Dr. J. van der Linde
- okt. 1984 -
- juli 1985 part-time betrekking als docente scheikunde aan de Chr. s.g.
"Johannes Calvijn" te Rotterdam
- juli 1985 -
- juli 1989 betrekking als assistent-onderzoeker aan de Technische
Universiteit Eindhoven bij de groep Polymeerchemie o.l.v.
Prof. dr. ir. A.L. German in het kader van het alhier
beschreven promotie-onderzoek
- 1989 toekenning Koninklijke/Shell reis-prijs
- vanaf 15
okt. 1989 betrekking bij DSM Research te Geleen, als researchmedewerker
op het gebied van de Ziegler-Natta-polymerisatie

STELLINGEN

behorende bij het proefschrift van J. van Welzen

"EFFECTS OF POLYCATIONS ON STRUCTURE AND CATALYTIC ACTIVITY OF COBALTPHTHALOCYANINE. Mechanistic study of the ionene-promoted thiol autoxidation"

1. Polymere katalyse is nooit homogeen.
2. Nevin et al. stellen ten onrechte, dat het electrochemisch door hen gegenereerde $\text{Co}^{\text{I}}\text{Pc}(\text{NaSO}_3)_4^-$ niet geaggregeerd is.
W.A. Nevin, W. Liu, M. Melnik, A.B.P. Lever, J. Electroanal. Chem. 213 (1986) 217
hoofdstuk 5 van dit proefschrift
3. De conclusie van Kobayashi en Lever, dat kroonether gesubstitueerde phthalocyanines onder invloed van zouten uitsluitend dimeren vormen, is gebaseerd op een onjuiste toepassing van de theorie en derhalve niet bewezen.
N. Kobayashi, A.B.P. Lever, J. Am. Chem. Soc. 109 (1987) 7433
4. Het mechanisme voor de katalytische oxidatie van cysteine, zoals voorgesteld door Yatsimirskii et al., wekt de schijn gedetailleerd en gecompliceerd te zijn, maar is in werkelijkheid een niet-realistisch, sterk gesimplificeerd model, aangezien alle reactiestappen voorafgaand aan de produktvormingsstap verondersteld worden in evenwicht te zijn.
A.K. Yatsimirskii, E.I. Kozlyak, A.S. Erokhin, Kin. Catal. 29 (1988) 305
5. De door Leung en Hoffmann gepresenteerde kinetische data voor de reactie tussen 2-mercaptoethanol en waterstofperoxide zijn niet betrouwbaar, aangezien de spectrofotometrische bepalingen werden uitgevoerd bij zeer lage thiol concentraties, waar storende invloed t.g.v. foto-oxidatie te verwachten is.
P.-S. K. Leung, M.R. Hoffmann, J. Phys. Chem. 89 (1985) 5267
S. Patai (ed.), "The Chemistry of the Thiol Group", Wiley, London, 1974, vol. 1, hoofdstuk 10 en vol. 2, hoofdstuk 17
6. De conclusie van Soldi et al. dat micellaire structuren uitsluitend voorkomen in 3,m-ionene oplossingen met $m \geq 14$ is voorbarig, aangezien de auteurs geen onderzoek hebben verricht in het concentratie-gebied $> 0.01 \text{ mol N}^+ \text{ dm}^{-3}$, terwijl te verwachten is dat 3,m-ionenes met $m < 14$, evenals vergelijkbare conventionele kationische zepen, pas bij dergelijke hoge concentraties micellen kunnen vormen.
V. Soldi, N. de Magelhaes Erismann, F.H. Quina, J. Am. Chem. Soc. 110 (1988) 5137

7. De conclusie van Wöhrle et al. dat polymeren geen significant effect hebben op de epoxidatie van 2,5-dihydrofuran m.b.v. Mn(III)porphyrines is voorbarig, gezien de grote verschillen in waargenomen selectiviteiten en gezien het gegeven dat het kinetisch onderzoek slechts heeft bestaan uit conversie-metingen na 4 uur reactie, waar reeds ca. 95 % omzetting had plaats gevonden.
D. Wöhrle, J. Gitzel, G. Krawczyk, E. Tsuchida, H. Ohno, T. Nishisaka, J. Macromol. Sci. - Chem. A25 (1988) 1227
8. Het betitelen van de activiteit van geïmmobiliseerd Fe(III)-tetracarboxyphthalocyanine als "catalase-like" door Shirai et al. getuigt van een te groot optimisme van de auteurs, aangezien de snelheidsconstante van catalase een factor $2 \cdot 10^4$ hoger is.
H. Shirai, S. Higaki, K. Hanabusa, Y. Kondo, N. Hojo, J. Polym. Sci., Polym. Chem. Ed. 22 (1984) 1309
9. Informatica-onderwijs in het basis-programma van de scheikunde-studie is overbodig, een cursus rapporteren daarentegen dringend gewenst.
10. Het is onjuist de titel doctor te verlenen zonder hieraan toe te voegen welke wetenschap betrokkene beoefent.
11. Het is niet terecht dat de personen die wezenlijk hebben bijgedragen aan de totstandkoming van dit proefschrift, t.w. Annie Tullemans, Hans Kramer, Timen Thijssen, Karel van Streun, Alex van Herk, Prof. German en Prof. Reedijk, niet in een dankwoord vermeld mogen worden.

Eindhoven, 3 oktober 1989